

SLOPE STABILITY INVESTIGATIONS
IN CASTLE HILL BASIN

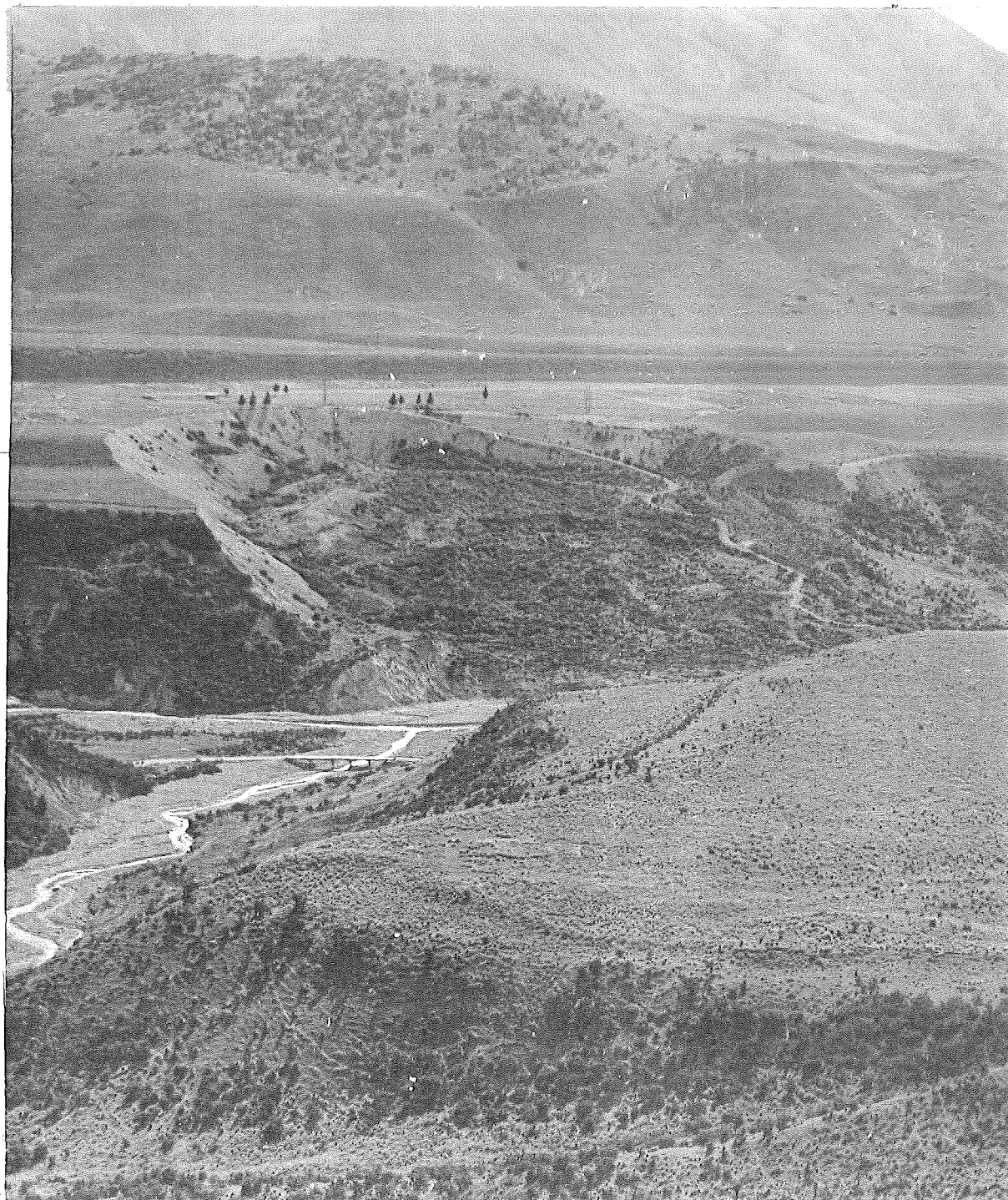
A thesis
submitted in partial fulfilment
of the requirements for the degree
of
Master of Science in Engineering Geology

by

J. M. Bryant

University of Canterbury
1975

i.e. 1978



FRONTISPIECE : LANDSLIDE COUNTRY.

TO GENEVIEVE

CONTENTS

CHAPTER	PAGE
List of photographs	iii
List of figures	v
List of tables	vii
Abstract	viii
 1 INTRODUCTION	
1.1 Thesis statement	1
1.2 Location and description of field area	1
1.3 Scope and organisation of thesis	6
 2 THE PHYSICAL ENVIRONMENT OF CASTLE HILL BASIN	
2.1 Physiography	9
2.2 Geological setting	19
2.3 Lithologies	21
2.4 Structure	27
2.5 Tectonism	30
2.6 Geomorphology	34
 3 GENERAL DISCUSSION OF SLOPE STABILITY IN CASTLE HILL BASIN	
3.1 Introduction	44
3.2 Classification of landslides	44
3.3 Types and distribution of landslides	53
3.4 Rates of degradation	65
3.5 Dating landslides	67
3.6 Engineering geological aspects of the Castle Hill Basin sediments	74
 4 SLOPE STABILITY IN THE ENYS FORMATION, BROKEN RIVER	
4.1 Introduction	85
4.2 Lithologies of the Enys Formation at Broken River	90
4.3 Structure	94
4.4 Geohydrology	96
4.5 Sampling and testing of the Enys Formation	98
4.6 Interpretation and significance of geotechnical testing	112

CHAPTER	PAGE
5 SLOPE STABILITY ANALYSIS OF THE BROKEN RIVER BRIDGE SLIDE	
5.1 Introduction	138
5.2 Field conditions	141
5.3 Mechanisms of movement	141
5.4 Stability analyses	144
5.5 Discussion of results	153
6 REASONS FOR SLOPE FAILURE IN CASTLE HILL BASIN	
6.1 Introduction	161
6.2 Classification of landslide processes and causes	162
6.3 Presentation of landslide susceptibility map	170
ACKNOWLEDGEMENTS	175
REFERENCES	176
Appendix 1 Glossary of terms	179
2 Notation	179
3 A method suitable for determing certain index properties of soils which are appreciably affected, both chemically and physically, on saturation with water	187
4 Particle size distrbution curves	189

LIST OF PHOTOGRAPHS

PLATE		PAGE
	Landslide country	Frontispiece
1	Present day topography in Castle Hill Basin	4
2a	Headwaters of Broken River and Craigieburn Range	10
2b	Dry Creek and Torlesse Range	10
3	Vegetation and failure patterns in Hogsback Stream	16
4a	Broken River oversteepening valley sides	18
4b	Lateral erosion in upper Porter River	18
5	Glaciofluvial terraces around Hogsback Stream	38
6	Limestone quarry in possible landslide in Thomas Formation	41
7	Steeply-dipping limestone beds of Hogsback Hill	42
8	Steep-sided gorge in limestone and Cave Stream outlet	42
9a	Arcuate configuration	46
9b	Uneffaced head scarp	46
9c	Drunken forest	47
9d	Swamps in backtilted depressions	47
9e	Boulder fields, derived from the terrace gravels	48
9f	Toe scarp eroded by diverted river channel	48
9g	Backtilted scarps	49
9h	Failure surface	49
10a	Two views of dormant landslides in Broken River	50
10b	Panoramic view of dormant landslides in Hogsback Stream and tributary	51
11a,b,c,	Three views of fossil landslides	52
12	Prebble Hill limestone escarpment with its numerous block slides	54
13	Aerial view of the Broken River Bridge slide	54
14	Earthflows in glauconitic muds of the Enys Formation	58
15	Debris avalanche in greywacke, Leith Hill	58
16	Soil creep on Gorge Hill	63
17	Badlands topography in Gorge Hill	

PLATE		PAGE
18	Incised gullies forming along Torlesse fault zone	63
19	Concordant terraces on both undisturbed ground and fossil landslide	66
20	Drop in terrace level at Broken River	69
21a & b	Two views of a recent slump in Broken River Coal Measures	71
22	Panoramic view of Iron Creek Greensand and Broken River Coal Measures country	76
23a	Aerial view of unusual slide on true left bank of Porter River	78
23b	Side view shows multiple slip circle failure planes	78
24	Persistence of unsuitable conditions leading to almost continuous instability at Hogsback Stream	80
25	Porter River where it passes through the two flanks of the Prebble Hill syncline	82
26	Small slide developed on Flock Hill syncline	82
27a & b	Two faults disrupting a terrace to the south of Porter River	84
28	View down Hogsback Stream towards Broken River	86
29	Suite of slides in upper reaches of Broken River	98
30	Uniaxial swelling strain testing apparatus	103
31a & b	Before and after specimens selected for uniaxial swelling strain testing	104
32a & b	Before and after specimens selected for slake durability testing	106
33	Broken River Bridge slide	139
34a & b	Incipient scarplets on valley sides of Hogsback Stream	166
35	Stable slopes in upper Trout Stream	167

LIST OF FIGURES

FIGURE		PAGE
1	Location of Castle Hill Basin	2
2	Castle Hill Basin	5
3	Mean monthly rainfall	12
4	Vegetation	13
5	Structural contour map of Castle Hill Basin	28
6	Location of earthquake epicentres in the vicinity of Castle Hill Basin	32
7	Hypothetical cross-section through slump in Porter Group tuffs and limestone	41
8	Cross-section of contemporary landslide showing swamp formed in back tilted depression	72
9	Engineering geology of part of Broken River	87
10	Geological cross-sections of Broken River and Hogsback Stream	88
11	Geological column of the Enys Formation	89
12	Hypothetical profile across part of Broken River just upstream from Hogsback Stream	98
13	Relationship between cohesion and water content	120
14	Plot of swelling strain index against dry density	124
15	Plasticity chart	128
16	Relationship between plasticity index and peak friction angle	130
17	Relationship between plasticity index, liquid limit and residual friction angle	131
18	Contour map of Broken River Bridge slide	142
19	Geological cross-section of Broken River Bridge slide	143
20	Contoured positions of factors of safety assuming a circular arc failure for the Broken River Bridge slide	148
21	Block and wedge analysis of the Broken River Bridge slide	150

FIGURE

PAGE

22	Topographical map S66/8, Castle Hill Basin	Inside rear cover
23	Geology and landslide distribution	"
24	Slope and map, Castle Hill Basin	"
25	Landslide susceptibility map	"

LIST OF TABLES

TABLE	PAGE
1 Vegetative cover of the Broken River Catchment	14
2 Gage's Cretaceous-Tertiary sequence	21
3 Estimated earthquake intensities	33
4 Advances of the Waimakariri Glaciers	36
5 Geotechnical property values of the Enys Formation	107
6 Grain mineralogy percentages	110
7 Cohesion values from unconsolidated undrained triaxial tests	112
8 Solid densities for mineral constituents	122
9 Relationship between rate of expansion and permeability	123
10 Relationship between plasticity index and swelling strain index	129
11 Effect of angularity and grading on peak friction angle	133
12 Representative values of ϕ for dense sands and silts	133
13 Cohesion values for varying ϕ values and groundwater levels	146
14 Computed forces and safety factors for block and wedge analysis	154

ABSTRACT

The field area of interest is an intermontane basin lying 100 km northwest of Christchurch on the West Coast Road. Within this roughly triangular, tectonic depression lies a sequence of marine and non-marine sediments of late Cretaceous-Tertiary age. The sediments have been modified by glacial and post-glacial events to leave steep-sided valleys, flights of terraces and limestone hills.

Landslides of all types (falls, slides, slumps, flows, complex movements and mass wasting) are found in the dense, heavily overconsolidated sands, silts and muds. The different types of landslides and their distribution with respect to lithology and structure is discussed, as is the rates of degradation and their relative age.

A select area around Broken River - Hogsback Stream is studied in detail and the stratigraphy, structure and geohydrology is presented. The sediments from the Enys Formation were sampled, tested for index and physical properties, and interpreted in terms of their significance towards slope stability. A major slump of this area is back-analysed using parameters gained directly or inferred from the geotechnical testing. Several methods are used and a circular arc mode of failure is rejected in favour of a block slide bounded by passive and active wedges.

Finally the landslide processes and factors that have been found operating in Castle Hill Basin are outlined and it is seen that the most important factors are those

relating to the area's intrinsic climatical, geological and topographical nature. These processes and factors are summarised in a series of maps, which, when overlain, produce a landslide susceptibility map showing predicted areas of likely movement.

CHAPTER 1

INTRODUCTION

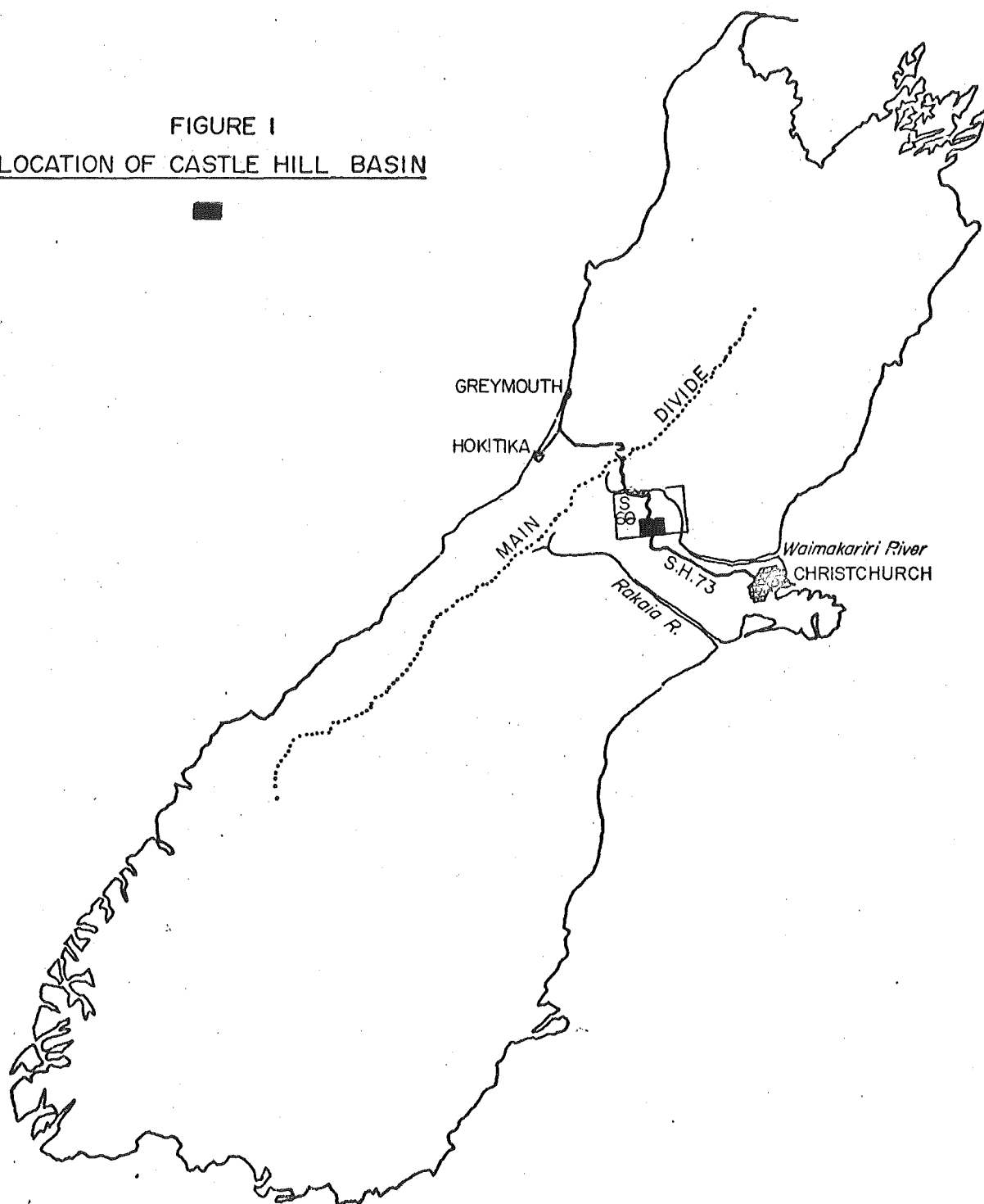
1.1 THESIS STATEMENT

The intention of this thesis is to investigate the various aspects of slope stability in a selected area, Castle Hill Basin. An attempt has been made to cover as many aspects of slope stability as possible within the resources normally available for a Master of Science thesis. As some aspects warranted a more detailed investigation a smaller area was selected for a more intensive study. The final aim is to determine the overall factors responsible for mass movement and to use this data for predicting the likely susceptibility of a slope to failure.

1.2 LOCATION AND DESCRIPTION OF FIELD AREA

The field area of interest, Castle Hill Basin, lies about 100 km from Christchurch on the West Coast road (State Highway 73) as shown in figure 1. Castle Hill Basin, formerly known as Trellisick Basin, is a roughly triangular, tectonic depression bounded by major faults at the foot of the Torlesse, Craigieburn and Broken Hill

FIGURE I
LOCATION OF CASTLE HILL BASIN



Ranges. Within this depression lies a sequence of Cretaceous and Tertiary formations which unconformably overlies greywacke basement rocks.

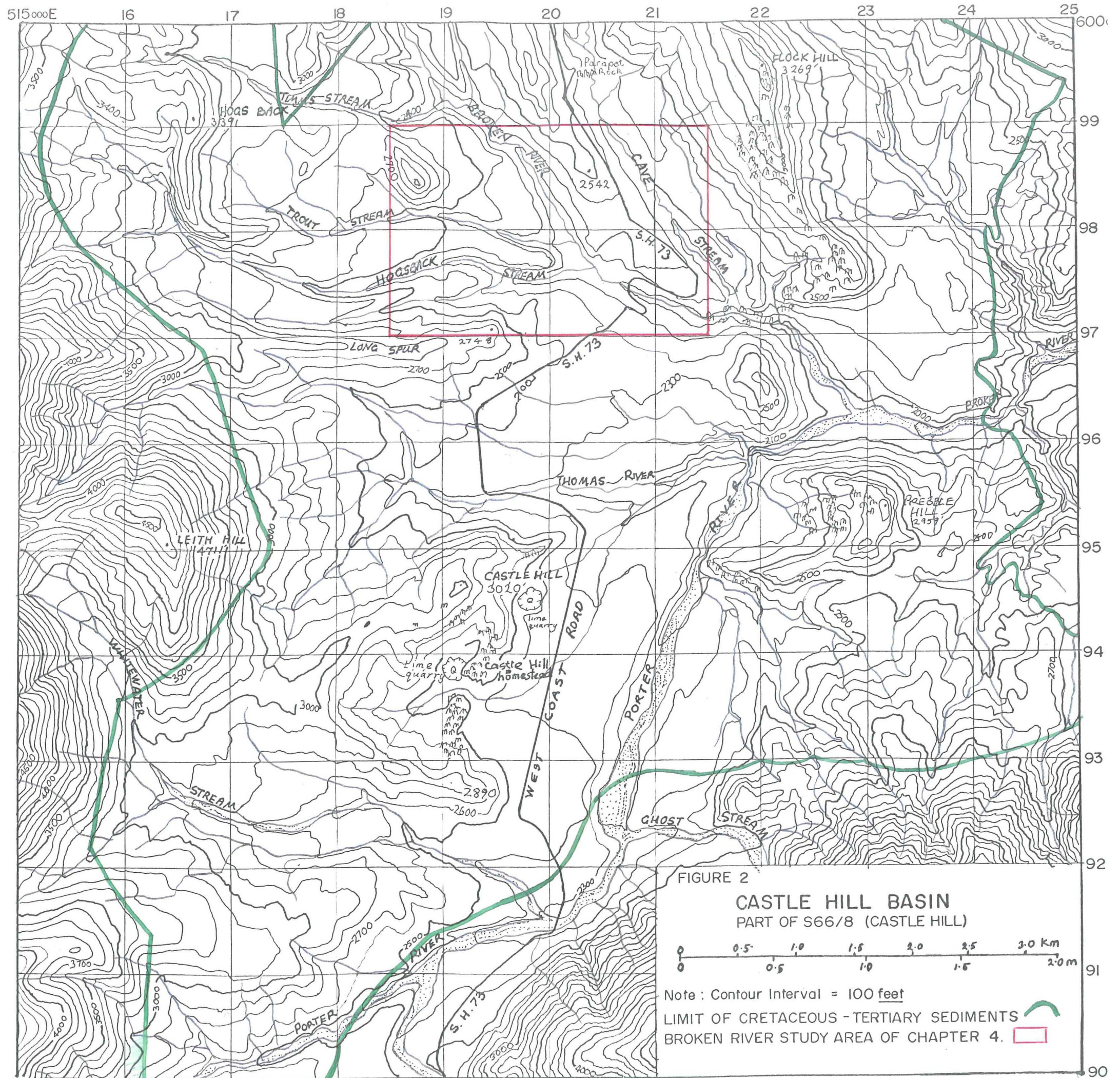
The Broken River system arises in the higher-standing, surrounding mountain ranges, flows through the broad lower part of the basin, then joins the Waimakariri River via a gorge between the Torlesse and Broken Hill Ranges. The lower part of the basin contains about 70 sq km of Cretaceous-Tertiary sediments that have been modified by glacial and post-glacial events to give a present-day topography of deeply incised rivers, broad glaciofluvial terraces and subdued hills, broken in various places by limestone escarpments (plate 1).

The area is covered by Sheet 18 (Hurunui 1:250,000) of the Geological Map of New Zealand and more specifically by the NZMS 1 map, S66/8 (Castle Hill 1:15840); a part of which is reproduced in figure 2 to delineate the bounds of this thesis. For the purpose of a slope stability investigation, the area shown in figure 2 is representative of the range of slope failures encountered even though small portions of the Cretaceous-Tertiary beds have been excluded to the north and south.

The only permanent inhabitants of the area reside at Castle Hill Homestead and manage a sheep and cattle run that covers most of the basin. The district sees heavy road usage, both as an access route to the Arthurs Pass National Park and the West Coast, and also by visitors who view the area for its scenic and



PLATE 1: Present day topography in Castle Hill Basin consists of deeply incised rivers, broad glaciofluvial terraces and subdued hills, broken in various places by limestone escarpment. View is looking towards northern part of basin and Craigieburn Range.



recreational values. Many of the visitors come during the winter months to ski at one of the four ski fields on the Craigieburn Range.

Future development that may take place in Castle Hill Basin includes realignment and upgrading of the State Highway, construction of an alpine resort village, upgrading of the access roads to the ski fields, and further exploitation of the limestone deposits. As in other areas of scenic, recreational and economic value, development is inevitable and this could perhaps proceed in a haphazard manner with little regard to the environment. The geological environment is most affected by mass movement, not only by natural agencies, but also as a result of man's activities.

1.3 SCOPE AND ORGANISATION OF THESIS

A preliminary field investigation revealed the presence of over 60 landslides, clearly indicating the applicability of a slope stability investigation in this area. The many examples of mass movement are of varying types, ages and stages of development and can be found in both rocks and soils. Landslides are particularly common in some areas and rare in others suggesting that a regional combination of factors peculiar to Castle Hill Basin as well as a local combination of factors is responsible for mass movement.

The aim of this study is to determine the overall factors responsible for mass movement at Castle Hill Basin and to delineate areas of known and possible slope

instability. Such a study would be of use to engineers involved with the development of the basin as a background to the problems associated with landslides in this area. A glossary of engineering geological terms is included at the rear (Appendix 1).

Initially discussion of slope stability is on a regional basis. A select area is then investigated in more detail to ascertain local influences.

The physiography, geology and geomorphology of Castle Hill Basin are examined in Chapter 2 as an introduction to slope stability in this area. Although much of this chapter is drawn from previous workers, many comments arise from the author's own field observations. Aerial photographs were stereoscopically examined and an aerial survey was carried out by the author in a light aircraft. These surveys pointed to areas worthy of ground inspection and most of the basin was covered on foot as a consequence.

Chapter 3 discusses the landslides in Castle Hill Basin in terms of a four-fold classification system and mention is made of rates of degradation and ages of landslides. Engineering geological aspects of the Castle Hill Basin sediments are studied with respect to the influence of lithology and structure on the distribution of landslides.

An area around Broken River-Hogsback Stream, where landslides are particularly common, has been chosen

for a detailed investigation in Chapter 4. In the next chapter, stability analyses are performed on a large landslide near the highway bridge at Broken River in an attempt to verify assumptions made about soil strength parameters. Finally the reasons for slope instability are collated and summarised in Chapter 6 and the data are used to predict likely areas of future mass movement.

CHAPTER 2

THE PHYSICAL ENVIRONMENT OF
CASTLE HILL BASIN2.1 PHYSIOGRAPHY

2.1.1 Climate:

Castle Hill Basin has a climate similar to other intermontane basins in the Southern Alps. The ranges to the north and west (of which the Craigieburn Range is the nearest) lessen the intensity and moisture content of the prevailing norwesterlies, and the Torlesse Range to the south-east interrupts airflows from the Canterbury Plains. The amount of annual precipitation decreases rapidly with altitude from the Craigieburn Range in the north-west then less rapidly in a south-easterly direction. The decrease in annual precipitation is best shown by the vegetation which changes from beech forest in the headwaters of Broken River to arid tussock grassland towards Lake Lyndon (see plates 2a, 2b and figure 4).

Meteorological observations (source: New Zealand Meteorological Service) at Castle Hill Station (altitude 741 m) can be regarded as typical for the basin, with



Plate 2a: Beech forest in headwaters of Broken River on Craigieburn Range. The Avoca Glaciation surface referred to in section 2.6.2 can be seen on the two low hills in the centre (Bridge Hill on the left and Nursery Hill on the right). The northern end of the Flock Hill escarpment can be seen to the lower left and Craigieburn cutting is towards the right. Note cirque-like basins above Nursery Hill.



Plate 2b: Dry Creek and Tarlness Range in the southern part of Castle Hill Basin. Note extensive erosion as compared to the forested slopes in the northern part of the basin (plate 2a). State Highway 73 is seen crossing the broad aggraded bed in centre and continuing to either side across the low-angle alluvium cone.

an average annual precipitation of 760 mm. The mean monthly rainfall ranges for this station are shown in figure 3.

At 900 m (Nursery Hill in the headwaters of Broken River) the annual precipitation averages 1,450 mm per year. At 1,500 m in the Craigieburn Range, the annual precipitation is about 1,780 mm; of this, 30% could fall as snow.

In the main basin itself, a few falls of snow are likely each year and in the winter of 1965, snow lay on the ground for five weeks. Frosts are not uncommon with an average of 37 per year.

Apart from rainfall, the Craigieburn Range also receives more snow than the Torlesse Range. On the Castle Hill Basin side of the north-east trending Torlesse Range, a high evaporation rate seems to disperse snowfalls more rapidly than on the shady side of the Craigieburn Range. During winter, the sun lies low in the northern sector of the sky depriving the south-facing slopes of sunlight. Shaded slopes have important implications for slope stability as it is on these slopes that shallow, permafrost-like conditions are seen to develop. Groundwater seepages (especially around unstable areas) often become frozen overnight and with little melting during the day these seepages are seen to form ice sheets up to 1 m thick on the shady side.

2.1.2 Vegetation:

Mass movement is influenced by different types of vegetation and also the ability these different types have of revegetating exposed ground. Figure 4 shows the

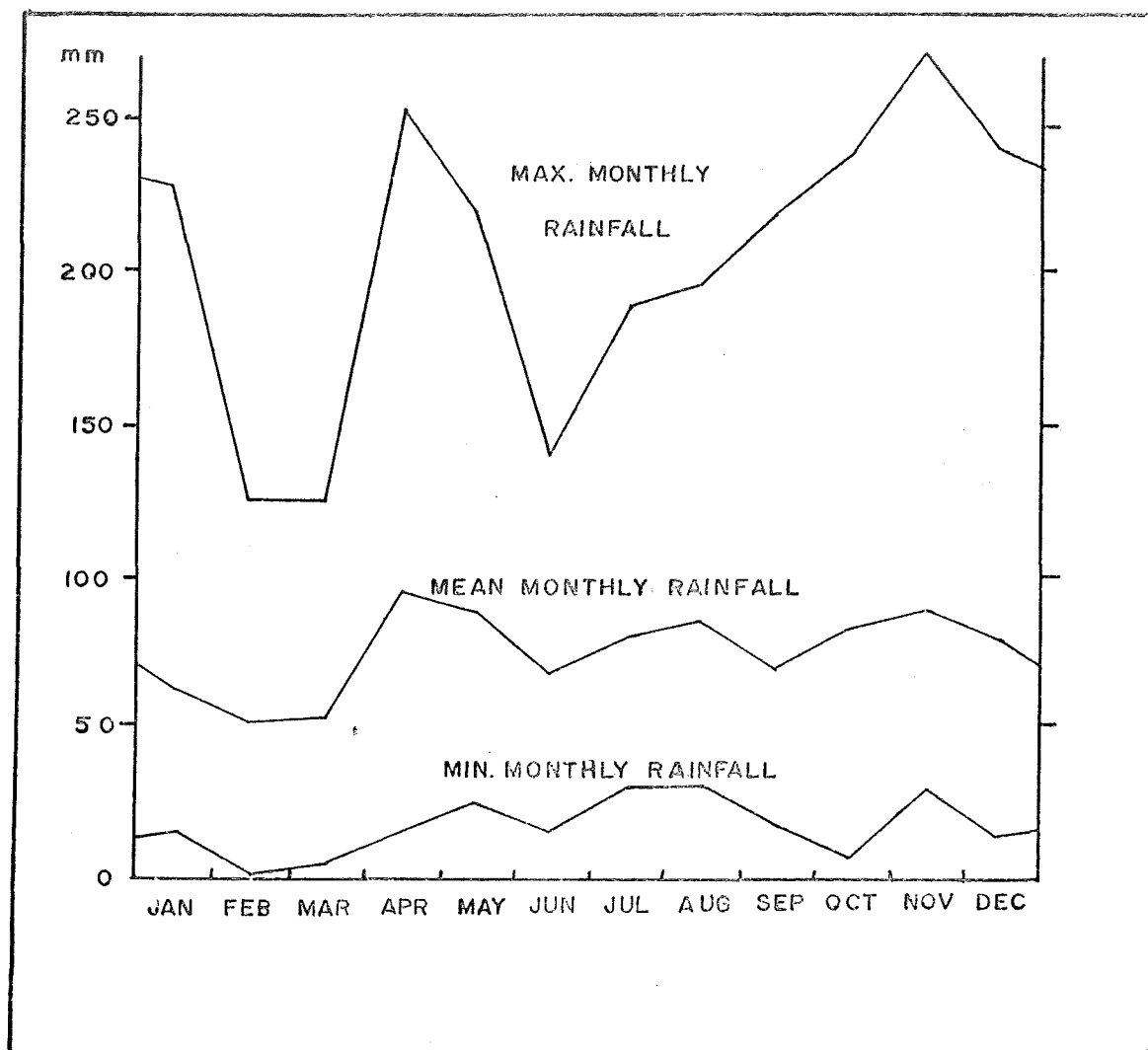


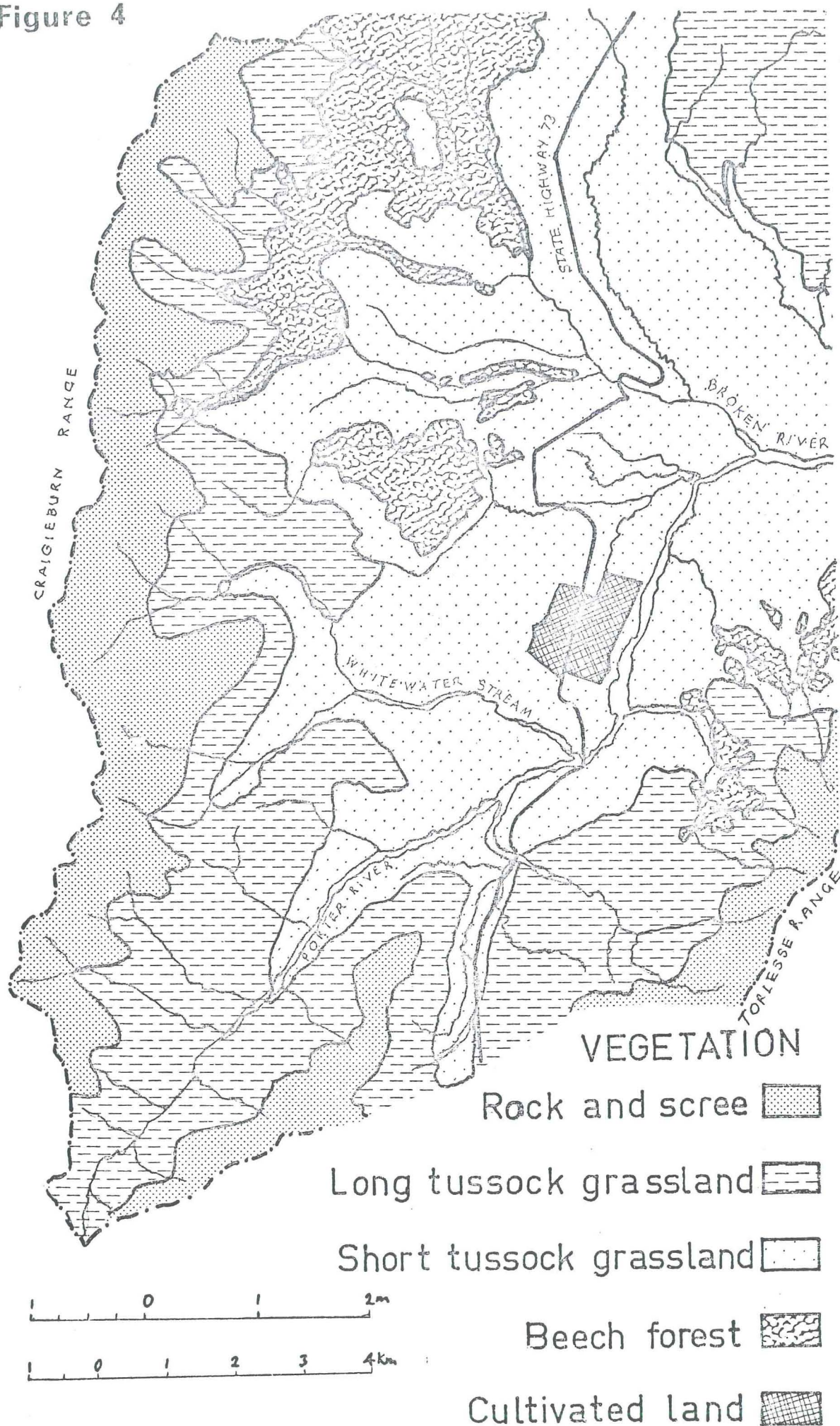
FIGURE 3:

AVERAGE MONTHLY RAINFALL CHARACTERISTICS

FOR CASTLE HILL BASIN.

Source: N.Z. Meteorological Service.

Figure 4



Compiled from air photographs and ground survey.

distribution of the major vegetation associations within the region and table 1 shows the relative proportions.

TABLE 1

Vegetative Cover of the Broken River Catchment
(source: Hayward and Boffa, 1972)

Grasslands	72%	- short tussock	61%
		- tall tussock	35%
		- scrub	4%
Beech forest	12%		
Alpine rock and scree	13%		
Riverbeds	3%		
	<hr/>		
	100%		

The existing vegetation pattern in Castle Hill Basin has been modified from the original forest cover by European burning and grazing and Polynesian era burning (Hayward and Boffa, 1972). The former forest cover is thought to have developed during the Climatic Optimum following the last glaciation (see section 2.6.2). Hayward (1967) estimates that over five times the present day forest cover existed in the Pre-Polynesian era and, from radiocarbon dates, gives an approximate date of burning at 700 years ago.

A forest cover may affect mass movement in several ways. Probably the most significant affects are in reducing the force of rainfall and retarding runoff. Other possible influences on mass movement are: a surcharge due to the weight of the trees, a delaying action in the rise of the ground water level and strengthening of the soil mass enclosed by the root system. The last factor just mentioned

seems to have influenced the mode of failure and frequency of landslides in Hogsback Stream (see plate 3). On the forested northern side of this stream landslides are of the slump or rotational slide type (see section 3.3.2) and the slip surface appears to undercut the strengthened zone of the root system. On the southern side the slopes are tussock-covered, the landslides are more frequent and appear to have a shallower slip surface than on the northern side. It is possible that other factors such as differences in bedding orientation and the amount of sunshine received also account for the differences in slope failure. It is interesting to note here that pine trees were planted, about 10 years ago, on the Utiku slip (a very large slump just south of Taihape) in an effort to retard movement. The planting has been ineffective in stabilising the area and it is now known that the slip surface is too deep-seated to be affected by the root zone (Brown, 1974).

Thus the affect of repeated burning of the forest cover is to increase erosion and decrease the resistance to mass movement. Once bare ground is exposed a considerable amount of erosion may take place before tussock and shrubs colonise and stabilise the ground surface. Castle Hill Basin, with its relatively harsh climate and high elevation, has a growing season (below 1,000m a.s.l) of only four months (Hayward & Boffa, 1972) so that revegetation is slow.

2.1.3 Hydrology:

Nine sub-catchments exist within Castle Hill Basin, six of which have their headwaters in the Craigieburn Range and the remaining three in the Torlesse Range. The



Plate 3: Vegetation and failure patterns in Hogback Stream. Forested slopes on right hand side of streams preferentially fail along deep-seated rotational failure planes which by-pass the strengthened root zones. Tussock and scrub covered slopes on left-hand side of streams fail as a flow or shallow-seated slump.

difference in runoff is indicative of the differing amounts of precipitation the two opposing ranges receive. Porter River, the dividing line between the two drainage systems, has been forced to flow almost at the foot of the Torlesse Range by the more powerful rivers flowing west (e.g. Whitewater Stream, Thomas and Broken Rivers). These rivers seem to have a greater capacity to carry debris as the main river terrace systems have developed on their banks. On the Torlesse side, the streams are steep, have yet to be graded and have large alluvial cones and fans where they enter the Porter River (see plate 2b).

The drainage pattern is clearly dendritic and must have developed on the thick glaciofluvial terraces during the last glacial advance (see section 2.6). With continuing erosion the drainage pattern has superimposed itself on the Tertiary and Cretaceous rocks leaving steep gorges where the rivers have cut through the limestone beds. Broken River, the main outlet for the basin has cut its way down through a rising Torlesse Range, incising a gorge in the greywacke.

As the rivers developed their valley morphology in a former period of much higher rainfall they are now slightly underfit for their valleys and aggradation is prevalent. With less discharge the rivers are now meandering from one side of the valley to the other (see plates 4a and 4b), laterally widening the valley floors by undercutting the already over-steepened terrace risers and thus providing ideal conditions for slumping or renewed movement of existing landslides.



Plate 4a: Broken River (just upstream from Hogsback Stream confluence) oversteepening the valley sides by meandering and lateral widening.



Plate 4b: Lateral erosion in upper Porter River. In both cases meandering is initiated by the rivers being underfit for their valleys. Local oversteepening contributes towards landsliding which enhances the meander pattern. The line segments (arrows) on the terrace to the left are recent fault traces shown closer in plates 27a and 27b. The road on the left gives access to Porter Heights skifield.

Where a meandering river is responsible for a landslide through lateral widening, the down-thrust toe of the slide is, in turn, responsible for pushing the river channel across the other side of the valley. Here the river may oversteepen and endanger the stability of the opposite bank. Thus an interacting system of migrating meanders and landsliding is developed. Such a system can best be seen in sections of Broken River and Porter River (see plates 4a and 4b).

Due to the proximity of the basin to the Main Divide, high intensity rainstorms are not uncommon and with the low storage potential of the basin (except where forested), flash floods are to be expected. Such floods are particularly destructive as they can quickly erode a far greater amount of material than that which occurs under the normal flow regime. Also, the rise in ground water level coupled with the lateral undercutting power of the river provides ideal conditions for mass movement.

2.2 GEOLOGICAL SETTING

The part of the geological environment which is of most significance to a study on slope stability is the physical nature of the sediments, i.e., the lithology of the beds and their thickness, distribution and structure. Time-related concepts such as stratigraphic relationships, mode of formation and structural history are only briefly mentioned as they have little engineering significance to the main topic.

Previous work in the area dates back to the 1870's and many workers have since studied the Cretaceous and Tertiary sediments in Castle Hill Basin. Of most interest is a study of the geology (Gage, 1970) and a study of the folds (Bradshaw, 1975) in Castle Hill Basin. Bradshaw has examined in detail the disposition of the prominent limestone strata and has subsequently modified the boundaries and structural interpretation of Gage. Gage's (1970) classification (table 2) of the Cretaceous-Tertiary sequence is retained here to provide a basis for describing the lithologies, even though the divisions have been made where breaks in deposition occur. Because of the large area (approximately 70 sq km) and the limited time available, the descriptions of the geology by Gage, as refined by Bradshaw, are accepted by the author as a basis for a general discussion on slope stability (see chapter 3). A more detailed investigation of slope stability in the Enys Formation is accompanied by a more intensive study of the geology in the Broken River-Hogsback Stream area (see chapter 4). The author's observations in this area have led to the doubt that past workers in the field may have been misled by the extensive landslide deposits which cover many slopes. As the source of error is greatest in the study area of chapter 4 the possibility of future refinement being necessary elsewhere is probably low.

The geology (see figure 23 at rear) consists of a late Cretaceous-Tertiary sequence of marine and non-marine beds deposited in a roughly triangular, complex, tectonic depression of faulted, Mesozoic basement rocks. The sequence represents an interval of marine transgression and regression

between the Rangitata-Kaikoura orogenies, which has been interrupted locally by uplift and tilting in the late Eocene (Gage, 1970).

TABLE 2

Late Cretaceous & Tertiary Sequence of
Castle Hill Basin
 (Source: Gage, 1970)

ENYS FORMATION:	marine sediments grading up to non-marine	Miocene-? Early Pliocene (Pa-?Wo)
	(unconformity)	
PORTER GROUP:	THOMAS FORMATION: marine basaltic tuffs & limestone	Late Oligocene (Ld-w)
	COLERIDGE & PUFFER FMNS	Early Oligocene (Lwh)
	(western area marine) (eastern area marine)	
	(local unconformity)	
IRON CREEK GREENSAND:	marine)	Late Cretaceous- Eocene (Mh-A)
BROKEN RIVER COAL MEASURES:	non-marine)	
	(unconformity)	

2.3 LITHOLOGIES

2.3.1 Pre-Cretaceous Basement:

The Cretaceous and Tertiary formations at Castle Hill Basin exist as infaulted outliers lying unconformably on and surrounded by non-schistose greywacke of the Torlesse Supergroup. The Torlesse basement rocks are prominent as

the higher-standing mountain ranges and are seen to consist of well indurated, dark grey sandstone, siltstone and argillite, replaced locally by tuffaceous mudstone, chert and jaspilite.

2.3.2 Broken River Coal Measures:

Lying unconformably above weathered Torlesse rocks are the carbonaceous and quartzose sediments of the Broken River Coal Measures. Gage (1970) describes this unit as consisting predominantly of unevenly stratified, current-bedded, white quartz sands, dark grey carbonaceous silts and sands, and lensoid beds of sub-bituminous coal. Thin beds and lenses of conglomerate occur at the base and near the top of this unit, the latter being interbedded with shell beds and carbonaceous sediments (Gage, 1970).

The thickness of the Broken River Coal Measures has been estimated by Gage to be about 60m at the type section in lower Broken River but local denudation has reduced this to between 0 and 30m in the south and north of the basin.

2.3.3 Iron Creek Greensand:

Gage (1970) defines this formation as:

"highly glauconitic sandy sediments overlying Broken River Coal Measures and succeeded by marls and sands of the Porter Group in Iron Creek".

Expanding on this, Gage gives the following description of the formation:

"Massive medium to coarse greyish-green glauconitic quartz sands predominate in the lower half of the formation. The upper part

consists of medium to fine current-bedded glauconitic sands with prominent bands of dark greensand."

Concretionary bands, shelly limestone beds and limonitic sands are also described in this formation.

Iron Creek Greensand is known to vary in thickness throughout the basin. In the upper Porter River, denudation has removed the beds so that younger sediments rest unconformably on basement rocks. Gage estimates about 240 m of Iron Creek Formation are present in sections on the eastern side of the basin and about 180 m of Greensand exists towards the north of the basin in Tims Stream. A minimum thickness of 275 m has also been estimated for the greensand below Whitewater Creek however there seems to be little evidence to support this. Bradshaw's (1975) more recent work suggests that the basement is not as deep in this area as Gage implies.

2.3.4 Porter Group:

This large group consists of the Coleridge and Thomas Formations which are characterised by highly calcareous strata, abundant quartz sands and volcanically-derived sediments.

Gage (1970) describes the Coleridge Formation as follows:

"A thin glauconitic mudstone bed resting directly upon Iron Creek Greensand is followed by calcareous grey muds with numerous bands of massive grey quartz

sand near the base and then by massive faintly stratified light-grey argillaceous limestone. Variations occur between sections, some for example, including a few thin beds of glauconitic mudstone and siltstone, while others consist entirely of limestone."

The thickness at the type locality in Porter River is 90 m and both greater and lesser thicknesses have been estimated by Gage from other sections.

Overlying the Coleridge Formation is the Thomas Formation; Gage's (1970) definition is as follows:

"The formation comprises a sequence of hard, buff- or cream-coloured limestones alternating with a basaltic tuff and conglomerate."

Throughout most of the area where the sinuous Thomas beds can be traced, two limestone and two tuff members exist, though local absence of one or more beds is not uncommon. The tuff members vary from fine to coarse grained, from current-bedded to evenly-bedded or laminated, and from a green to a reddish-brown colour, with abrupt lateral textural variations. The limestone members are just as variable with massive to flaggy bedding, and yellowish-white to buff coloured where tuffaceous material is included.

Eight sections through the Thomas Formation in Castle Hill Basin were studied by Gage (1970) who found that many correlation uncertainties and thickness variations exist

between sections. At the type locality in the Broken River-Cave Stream confluence the thickness is about 100 m but sections in the Thomas Formation further to the south (in Whitewater Stream and Porter River) have given values up to 150 m (Gage, 1970).

2.3.5 Enys Formation:

Gage's (1970) definition of the Enys Formation is:

"A thick succession of sediments marking a transition from shallow marine to estuarine and possibly lacustrine and fluvial conditions rests unconformably or disconformably on Porter or older beds and is overlain with strong unconformity by late Pleistocene glacial and glaciofluvial deposits."

A more complete subdivision of the Enys beds into members has been made following detailed mapping at Broken River and is described in section 4.2.

The Enys Formation begins with interbedded grey sands, shell beds and sandy limestone, resting unconformably on the Thomas beds. Above this lies a series of thick, massive, fine grained, grey quartz sands which contain occasional mud and carbonaceous laminae and iron-stained concretions. The sands are interbedded with silts, grey and green muds, interlaminated muds and silts, and occasional lensoidal, impure lignite seams. Towards the top of the sequence, a series of graded-bedded, glauconitic sands, silts and muds appear which are finally overlain by a greywacke pebble and cobble conglomerate.

Enys beds attain their maximum thickness in the deepest parts of the basin near the head of Thomas River and in Hogsback Stream. Elsewhere the beds have been peneplaned by postglacial erosion to give an incomplete sequence and hence a lesser thickness. Estimations of thicknesses vary between Gage and Bradshaw. Bradshaw (1975) estimates the Enys Formation to be as much as 1000m thick but the deepest thickness that can be inferred from his structural map (figure 5) is only about 700m. The latter depth is consistent with Gage's estimate in the same area (upper Thomas River). Elsewhere, in the Whitewater Stream area, Gage's cross-section accompanying his geological map suggests a thickness of over 900 m and the relevant text says:

".....probably more than 300 m."

Bradshaw (1975) advances an alternative interpretation for this part of the basin (see section 2.4) which suggests a thickness of 400 m. The author's own observations in Broken River-Hogsback Stream lead to a maximum thickness of 500 m (see figure 11) agreeing with Bradshaw's structural interpretation.

2.3.6 Pleistocene Glaciofluvial Deposits:

Overlying the Cretaceous-Tertiary sediments with strong angular unconformity are the Pleistocene terrace gravels of glaciofluvial origin. These gravels consists of poorly sorted, rounded to sub-rounded, greywacke-derived, sandstone and mudstone fragments with minor vein quartz and chert fragments. Grain sizes range from boulders up to 50 cm, down to silt sized particles. In general, the mean size decreases gradually with distance from the main source, the Craigieburn

Range. The gravels represent the depositional products of the many glacial and periglacial periods of the Porika, Waimaungan and Otira Glaciations (see section 2.6). They have accumulated in essentially tabular sheets with thicknesses ranging from 1 m to 28 m. Successive periods of degradation and aggradation have left these gravels as flights of terraces, which infill the basin and represent the top of the stratigraphic column.

2.4 STRUCTURE

The Cretaceous and Tertiary sediments of Castle Hill Basin lie in a complex, structural depression and represent part of the few surviving remnants of a once extensive cover. The Castle Hill Basin outlier is separated from other similar remnants at Iron Creek, Avoca, Esk and Harper valleys by denuded, higher-standing blocks of Torlesse basement rocks which owe their differential elevation mainly to Kaikouran orogenic movements.

The intensity and complexity of deformation is easily shown by the prominent homoclinal limestone ridges which meander around the basin and generally converge towards the structurally-deepest, western part of the basin. (Gage, 1970). The folds are non-cylindrical structures of highly variable profile, plunge and trend that tend to die out towards the centre of the basin. (Bradshaw, 1975). From figure 5 it can be seen that the largest structure is a west-plunging boxfold bounded by

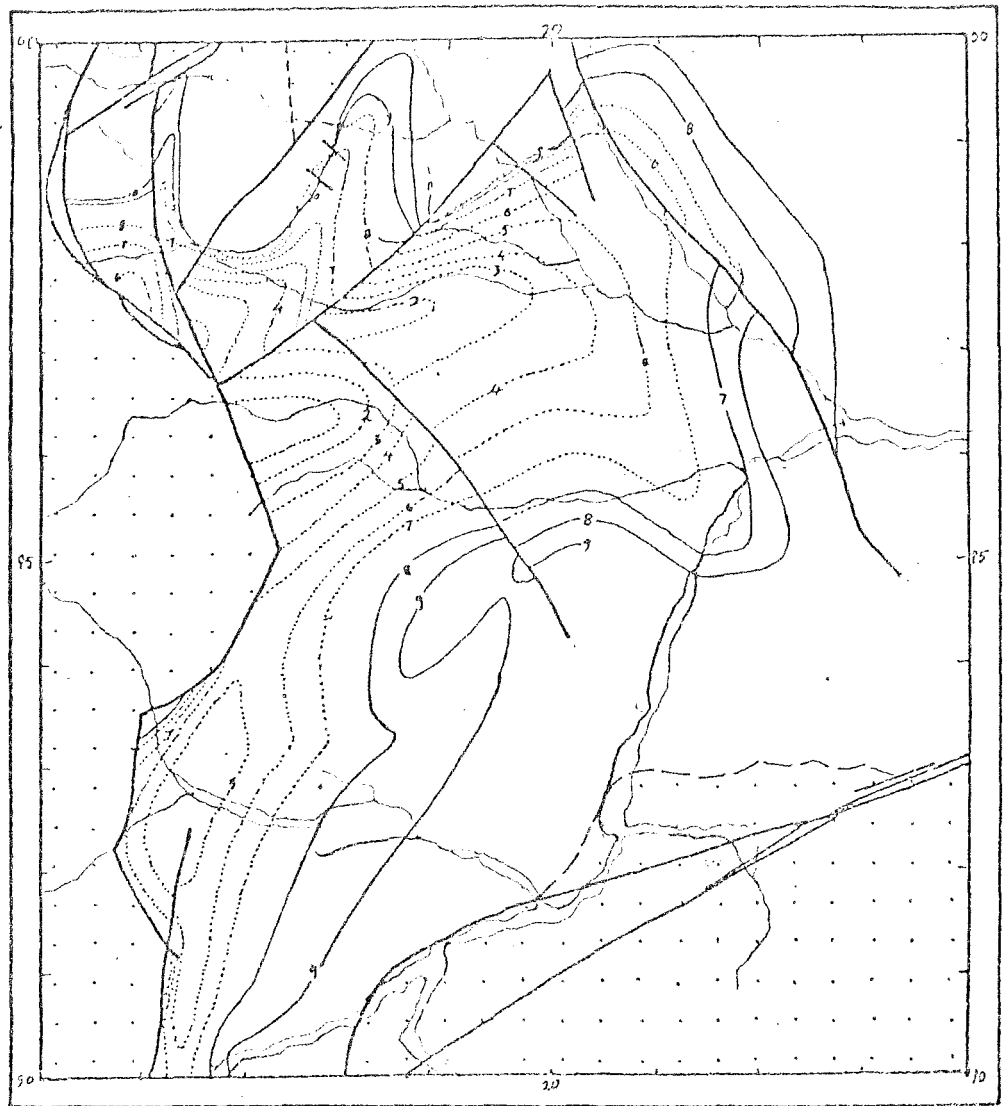


FIGURE 5 : STRUCTURAL CONTOUR MAP OF CASTLE HILL BASIN.
(Bradshaw, 1975)

Structure contours and form lines (dotted) on the upper surface of the Thomas Formation; contour interval 100m. Heavy lines represent faults, shaded area represents greywacke. Approximations of the axial plane traces of the various folds may be obtained by joining the points of maximum curvature in successive structure contours.

synformal bends at Flock Hill and Prebble Hill. To the south and northwest the folds become more angular and complex. At a few places along the Cheeseman Fault, there exist small outcrops of limestone which have been interpreted by Gage (1970) as fault-involved drag blocks. Bradshaw interprets these outcrops as belonging to the western limb of a trough centred over Whitewater Stream. The author favours the latter opinion as it is difficult to visualise intact blocks of limestone surviving shearing along a fault for distances up to 1000 m. Intensely shattered limestone in upper Porter River (see plate 27b) adjacent to the Torlesse Fault zone, indicates the effects of faulting on Tertiary limestone. It is quite possible that movement on the Cheeseman Fault is responsible, in part, for the development of the synclinal trough in the Whitewater Stream area.

When interpreting Bradshaw's structural map (figure 5) a few points must be kept in mind. Firstly the structural contours are schematic and are often drawn where limestone is thought to be or have been.

There is, for example, a 300 m height difference for the same contour between Flock Hill and the Broken River-Porter River confluence (where no limestone exists). There are also inconsistencies between Bradshaw's field observations and his structural interpretation, particularly around Hogsback Hill. Obviously there is room for alternative opinions and thus estimates of thickness of sediments overlying the limestone can only be approximate.

2.5 TECTONISM

2.5.1 Orogenic movements:

It is generally recognised (Gage, 1970 & Bradshaw, 1975) that Castle Hill Basin has undergone significant tectonism. This tectonism has been responsible for the regional basin-and-range topography, the resultant rapid erosion of the ranges, deposition in the basins and folding of the sediments. The development of Castle Hill Basin began with regional folding and faulting of basement rocks during the late Jurassic-early Cretaceous Rangitata Orogeny (Gage, 1970 & Bradshaw, 1975).

Transgressing seas laid the first of the sediments in late Cretaceous times (Broken River Coal Measures) and sedimentation continued through to Miocene times. A change in the Enys Formation from marine to non-marine sediments is attributed by Gage (1970) to uplifted basement rock being vigorously eroded nearby. This change marks the beginning of the Kaikoura Orogeny which reached a peak in the late Pliocene-early Plietocene (Gage, 1970). Kaikouran movements are considered by Gage (1970) and Bradshaw (1975) to be responsible for the major differential elevation between basin and ranges, the propagation of basement faults into the cover and the fold form. Minor orogenic movements have continued to till recent times with fresh scarps cutting Blackwater terraces (see section 2.6.2) in upper Porter River (see plates 27a and 27b) and troughs visible along parts of the Torlesse Fault. Measurements on terraces around glacial Lake Speight in the Waimakariri Valley and on terraces in the Kowhai Valley (just south of Castle Hill Basin) have been made (D.H. Bell, pers. comm.).

These measurements indicate continuing uplift about an axis centred over the Southern Alps.

2.5.2 Seismicity:

A request was made to the Seismological Observatory, Geophysics Division, D.S.I.R. for information on seismicity. The Seismological Observatory has compiled a computer file of earthquakes that have occurred between 1860 and 1976 and can retrieve data satisfying specified criteria. The information required was of two types. Firstly a list of all earthquake epicentres that have fallen within a 60 km radius of Castle Hill station (latitude 43.22°S , longitude 171.22°E) was requested. A list of 236 shocks that occurred between 1876 and 28 September 1976 was supplied and their epicentres have been plotted in figure 6. A clustering of epicentres at grid points (latitudinal and longitudinal intersections) is a characteristic of this map and merely reflects the accuracy with which earlier epicentres could be located.

All the foci are crustal and most of the earthquakes are of low magnitude. Castle Hill Basin appears notably aseismic indicating that no faults within the Basin have moved in the time span mentioned above. The nearest epicentres lie 9 km south of Castle Hill Station and are situated on the Porter Pass Fault.

The second request was for a list of earthquakes which would have had a high intensity in the area of interest. Intensity is measured on the Modified Mercalli scale and is based on ground motion and damage. In table 3 are listed major earthquakes which are estimated to have had an intensity

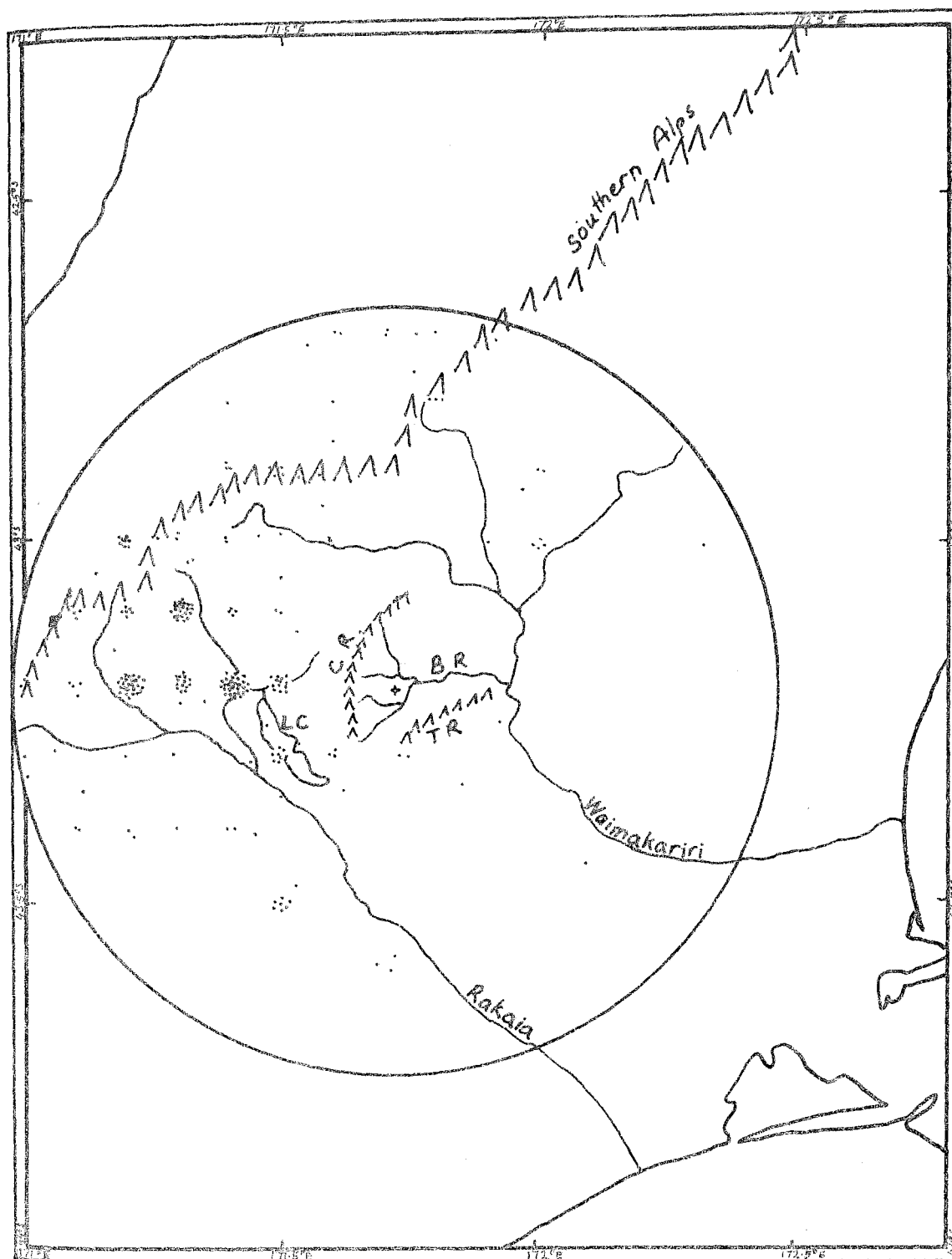


FIGURE 6

0 10 20 30 Km

EARTHQUAKE EPICENTRE LOCATIONS WITHIN 60 KM
OF CASTLE HILL STATION (+).

LC Lake Coleridge

BR Broken River

CR Craigieburn Range

TR Torlesse Range

of M.M.6 or greater. These intensities have not actually been reported from Castle Hill Basin, but have been inferred by the Seismological Observatory. As the scale is only sensitive to the nearest integer it is presumed that the values given for Castle Hill Basin have been interpolated between the nearest isoseismals for each earthquake.

TABLE 3

Estimated Earthquake Intensities for
Castle Hill Basin (1876-1976)
(Source: N.Z. Seismological Observatory)

YEAR	DATE	LAT.	LONG.	MAG. ^a		DIS. ^b	INT. ^c	
1876	FEB 26	45	171	B	F	206	6.2	
1881	DEC 04	43	172	B	F	33	8.7)	Nth Canterbury
1888	AUG 31	43	172	7	F	33	8.7)	
	OCT 23	43	172	B	F	33	8.7)	
	DEC 27	43	172	C	F	33	6.6)	
1901	NOV 16	43	173.5	B	F	147	6.9	Cheviot
1922	DEC 25	43.0	173.0	B	F	107	7.4	
1929	MAR 09	42.5	172	6.9	F	83	7.5	Arthurs Pass
	JUNE 16	41.8	172.2	7.7	F	163	8.1	Buller
	AUG 23	42.9	171.4	6.0	F	44	6.4	
	JUN 26	43.2	171.5	6.2	F	18	7.6	
	JUN 28	43.2	171.4	5.8	F	26	6.5	
1968	MAY 23	41.77	172.01	7.1	F	163	6.6	Inangahua

13 earthquakes in all

a - Richter's local magnitude scale. Some early shocks have an alphabetic classification: A (7.5 and greater), B (6 to 7.5), C (4.5 to 6), D (less than 4.5). The letter F following the magnitude implies that the earthquake is known to have been felt.

b - Epicentral distance from Castle Hill Station in Km

c - Intensity. At M.M.6 furniture is moved or overturned, weak plaster and masonry are cracked, trees and bushes are shaken. At M.M.8 there is some damage to moderately reinforced masonry, falls of chimneys, movement of frame houses on foundations, branches broken from trees, cracks in wet ground and on steep slopes.

The effect of earthquakes on slope stability is to impart transitory horizontal and vertical accelerations to the soil or rock mass. In slope stability calculations, it is normal practice in designing for seismic risks in New Zealand, to assume a maximum horizontal ground acceleration of 0.1 that of gravity. Although this approach grossly oversimplifies the likely ground behaviour it does result in a large driving force with a subsequent conservative factor of safety (see chapter 5 for a discussion on slope stability calculations).

A total of four earthquakes, of an intensity sufficient to cause slope damage, in a century indicate that seismicity could be a significant factor in landslide development. However, several other factors (direction and duration of shaking, existing static factor of safety and the pore pressure response of the material) are known to influence the extent of seismic slope failures (Seed, 1967). There is no evidence to suggest that in the last century, fault movement within the basin has been directly or indirectly responsible for landsliding.

2.6 GEOMORPHOLOGY

2.6.1 Geomorphological Setting:

The geomorphological development of Castle Hill Basin began with the main Kaikouran Orogenic phase. It was during that phase that the complex folding and faulting of the Cretaceous-Tertiary cover and the characteristic basin-and-range topography of the region was developed. During the Pleistocene glaciations, the uplifted greywacke basement

deposited in the basin and subsequently modified to form flights of terraces. It is these terraces which form the most prominent feature in Castle Hill Basin and provide the most marked contrasts in slope stability. The terrace surfaces are the most stable slopes within the basin whereas the steep terrace risers are commonly unstable (movement arising in the latter slopes often involves a small portion of the former however).

2.6.2 Pleistocene River Terraces:

Two important phases of erosion have occurred to form the terraces. The first phase is associated with glacial times when large glaciers in cirques and neves were actively eroding the bedrock. Evidence for past glaciation in Castle Hill Basin has been recorded by Speight (1938, vide Breed, 1958), Breed (1958), Gage (1958) and Chinn (1975) who note the prominent cirque-like basins on the upper Craigieburn Range (see plate 2a) and the presence of morainic dumps in the headwaters of some of the tributaries of Broken River (see plate 7).

The second phase of erosion occurred during the interglacials and was probably more active as the glaciers were rapidly retreating. The outwash gravels deposited in tabular sheets from the first phase of erosion were extensively degraded to leave incised valleys with steep sides.

Pleistocene glacial history has been well documented for the nearby Waimakariri Valley (Gage 1958) and table 4 outlines the advances of the Waimakariri glaciers in terms of New Zealand glacial stages.

TABLE 4

Advances of the Waimakariri Glaciers
(Taken from Geology Dept Museum, Canterbury University)

Poulter Advance		Interglacial)	
		Short Interstadial)	The Otira
	II)	Glaciation
Blackwater Advance	I	Brief recession)	
		Interstadial)	
Otarama Advance		Relatively long interglacial		
Woodstock Advance		Long interglacial		The Waimaungan Glaciation
Avoca Advance				The Porika Glaciation

Breed (1958) correlated the Castle Hill Basin terraces with the Waimakariri Valley terraces (via the Broken River gorge). His work has been extended by Chin (1975) who studied late Quaternary snowlines and cirque moraines in the Waimakariri catchment. Chin found evidence for three other minor advances but the resultant terraces are of insignificant size and distribution in Castle Hill Basin to be of importance to slope stability. Breed's descriptions of the terraces from the three main glaciations have been summarised here to account for the geomorphic development of the area.

The oldest glaciofluvial deposits in Castle Hill Basin belong to the Avoca advance and have been attributed by Breed to the Porika Glaciation. This major advance has left faintly discernible benches around the basin and scarce outwash deposits around Broken Hill (to the northwest of the basin) and

basin to have been a huge neve during the Porika Glaciation while only small glaciers and snowfields existed in the surrounding ranges during subsequent glaciations.

Active downcutting during the long interglacial between the Porika and Waimaungan Glaciations has led to a 105 m height interval between the Avoca and Woodstock surfaces. About 28 m of gravels were deposited during the Woodstock advance (Breed, 1958) which is best represented by Long Spur (see plate 5), between Thomas River and Hogsback Stream. The bulk of the remaining terraces have been attributed by Breed to the Otira Glaciation which can be clearly differentiated into three major advances, namely Otarama, Blackwater and Poulter.

Following the Woodstock advance an interglacial period led to a degrading of the basin by about 60 m. The most prominent Otarama terrace is given by Breed as lying at the foot of Long Spur (see plate 5) with smaller remnants in Cave Stream, Flock Hill Stream and on the Porter-Whitewater divide (see plate 23a).

Extensive degradation during the Post-Otarama deglaciation removed most of the terraces in the basin and considerably lowered the bedrock surface. The degradation was followed by a succession of two sub-advances, collectively known as the Blackwater advance, which produced the most extensive and widespread terraces in the basin. About 30 m separates the Otarama surface from the upper Blackwater surface and there is a 10 m height difference between terraces of the two Blackwater advances. The most prominent



Plate 5: Glaciofluvial terraces at the junction of
Hogsback Stream (in shade) and Broken River

- A Avoca surface
- B Woodstock surface (Long Spur)
- C Otarama surface
- D Blackwater I and II surfaces
- E Approximate level of Poulter surface

of the Blackwater terraces is that on which Castle Hill homestead is built (see plate 6) and that on which the Canterbury Winter Sports club road is placed (see plate 7) (Breed, 1958). The terrace gravels reach a thickness of 28 m near the Broken River bridge.

The last major advance is not very well represented in Castle Hill Basin (Breed, 1958) but is well preserved in the nearby Waimakariri Valley (Gage, 1958). The best evidence for a Poulter surface is described by Breed as that where the Canterbury Winter Sports Club road joins the state highway by the Broken River bridge (see plate 5). This surface is 60 m lower than the younger Blackwater terrace and is of limited distribution and thickness.

Several other small and discontinuous terraces can be found below the Poulter surface, especially around the Broken River bridge area. These have been attributed by Chin (1975) to minor advances and other climatic effects (e.g. increase in average annual precipitation).

2.6.3 Other Geomorphic Features:

The present day landscape has been only slightly modified from a Poulter landscape by erosional, depositional and man-induced agencies. Perhaps the most significant influence on the geomorphology since the last glaciation has been the active landsliding which has imparted a characteristic appearance to the basin. A full description of this phenomenon along with its relation to the geology and other intrinsic factors will be presented in the next chapter.

The limestone beds of the Thomas Formation have resisted the degradation phases of the interglacial periods and are now left elevated above the peneplain surface. After a partial reburial with terrace gravels the beds now stand out as hills or cuerdas (see plate 7) in many places (for example; Flock Hill, Castle Hill, Prebble Hill and Hogsback). Where the rivers have had to cut their way down through the limestone, steep-sided gorges have formed with predominantly stable slopes (see plate 8).

Where the limestone has been exposed for a lengthy period, such as during the interglacial periods (for example; Castle Hill and Flock Hill), a Karst-like topography has developed. Here fluted limestone tors are exposed and deep solution channels have formed along joints and bedding planes. Solution cavities are seen to be quite widespread throughout the limestone, often linked to the surface by sinkholes. Several underground stream channels are known to exist, the most prominent of which is Cave Stream where the stream has abandoned the former surface channel to follow a solution-enlarged joint system (see plate 8).

Historical modification of the landscape by man and man-induced agencies is slight. Apart from the indirect effects of man-induced changes in vegetation (see section 2.1.2) the only appreciable impact on the geomorphology has been the construction of State Highway 73. The highway does not seem to have affected slope stability; even the cuts on the already over-steepened banks near the Broken River Bridge have remained stable. Several quarries and borrow pits have been

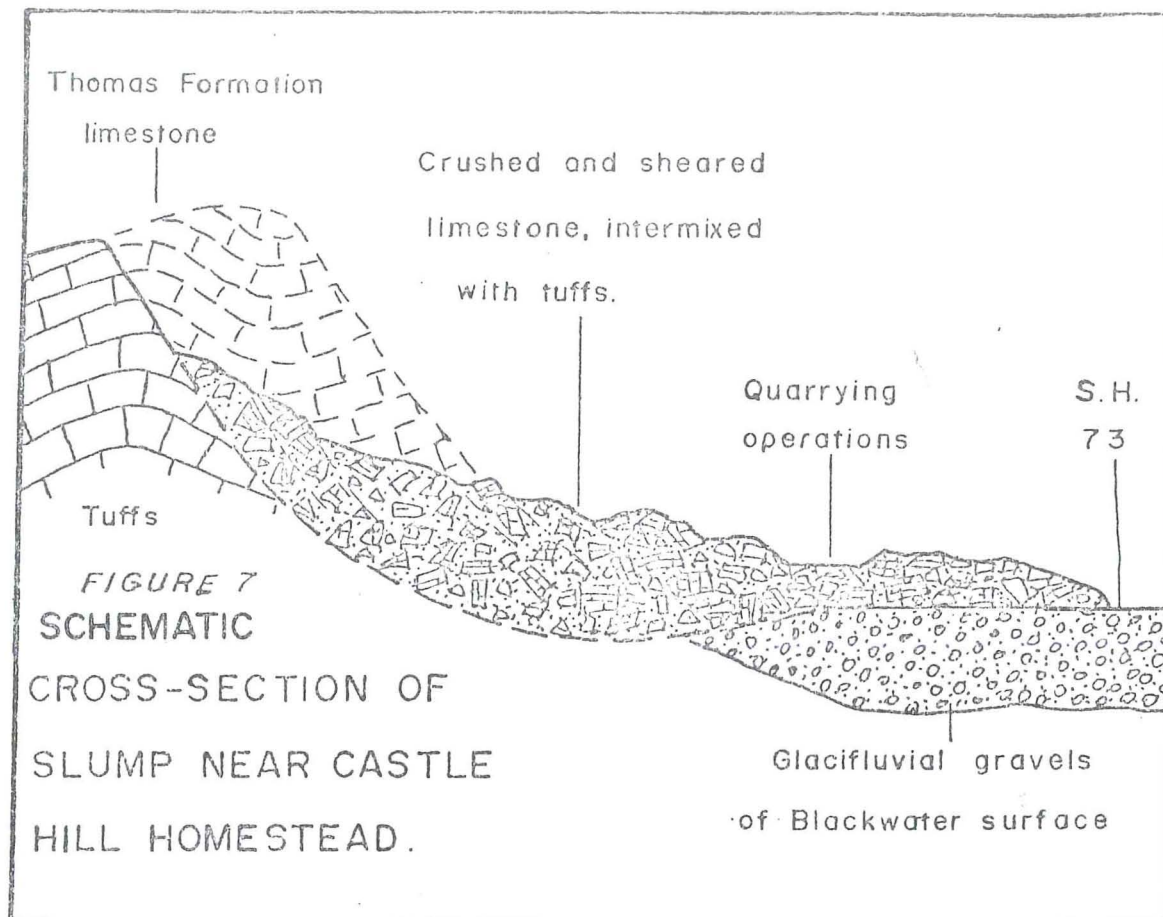


Plate 6: Limestone quarry in what appears to be an old landslide (outline dotted) developed in the Thomas Formation. See figure 7 for an interpretation of the cross-section through the landslide. Castle Hill homestead is situated on Blackwater I terrace just out of picture to left. Note limestone tors on crest of Castle Hill towards upper left.



Plate 7:
 Steeply-dipping limestone beds of Hogsback Hill. Remnants of a fossil slide in the sediments in front may be inferred from the hummocky topography. Toe of slide has been buried by terrace gravels of Blackwater 1 advance. Behind Hogsback Hill, terminal moraines have been identified by Breed (1958) in Hogsback Stream (left) and Tims Stream (right). Cross marks hummocky terrain attributed by Breed to a debris avalanche.



Plate 8: Broken River flowing through limestone gorge just above confluence with Thomas River. Note the outlet of Cave Spring to right.

excavated in the limestone and the largest of these is in a very old landslide near the Castle Hill homestead (see plate 6). Quarrying is facilitated by the crushed nature of the disturbed limestone (see figure 7 for an interpretation of the cross-section).

CHAPTER 3

GENERAL DISCUSSION OF SLOPE
STABILITY IN CASTLE HILL BASIN3.1 INTRODUCTION

An initial survey of Castle Hill Basin was carried out by stereoscopically viewing the appropriate aerial photographs to pinpoint possible areas of slope instability. The aerial photograph survey was proceeded by a visit to each area to verify the presence of a landslide and to make observations on its nature. Over 60 landslides have been mapped and they are presented with respect to their geology in figure 23 (at rear).

3.2 CLASSIFICATION OF LANDSLIDES

Within a certain lithology, slides are seen to have varying degrees of development and stabilization and also to have moved at times ranging from recent to pre-historic times.

Contemporary (generally active) landslides are easily recognised by their arcuate configuration, uneffaced head

scarp, trees tilted or with snapped trunks ("drunken forest") tension cracks, swamps in back tilted depressions, boulder fields, frequent groundwater seepages and diverted stream channels - often cutting into the toe to form a steep scarp. Some contemporary landslide features are shown in plates 9a to 9h.

Dormant landslides are those that have formed in historic times and have since been modified by rainwash, stream erosion and the growth of vegetation. Although traces of their last movement are not readily discernible, the causes of their origin remain, so that movement may be renewed. Drainage patterns have started to develop which easily incise themselves into the disturbed material. Small scarplets within the main body of the slide indicate that the mass is not yet fully stabilised. Views of dormant landslides are shown in plates 10a and 10b.

Fossil landslides are characterised by a concave upper half and a convex lower half with ubiquitous hummocky topography. The old landslide site is now a small stream valley whose tributaries have done much to modify the typical landslide shape. A distinctive vegetation association has developed within the slide, often with a higher proportion of woody shrubs (e.g., matagouri, sweet briar and box thorn). Soil creep both on the surrounding hillside and in the landslide area has further modified the fossil slide making recognition difficult and in some cases dubious. Three examples of fossil landslides are shown in plates 11a to 11c.

Plates 9a-9h: Some contemporary landslide features.

Plate 9a: Arcuate configurations (see also plate 13).

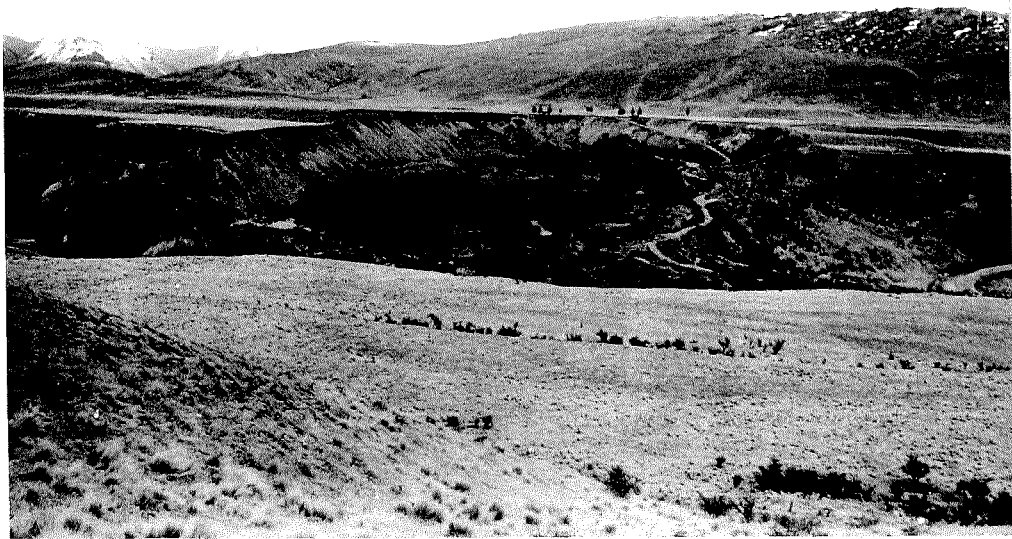


Plate 9B: Rear scarp that is largely unaffected by erosional processes and revegetation.

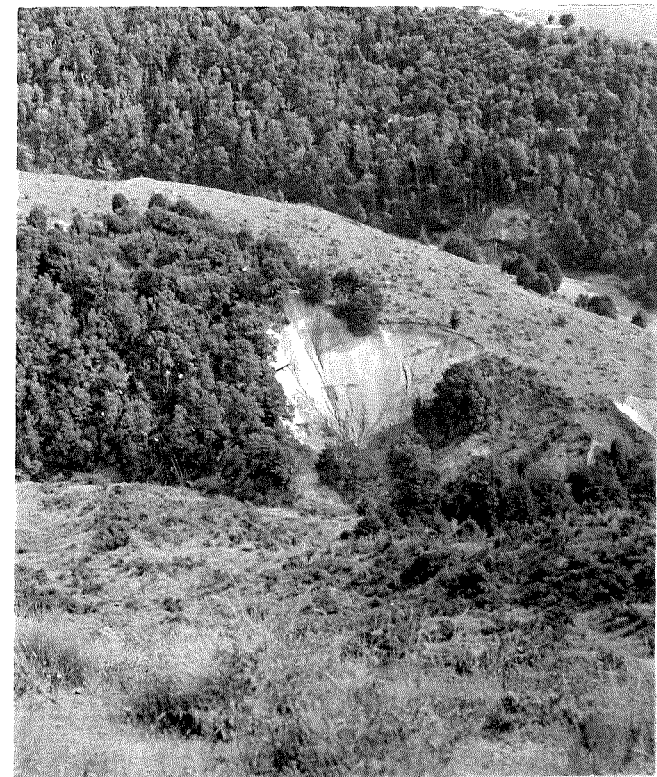


Plate 9d: (left) Swamps or ponds often form in the undrained depression formed between a rotated slump mass and the rear scarp. See also plates 21a and 21b.



Plate 9c: (right) Slumps developed on forested terrace risers (e.g. north bank of Hogsback Stream) disrupt the forest cover resulting in snapped trunks, and uprooted and tilted trees (drunken forest).



Plate 8a: (right) Boulder fields are often found towards the rear of many of the larger landslides. The boulders originate from the terrace gravels and are transported and deposited in irregular heaps by landslide movements.



Plate 9f: (left) Eroded toe of a large landslide that has traversed the valley floor (Broken River). The toe effectively buttresses the remaining landslide mass until the support is removed by erosion.

Plate 9g: (right) Blocks rotated by landslide movement show a backtilting or opposition of general slope angle and direction. Photograph shows slope in foreground disrupted into a series of backtilted steps by landsliding. See also plates 23a and 23b for more views.



Plate 9h: (left) Failure surfaces are sometimes seen where rivers (in this case Hogsback Stream) are rapidly eroding their banks. Failure surface (arrowed) consists of occasional terrace gravels and plant debris set in an argillaceous matrix.

Plates 10a; Two views of dormant landslides in Broken River
(Flock Hill in background). See also plate 20.



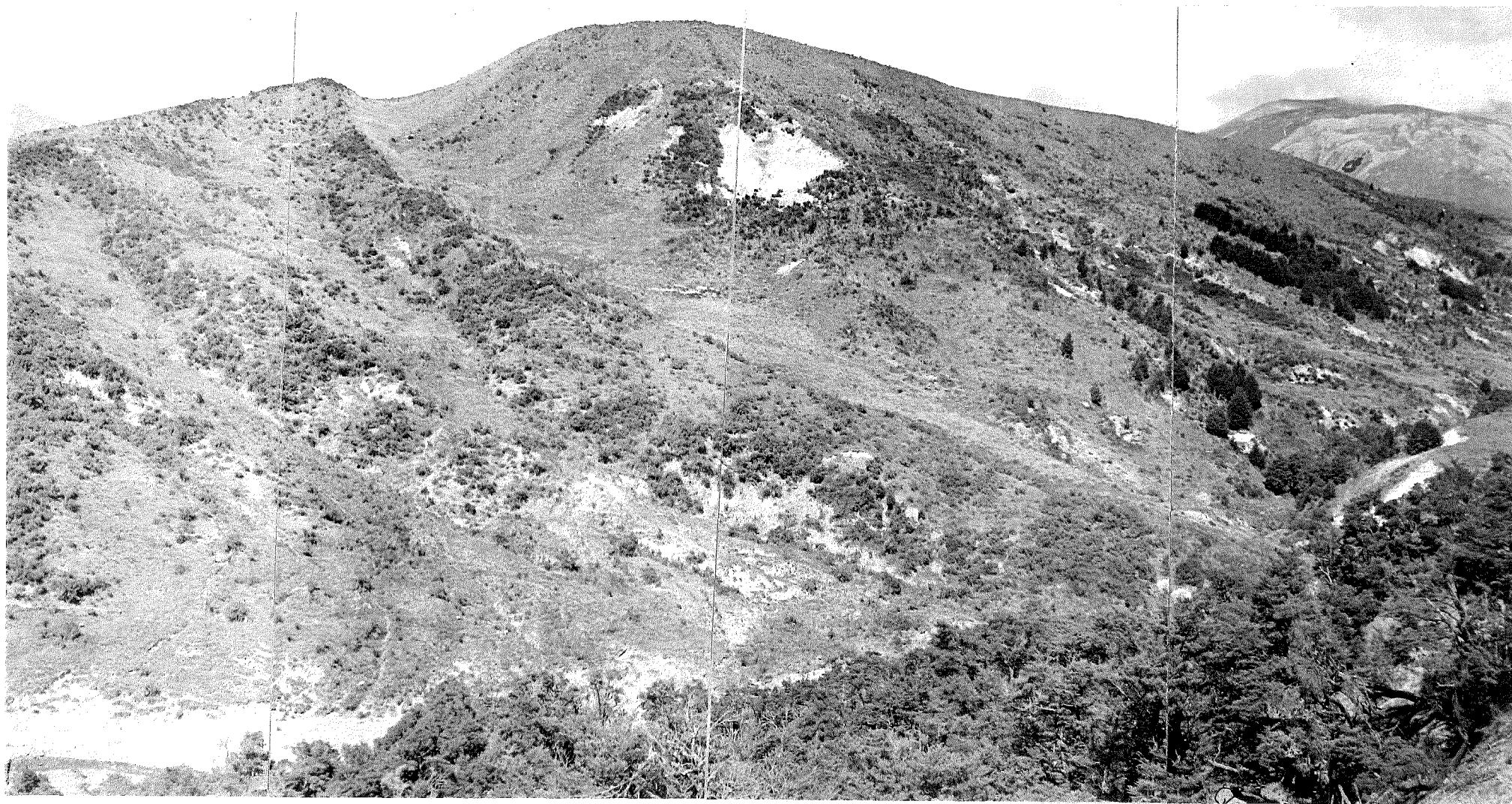
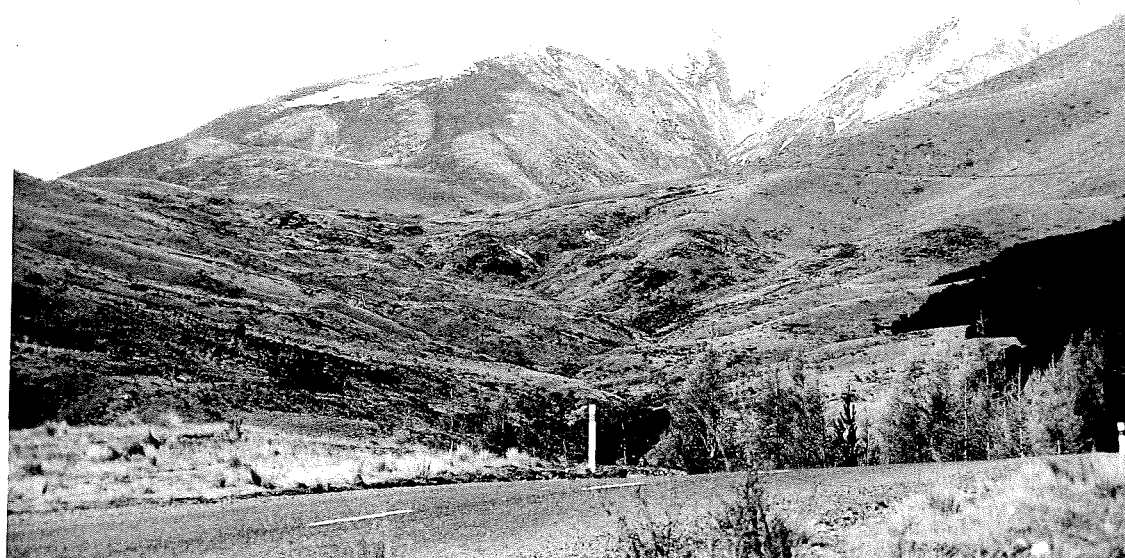
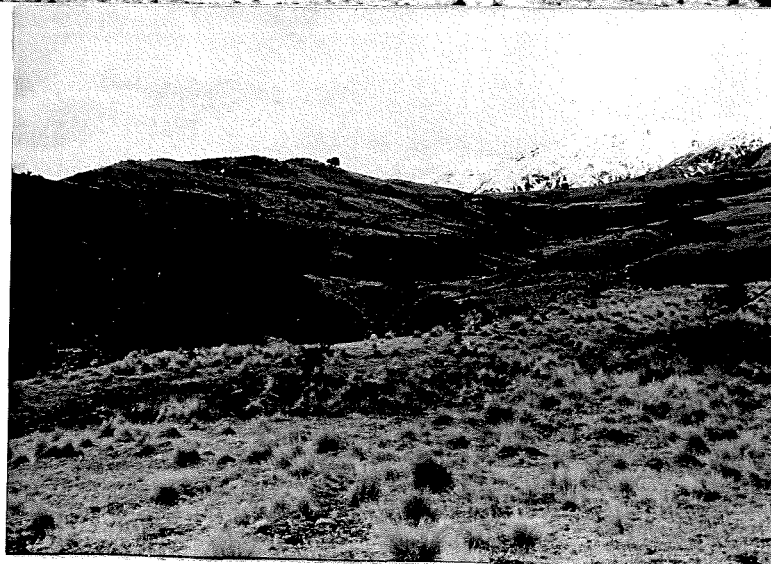


Plate 10b; Panoramic view of dormant landslides in Hogsback Stream and tributary to south.
Note sand outcrop in upper centre where reVegetation has been hindered by groundwater
flushing surficial debris away.



Plates 11; Note the hummocky topography, modification by stream erosion and soil creep, and preferential colonisation by woody shrubs; characteristic features of fossil landolides.

3.3 TYPES AND DISTRIBUTION OF LANDSLIDES

The term landslide has so far been used in a broad generic sense and is here taken to include a generally accepted, four-fold classification comprising falls, slides, flows and complex movements. A fifth class of mass movement will also be mentioned to include the superficial, mass wasting processes which play an important part in natural slope degradation.

3.3.1 Falls:

Falls occur where blocks of soil or rock are left unsupported either laterally by a steep slope or below by an overhanging slope. The soil-like sediments at Castle Hill Basin tend to form massive unjointed beds that are more effected by other forms of slope degradation than by block falls. Thus very steep or overhanging slopes are seldom seen except on a very small scale as in river banks. The only slopes in the basin that are steep enough to promote falls are the edges of the limestone escarpments and occasionally on greywacke faces. Ice wedging in cracks associated with cooler climates is thought to be responsible for most rock-falls. Differential weathering and slope degradation between the limestone and the tuffs would give rise to overhanging conditions in the limestone. On failing there would be a limited amount of free fall, followed by some leaping, bounding or rolling before the movement, finished with some sliding. Prebble Hill escarpment (see plate 12) has had many blocks fall off it in the past.



Plate 12; Prebble Hill limestone escarpment with its numerous block slides. Some have travelled as far as the river, involving both falling and sliding movements.

Plate 13; Aerial view of the Broken River bridge slide with its ubiquitous arcuate features. Although failure is thought to be along planar surfaces overall movement is rotational in nature.



3.3.2 Slides:

Slides can be further classified according to the surface of failure; those with a curved surface are known as rotational slides or slumps, and those with a surface approximately planar are termed translational slides.

(a) Rotational Slides: In rotational slides, the failure plane is usually circular and deep-seated (although this is not always the case). Wilun and Starzewski (1972) report that circular failure planes are characteristic of slumps in uniform clay or shale, whereas non-circular failure planes are commonly found in overconsolidated and non-homogeneous clays.

Slumps are the most widespread mass movement feature within the younger rocks of the basin and occur in all the formations except the Thomas Formation and the glaciofluvial gravels. A landslide involving a large proportion of Thomas limestone just north of Castle Hill homestead (see plate 6) is thought to have a curved failure surface. Large amounts of crushed limestone are seen in a quarry and access road within this landslide where the crushed rock is recovered. It is thought that the landslide primarily developed in the underlying tuffs and brought down with it a large cap of limestone (see figure 7 for a possible interpretation of the cross-section).

Apart from the fossil landslides, the slumps in the formations underlying the Thomas rocks all appear to have a steeper and less-curved failure surface than those in the younger Enys Formation. A possible reason is that the older

materials are slightly more indurated and consolidated and hence able to mobilize a greater shearing resistance against sliding. Slumps in the Enys Formation are particularly common, especially where topography and geology are favourable. Where these conditions are continuous along a section of river bank, a complex series of interlapping slumps of different ages and degrees of development may be found (as in Hogsback Stream - see plates 10b and 24). The contemporary slumps are distinguishable by their ubiquitous arcuate features (scarps, pressure ridges, tension cracks and toe) which are characteristic of the rotational slide (see plate 13).

(b) Translational Slides: Wilun and Starzewski (1972) describe translational slides as resulting from the presence of a heterogeneity, usually in the form of a weak soil layer or structural discontinuity, located at shallow depth beneath the slope. The planar failure surface is usually parallel to the surface and the overlying material moves as a slab or block with little distortion of the sliding mass.

Translational slides occur under two different circumstances at Castle Hill Basin. In the first instance, block slides may be found below the limestone escarpments. Here fallen blocks of limestone continue their movement by sliding on the superficial weathered layer of the underlying tuffs and Coleridge Formation (see plate 12). The second case involves slabs of weathered soil sliding at the interface between weathered and unweathered material. These slab slides are small and infrequent and are really only an extension of some of the mass wasting processes (see section 3.3.5). It is probable that small blocks

... of the soil along steeply inclined

joints or fissures but they are not of a large enough magnitude or frequency to become noticeable as a prominent form of mass movement.

3.3.3 Flows:

The form taken by the moving material in flows resembles that of viscous fluids and the name implies that water plays a major role. However, the material may range from dry rock fragments to a saturated plastic clay (Varnes, 1958). Slip surfaces are not as well developed as in slides and the boundary between moving and stationary material is often diffuse.

Varnes (1958) contends that at the time of flow, the material must be unconsolidated, implying that the heavily overconsolidated Castle Hill Basin sediments would not flow. However many slope failures with a flow-like form are seen to have developed, especially in the upper Enys Formation. These landslides are more elongate and have a smoother topography than the translational or rotational slides. Movement appears to be distributed unevenly throughout the material of the moving mass rather than occurring solely along the boundaries of blocks and wedges as in falls and slides. The rate of movement is slow and discontinuous, scarps are seldom seen and vegetation covers the moving mass (see plate 14). It is thus thought that flow movement does not originate in the consolidated ground mass but rather in a superficial layer of weathered material, landslide debris, rock fragments, etc..

Two types of flow movement, defined by Skempton and Hutchinson (1969) as earthflow and mudflow, are relatively common in Castle Hill Basin. The argillaceous Greenmud



Plate 14; Earthflow
in glauconitic muds
of the Enys Formation
at Hogsback Stream.

Plate 15; Debris avalanche in greywacke
Leith Hill. Beech forest on toe
exhibits a typical 'drunken forest'
appearance.



member of the Enys Formation (see section 4.2.7) is particularly prone to failure by flow mechanism. The earthflow form merges into the mudflow form with decreasing particle size and increasing water content. These conditions are usually found at the toe of landslides and earthflows in particular where rainwash (see section 3.3.5) and weathering have reduced the debris to ill-sorted remnants set in a clayey matrix. In Hogsback Stream (see plate 10b) earthflows have developed in what is suspected of being a series of former slumps. The landslide debris has been softened and weathered with considerable structural breakdown to form an unconsolidated mass that renews movement by flowing.

Mudflows may be found at the base of landslides in Hogsback Stream, Broken River (just upstream of Hogsback Stream confluence) and upper Porter River. They are typically small and localised, have a glacier-like form and are able to flow at very low angles. Rates of movement appear to be related to rainfall and the author found fresh signs of renewed movement, tension cracks and compression folds in the disrupted grass cover in the course of field work during the winter. During prolonged periods of dry weather, the flow dries up into a series of discontinuous chunks separated by tension cracks and scarplets. The cracks must facilitate entry of water at the end of the dry spell and the material would easily become quickly saturated, soften and flow.

A third form of flow movement, although rare, deserves some mention. This is the rockslide or rockfall avalanche

which is described by Varnes (1958) as initiating as a large rockslide or rockfall which later turns into a rock fragment flow of unusually high velocity and volume. The rapid movement and large distance travelled is attributed by Varnes to a large amount of internal interaction between the rock fragments and to highly compressed air, entrapped by the fragments, providing internal lubrication. Despite the lack of evidence and the difficulty in visualising such processes, this theory has been the only one available until quite recently. Habib (1975) has suggested that the unusual mobility associated with rock avalanches may be due to the production of gaseous pore pressures. When a rock mass slips, local heating of the slip surface transforms pore water into water vapour which buoys up the sliding mass in a manner similar to that of the hovercraft principle.

In the nearby Arthurs Pass National Park, Chin (1975) and Speight (1932) relate rock avalanches to the 1929 Arthurs Pass earthquake. A particularly good example is seen in the west branch of the Otehake River (NZMS1 map S59, Arthurs Pass) where a large crater can be seen on the side of Falling Mountain and a trail of debris extends down valley for 4 km. In Castle Hill Basin, at least two such avalanches can be seen on the Craigieburn Range. Although not of the magnitude of the Arthurs Pass rock avalanches they have similar characteristics. A distinguishable rock avalanche has originated from Leith Hill (see plate 15) and fallen towards Thomas River, coming to rest on Blackwater terraces. Although forested, the toe of this avalanche readily stands out from the air as a series of concentric

troughs and ridges. A similar landslide investigated by Breed (1958) perhaps explains the hummocky terrain behind Hogsback Hill (see plate 7). However, the lack of a suitable source area and the manner in which the material chose to come to rest atop a ridge casts serious doubt on this contention. A hypothesis advanced by Speight (vide Breed, 1958) that the hummocky area was a moraine was discounted by Breed because it was on the wrong level for any of the glacial advances.

3.3.4 Complex Movements:

Complex movements are a combination of other forms of mass movement, either occurring together as different parts of a landslide or at different stages of development. Thus a block of limestone involving falling and sliding movements would be classified as a complex movement.

Where a plane of weakness lies at a moderate depth beneath the surface a compound slide of partly rotational and partly translational character will develop. The superficial features of such a landslide closely resemble those of a slump but their greater length often indicates that a significant portion has slid along a planar surface. As the planar portion of the failure surface approaches a shallower depth the failed material more closely approximates a translational slide even though small rotational portions of the slip surface remain at the rear scarp and toe. A large slide situated just upstream from the Broken River highway bridge (see chapter 5) is thought to be a compound rotational-translational slide and it is quite likely that many others

translational-flow and rotational-flow movements are also thought to exist. Whether a distinct slip surface or a zone of shearing is developed is difficult to say, but superficially, a large part of the slide appears as a flow.

Quite often the landslides that have developed in the Enys Formation display a slump form in the initial stages then develop into a flow form as the root area becomes exhausted. This phenomenon is due to the initial slump movement destroying any pre-existing discontinuities such as bedding or joints, and remoulding the material to a plastic state. Renewed movements heighten this effect so that several mudflows may push forward as frontal lobes, away from the toe.

3.3.5 Mass Wasting:

Mass wasting is a comprehensive term covering all aspects of superficial mass movement. Although small compared to landslides, mass wasting movements are nevertheless significant as they can move far greater amounts of material in the course of time. Two classes can be distinguished on the basis of speed of erosion and both act semi-continuously depending on the amount of water available.

(a) Soil creep: The first class is soil creep which is characterised by the slowness in which the material moves. Soil creep occurs on most soil-covered slopes but is more active on the slopes above the Blackwater terraces and in particular the shady side of hills (see plate 16).



Plate 16; Soil creep on Gorge Hill (centre)



Plate 17; Badlands topography in Coleridge Formation sands.

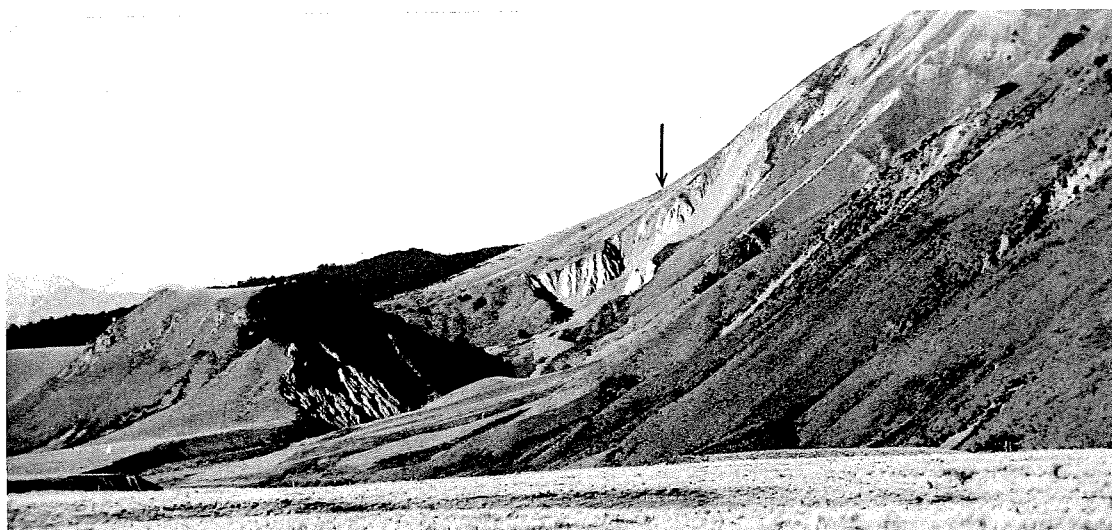


Plate 18; Incised gullies forming along Torlesse fault zone (arrowed).

It is these slopes that have been exposed to weathering and frost heave the longest. During cooler climates, when interstitial ice in the soil cover would have been prevalent, the soil creep form would have changed to solifluction. Although frozen sub-soil conditions were found in the winter of 1975, it is doubtful if solifluction exists today. An equivalent process in rocks, termed talus creep, occurs on the extensive screes that drape the surrounding greywacke mountains.

Other observable, slow, mass wasting agencies are the degradation of slopes by frost heave and cyclic wetting and drying. These processes are seen to actively erode bare or scantily-vegetated slopes at a surprising rate. Tests on the Enys Formation muds and silts (see section 4.6) show that they mostly have a very low slake durability, and therefore tend to erode quickly.

(b) Rain wash: The faster mass wasting agencies are associated with high intensity rainstorms and include the processes of slope-wash and rill-wash. Slope-wash is the rapid erosion of a superficial sheet of weathered material which retreats essentially parallel to the slope. Rill-wash on the other hand is the formation and rapid erosion of gullies and appears to be a deeper development of the latter form. Erosion by these mechanisms attacks any unvegetated ground and can be so severe that the resultant landform with its arcuate scarp may easily be confused with that of a landslide. Where the tuffs and sands of the Coleridge Formation are exposed, rill-wash gives rise to a badlands topography (see plate 17).

Slope-wash and rill-wash are highly erosive in the crushed and shattered greywacke near the Torlesse, Craigieburn and Cheeseman Fault zones. In particular, parts of the Torlesse fault zone are being deeply eroded to form incised gullies with near-vertical headwalls (see plate 18).

3.4 RATES OF DEGRADATION

It is interesting to note here how the different rates of movement of the various mass movement agencies affect slope retreat. No quantitative measurements have been made of rates of soil creep, rain wash, landslides, and solution but by comparing observations it is possible to postulate on the relative rates of slope degradation.

Mass wasting processes are considered to be very active in the Castle Hill Basin environment. Overseas estimates of slope retreat (Young, 1974) show a concurrence of results for similar environments and slope angles; the effect of parent material being negligible. Rates of 20 mm (measured perpendicular to ground level) per 1000 years for soil creep and 1 to 10 mm/1000 years for rain wash have been given by Young. The rate for soil creep seems reasonable for Castle Hill Basin but the rate for rain wash is probably several orders of magnitude too low.

Solution of limestone is minimal in comparison to the rate of scarp retreat through block falls. The overhanging conditions necessary for block falls are created by the relatively rapid mass wasting in the underlying sediments.

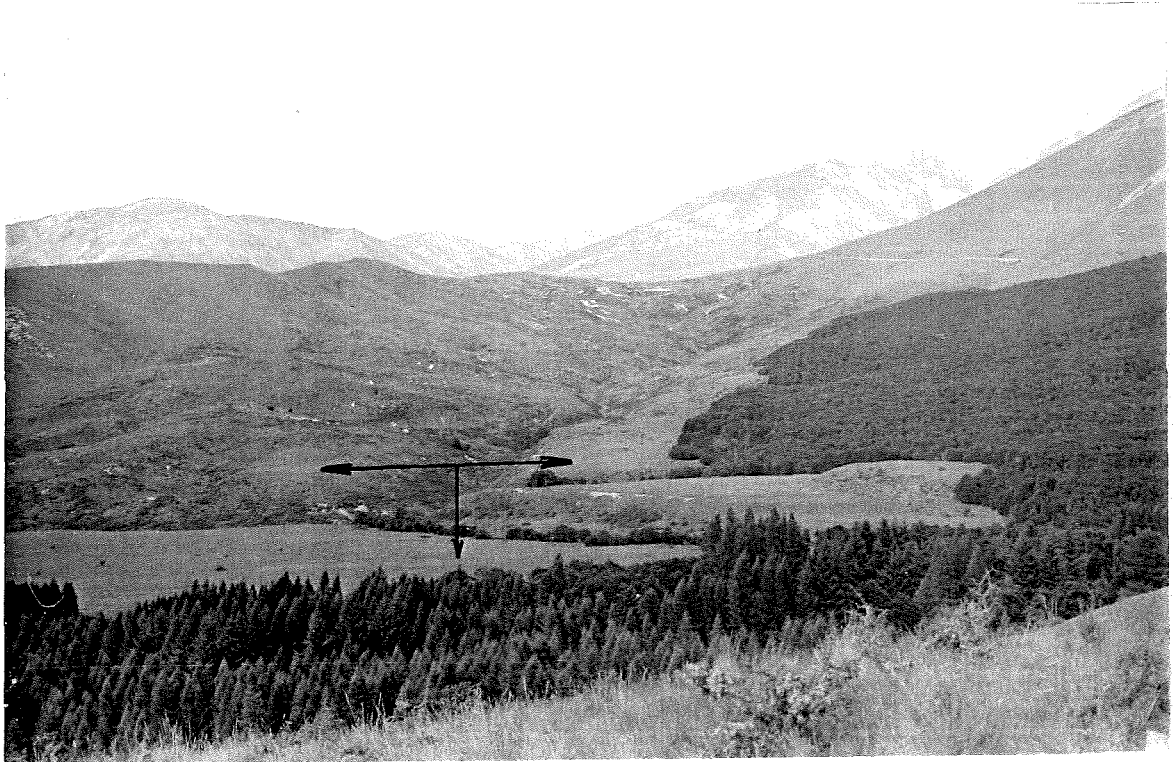


Plate 19: Concordant terraces (arrowed) of upper Blackwater surface. Terrace remnants in background have been formed on toe of fossil landslide whilst terrace gravels on near side of river rests on undisturbed Enys Formation. As the terrace levels are the same on both sides of the river, then terraces must have been formed after landslide movement.

Landsliding differs from the superficial processes in that it is essentially a catastrophic event with a very low recurrence interval. Although some parts of a slope retreat drastically on initial sliding, the lower part of the displaced material usually builds up (see plate 9f) and effectively buttresses the slope against further movement. The average rate of landslide retreat is considered by Young to be less than the more dynamic forms of soil creep and rain wash.

3.5 DATING LANDSLIDES

Attempting to date landslide movement is essentially a speculative procedure. Any dateable material (for example charcoal) contained within a landslide need not necessarily date the movement but merely indicates the date the preserved material was formed.

Two phases of movement may be distinguished on the basis of landslide defacement. An assemblage of younger landslides is clearly discernible from a series of older, fossil landslides although some of intermediate age exist.

3.5.1 Age of Fossil Landslides:

The age of fossil landslides may be roughly determined from the glaciofluvial terraces formed on them. In most cases, the initial formation of the fossil landslide predates terrace formation as the terrace surfaces are concordant with nearby surfaces on undisturbed ground (see plate 19) and do not show the backtilting associated

with slumping. However, one slide in Broken River (see plate 20) does show a slight drop in terrace level and the author attributes this to renewed movement as the height difference is disproportionate to the size of the slide. The mapping of the terraces by Breed (1958) has shown that the fossil landslides date back to either a pre-Blackwater or a pre-Poulter period.

The fossil landslides are thought to have first moved in a period of intensive degradation during the interglacial before the glaciation responsible for the terrace gravels. Rapid down-cutting in the valleys could occur at the beginning of an interglacial period when the glaciers were rapidly melting or possibly towards the end of an interglacial when a cooling climate brought increased rainfall. As the interglacials were long compared to the time scale of man's activities, this method of dating is only approximate. Apart from the actual time of movement, the greater magnitude of the fossil landslides suggests that the environment was substantially different from that under which the more recent slides have been established.

The blocks that have fallen from the limestone scarps have an aged appearance. These blocks, some of which are estimated to be as much as 8 m across, have moved up to 200 m in a down-slope direction. Evidence for a lengthy period of time elapsing since movement is given by the degree of weathering of the limestone blocks, a revegetated slide scar, vertical and oblique solution

channels on the block and exfoliation litter around the base. Also, substantial soil creep has buried the bases of the blocks to what seems to be a depth of several metres. It is the author's opinion that these block slides were initiated under glacial or periglacial conditions when ice wedging was an important factor in dislodging rocks.

3.5.2 Ages of Contemporary Landslides:

The more recent slides appear to have formed since the last glaciation. Most of the slumps have undrained depressions as a result of backtilting associated with rotational movement. A pollen analysis of material from the swamps was originally thought to be invaluable in assigning an age to movement. However, the pollen or other vegetable matter may not necessarily have been deposited at the time of swamp formation, and even if it had, the pollen may be no different from that derived from present day plant associations. The only significant vegetation changes have been those resulting from the Polynesian and European burnings (see section 2.1.1) and it seems likely that these burnings substantially affected the slope stability of the region. A more definitive method using swamps is to measure their depth and estimate their age from the rate of organic accumulation. From a slump in the Broken River Coal Measures which has a well-defined geometry (see plates 21a and 21b and figure 8), a minimum age of about 250 years has been estimated (Dr T. Dodson*).

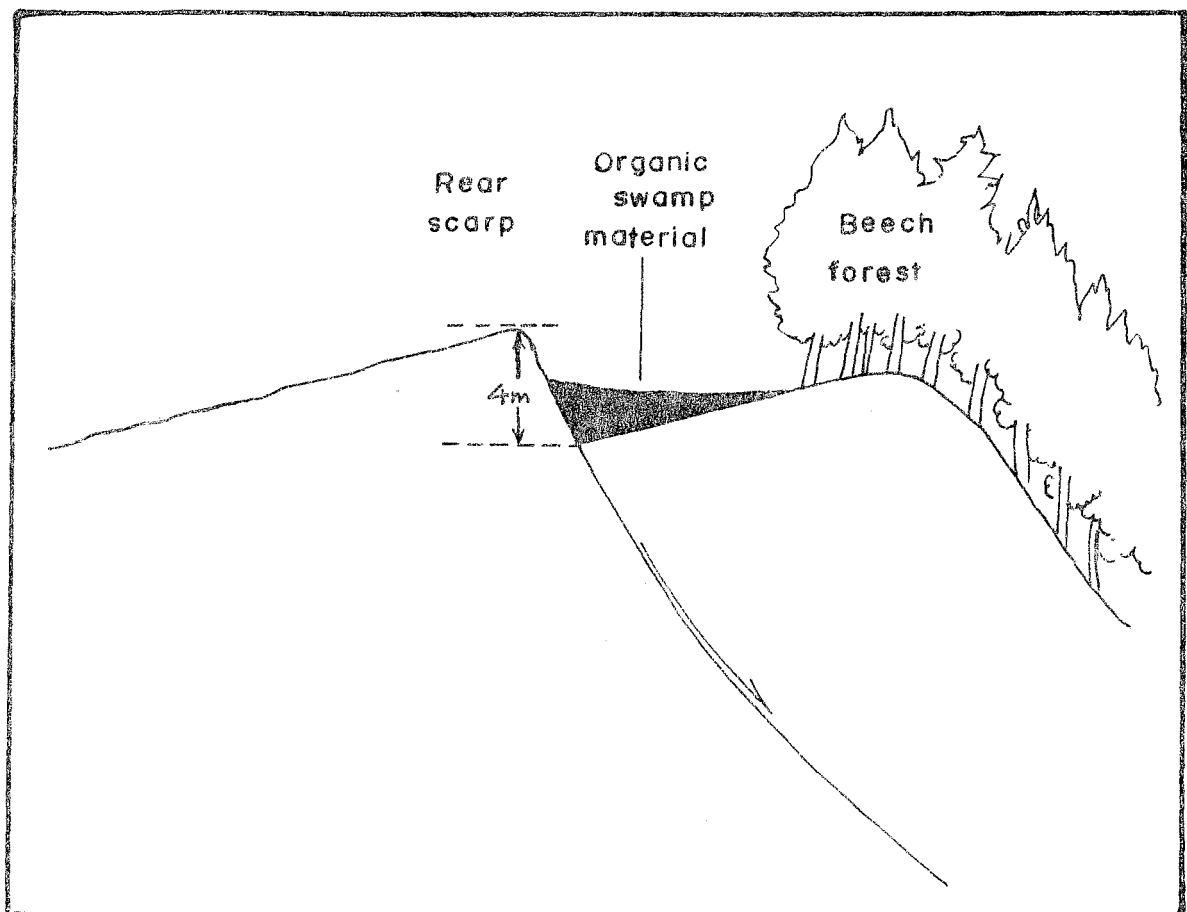
*Pers. comm., Geography Dept., University of Canterbury



Plates 21a and b: Two views of a recent slump in Broken River Coal Measures showing swamp formation in the back-tilted depression. For a cross-section see figure 8.

figure 8:

CROSS-SECTION OF A
CONTEMPORARY LANDSLIDE SHOWING
SWAMP FORMED IN A
BACK-TILTED DEPRESSION



For the younger slides a more reliable method has been to count the annual rings of shrubs growing on the scarp. An age of 150 years has been determined for the largest matagouri shrub found growing on the scarp of the Broken River bridge slide (see plate 26). However, the time of colonisation must be added to this age and for such an inhospitable place (loose, dry gravels) anything from 1 to 100 years is possible.

A very recent slump situated on the forested side of Hogsback Stream (see plate 9c) has dislocated a large number of the beech tree trunks. The rate of decay of the dead leaves and branches affords another method of dating. In this case an approximate age of 1 to 10 years seems likely as the leaves have not yet fallen from the branches.

The older, dormant slides are difficult to date, especially if movement has been semi-continuous or retrogressive. A method developed by Chin (1975) for dating moraines involved measuring the thickness of the weathering rind on greywacke boulders. Although afflicted by a complexity of variable factors, a time-thickness curve was developed which gave a youngest, measurable age of 1,000 years for a 1 mm weathering rind. With this method in mind, several boulders from the boulder fields of some of the older slides were cracked open and examined. The weathering rind thickness was seen to vary but never to exceed 1 mm (except on corners). A likely maximum age of 1,000 years is indicated.

3.6 ENGINEERING GEOLOGICAL ASPECTS OF THE CASTLE HILL SEDIMENTS

3.6.1 Lithological Control of Slope Stability:

It is possible to subdivide the Castle Hill Basin sediments according to their engineering geological characteristics. Apart from the greywacke basement rocks and the limestone beds, the sediments can be classified as either weakly compact and unindurated "rocks" or dense and heavily over-consolidated "soils" (see section 4.6). As these sediments fail in a manner unlike rocks, they will be considered here as engineering soils.

(a) Basement rocks: The hard, indurated and cemented greywackes are transected by at least four sets of closely-spaced joints of variable attitude. Although of high mechanical strength, the brittle rocks are highly susceptible to disintegration by heating and cooling, and frost action especially at high altitudes. There seems to be an increase in induration from the Torlesse Range to the Craigieburn Range with a corresponding decrease in talus development. Because erosion is so active, no weathering profiles seem to have developed except perhaps towards the lower parts of the basin where basement rocks are covered by younger sediments and glaciofluvial gravels. The rock itself is relatively non-porous but being highly fractured, groundwater is free to permeate. Examples of block falls, block slides and mass wasting are to be found on a small scale, but only the mass wasting (primarily frost action) is extensive. Very rarely, a debris avalanche has occurred, covering a large area.

(b) Broken River Coal Measures, Iron Creek Greensand and Coleridge Formation: The Broken River Coal Measures, Iron Creek Greensand and Coleridge Formation have been classed together as they all have a high proportion of sandy sediment. Occasional beds or lenses of carbonaceous material, silt, and mud in general, increase the likelihood of mass movement. On the other hand, cemented bands of ironstone and calcified shelly concretions have a strengthening effect. The compacting effect of 1,000 m to 1,300 m of overburden has imparted a certain degree of induration and the increased cementation of these older sediments has contributed to the mechanical strength. Geotechnical testing of the Enys Formation sediments (section 4.5), has shown the sand beds to be very dense with a relatively high bulk density and the muds to be highly overconsolidated. The older Broken River Coal Measures, Iron Creek Greensand and Coleridge Formation can be expected to be denser and more consolidated than the younger, overlying Enys Formation.

Sediments with a high proportion of sand are more susceptible to degradation by mass wasting, though several large fossil landslides show what can happen when excess water is available. A panoramic view of a typical topography developed in Broken River Coal Measures and Iron Creek Greensand can be seen in plate 22.

(c) Thomas Formation: The Thomas Formation consists of interbedded tuffs and limestone of widely differing engineering geological behaviour. The tuffs and limestone are being considered together here because of their interacting relationship whereby movement in the lower tuffs invariably involves movement in the limestone.



Plate 22: Panoramic view of Iron Creek Greensand and Broken River Coal Measures country in between Torlesse Range at back and Blackwater terrace in foreground. Southern limb of Prebble Hill syncline at left.

Several small-scale slumps and examples of mass wasting may be found on the banks of the larger rivers but by far the most common form of mass movement is block falls and block slides from the limestone beds (see plate 12). Although relatively small in volume, the block movements are so common that they probably outnumber all other forms of landslides.

The limestone is very porous and along with jointing and solution cavities, is highly permeable. The average unconfined compressive strength has been calculated by the Point Load testing method (B.W. Riddolls*) to be 81 Megapascals. The main difference between limestone and the other uncemented Cretaceous-Tertiary sediments is in the manner in which they fail. Cemented "rocks" fail in a brittle manner whereas the uncemented "soils" deform plasticly.

Some large scale slumps may be found in the tuffs on Flock Hill, Hogsback Hill and Castle Hill. The slumps appear to be prehistoric features and very few signs of recent movement can be detected. An unusual landslide of unknown age and mechanism is seen to have developed just upstream from the confluence of Porter River and Dry Stream (see plates 23a and 23b).

(d) Enys Formation: The Enys Formation will be the subject of a closer investigation in the next chapter but it is convenient here to compare it to the older sediments. The Enys Formation has a higher proportion of argillaceous material than the underlying formations. The fine-grained



Plate 23a: Aerial view of unusual landslide on true left bank of upper Porter River. Gravels of the Woodstock advance are exposed beneath a thin tussock cover at top.



Plate 23b: Side view of same landslide in Plate 23a. Backtilted scarps indicate rotation of blocks along multiple slip circle failure planes. See also plate 2g for downhill view of scarps.

sediments occur as thin seams interbedded with silts, sands and occasional lignite lenses. As a unit these sediments are heavily overconsolidated, uncemented and weakly bonded except on rare occasions where ferruginous and calcified lenses are present. There is a distinct difference in consolidation and induration between the Enys Formation and the Cretaceous-Tertiary sediments underlying the Porter Group. This difference is shown by the greater number of mass wasting instances in the Enys Formation and the ease of excavation with a geological hammer which decreases with depth.

Sandy members in the lower part of the Enys Formation (as in the Broken River Coal Measures and Iron Creek Greensand) are characterised by stable slopes (for example, the slopes between the limestone gorge and the highway bridges in both Broken River and Thomas River). It is likely that these slopes have not failed because the permeable nature of the sands allows water to discharge rapidly. The members above the sands are highly susceptible to both slumps and flows and where unstablising conditions persist for any distance alongside a river almost continuous mass movement is seen to occur (see plate 24). Failure planes are usually associated with the muds which have a moderate to high plasticity, high swelling strain coefficient and most have a low slake durability (see section 4.6). The interbedding of the permeable sands with the muds allows saturation of the latter with subsequent decrease in shearing resistance.

(e) Pleistocene gravels: Landslides do not occur solely within the gravels but slumps which have developed in the



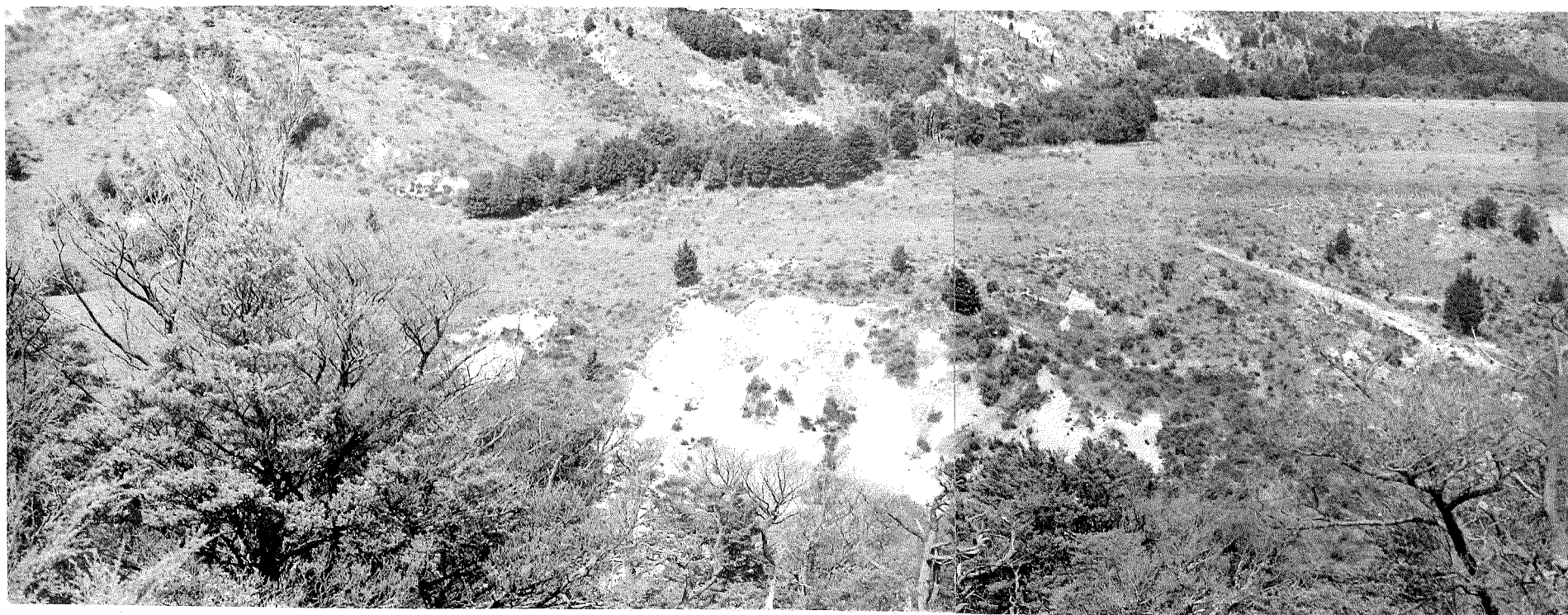


Plate 24: Persistence of unsuitable conditions leads to almost continuous instability
at Hogsback Stream.

underlying Tertiary sediments often involve the gravel capping. The fact that these gravels are sometimes exposed with nearly vertical faces suggests that their frictional component of strength is due to the sediments' angularity and packing density. The thin loess deposits which cap the terrace gravels are readily vegetated so that mass wasting processes are uncommon. The gravels are highly porous, and seldom have streams developed on them although several dry valleys exist.

3.6.2 Structural Control of Slope Stability:

The clastic sediments of Castle Hill Basin show little regard for failing along structural discontinuities. A probable reason is the general lack of well-developed sets of discontinuities and the overriding influence of the sediments' low mechanical strength. Landslides are seen to have developed in massive beds and in thinly-bedded sediments. The strata underlying the slope may be oriented in any direction and there is only a slight preference for landsliding where the beds dip outwards. Sections of Broken River (between Hogsback Stream and Tims Stream) and Cave Stream have strata dipping towards the valley floor but only Broken River has developed slides (see figure 12 and plate 29). Again, where the Prebble Hill syncline is cut through by Porter River, an active landslide has developed where the syncline plunges into the slope but there remains only the suggestion of a slide on the opposite, more favourable side (see plate 25). However, a small fossil slide has clearly taken advantage of its favourable structural position in the Flock Hill syncline (see plate 26).

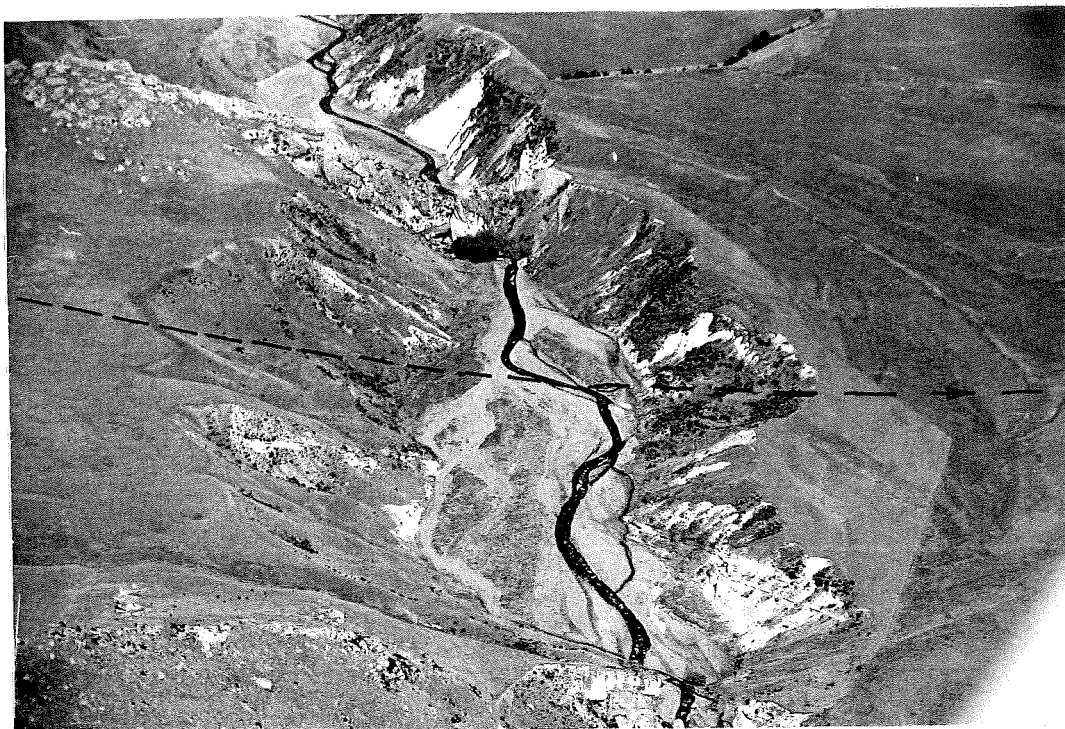


Plate 25: Porter River where it passes through the two flanks of the Prebble Hill Syncline. Active slide on right has moved in opposite direction to plunge of syncline (arrowed).



Plate 26: Small slide (centre) developed on Flock Hill Syncline. Note line of shrubs growing on scarp of Broken River bridge slide in foreground.

Faulting appears to have some influence on slope stability as the large slump by Broken River bridge, and two small slumps on the true right of Porter River (just upstream of the Porter River-Dry Creek confluence) have faults traversing them. The Porter River slumps in particular have recent fault traces disrupting the terrace on which the slides have developed (see plates 27a and 27b). It seems likely that the presence of a fault is partially responsible for the landslide through allowing groundwater to become more readily accessible to the surrounding sediments. Similarly the disposition of the strata may not necessarily control the failure surface but it may control the flow of groundwater.

Thus the emphasis in slope stability in Castle Hill Basin is more on a combination of weaker beds being unfavourably exposed by over-steepened slopes rather than on structural control.



Plates 27a and b: Two faults disrupting a terrace to the south of Porter River (for their position, see plate 4). Note how a slump has formed where the fault cuts the terrace. Quarrying operations (far right below) are in shattered limestone adjacent to Torlesse Fault (at foot of hills at rear).

CHAPTER 4

SLOPE STABILITY IN THE ENYS
FORMATION, BROKEN RIVER4.1 INTRODUCTION

The area described in this chapter was chosen for a more intensive study of mass movement because contemporary landslides are particularly common and active. The study area is centred around the confluences of Broken River, Trout Stream and Hogsback Stream as shown by figure 2 and figure 9. The Enys Formation sediments form a wedge bounded by the axial plane of a southwest plunging syncline and the lower limit of figure 9. The wedge of sediments rests on the Thomas Formation limestone and is capped in places by terrace gravels. Views of this area can be seen in plates 10b, 24 and 28.

The abundance of landslides in this area suggests that a peculiar combination of factors may account for the widespread slope instability. A major contributing factor appears to be the geotechnical nature of the Enys Formation sediments and in this chapter the geology and the geotechnical properties are discussed. The other contributing factors are by no means confined to this area alone and these are outlined as regional causes of slope failure in Chapter 6.

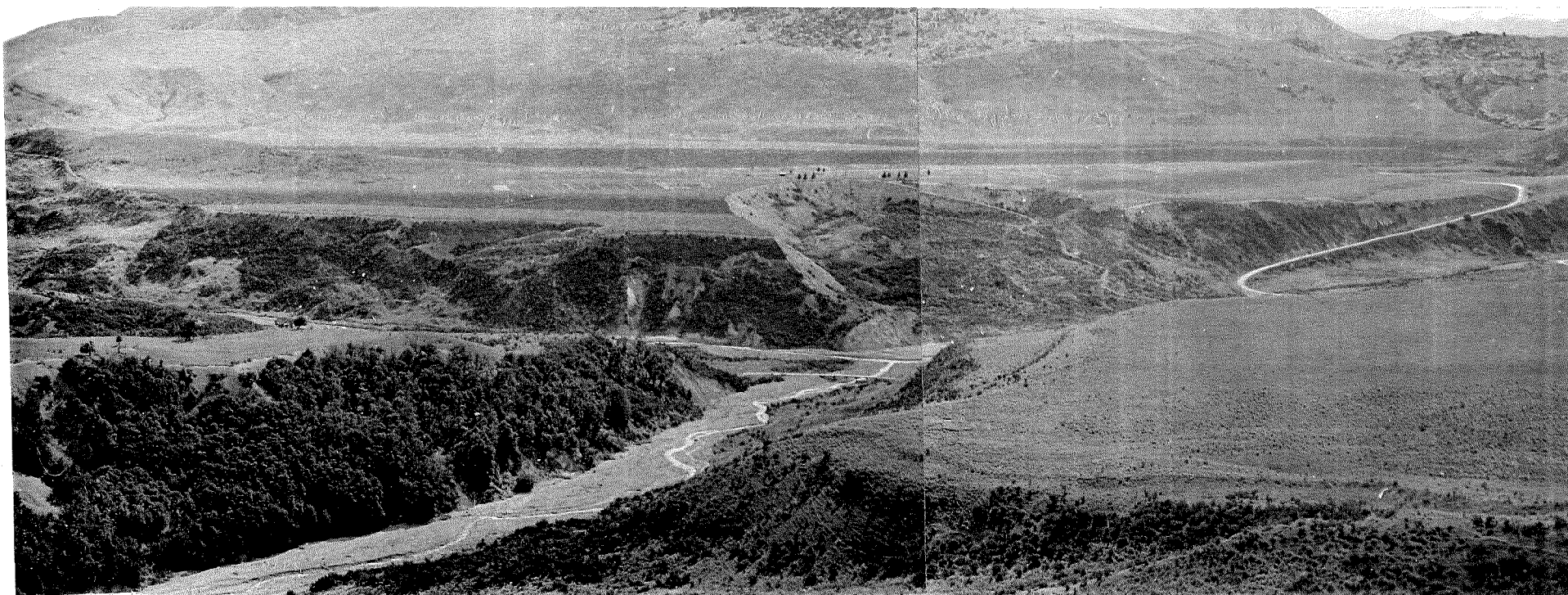

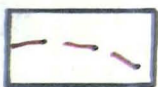

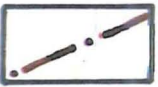


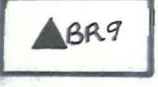
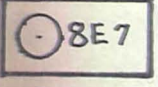


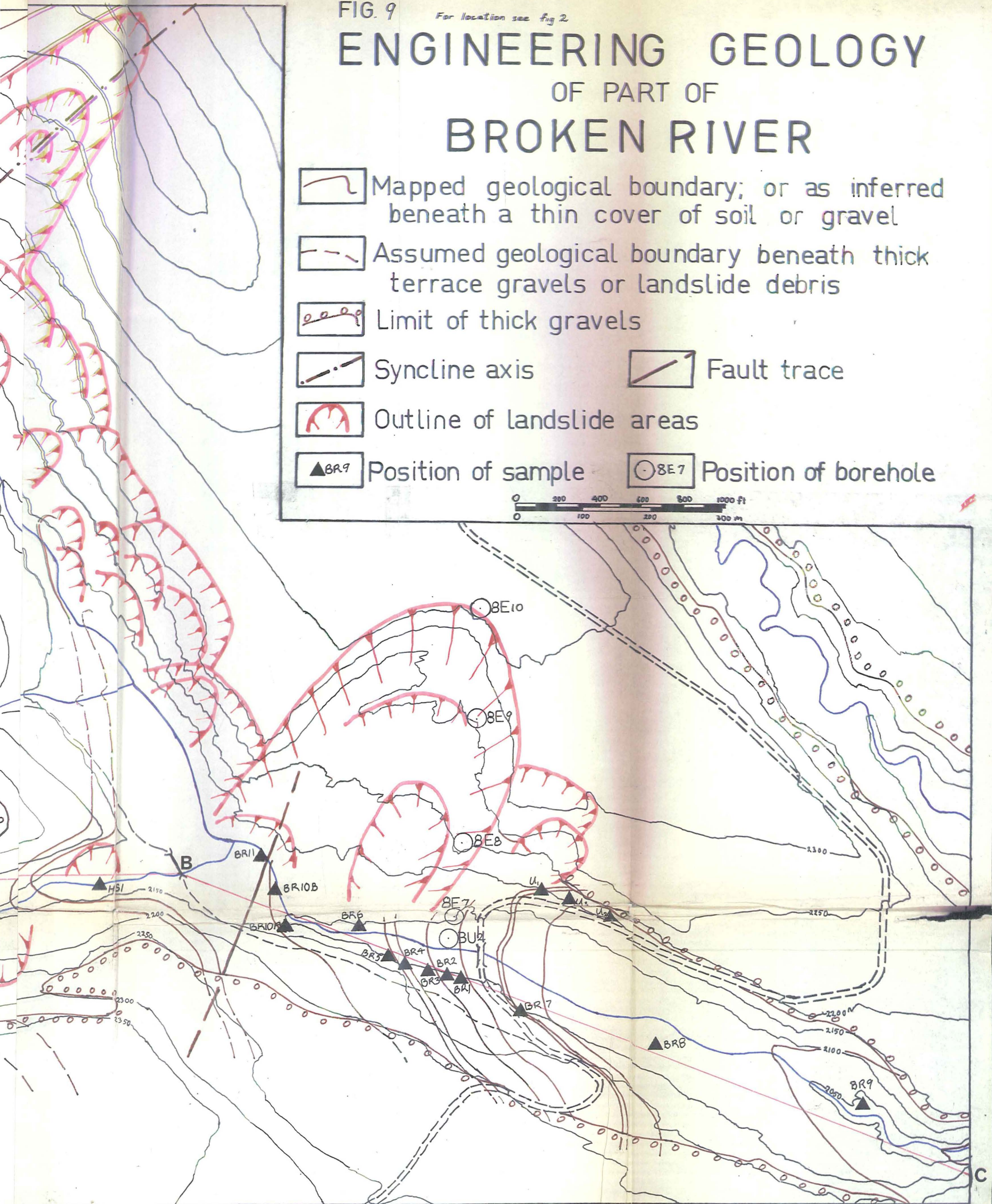
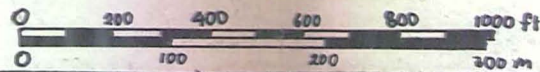
Plate 28: View down Hogsback Stream towards Broken River and Flock Hill beyond.

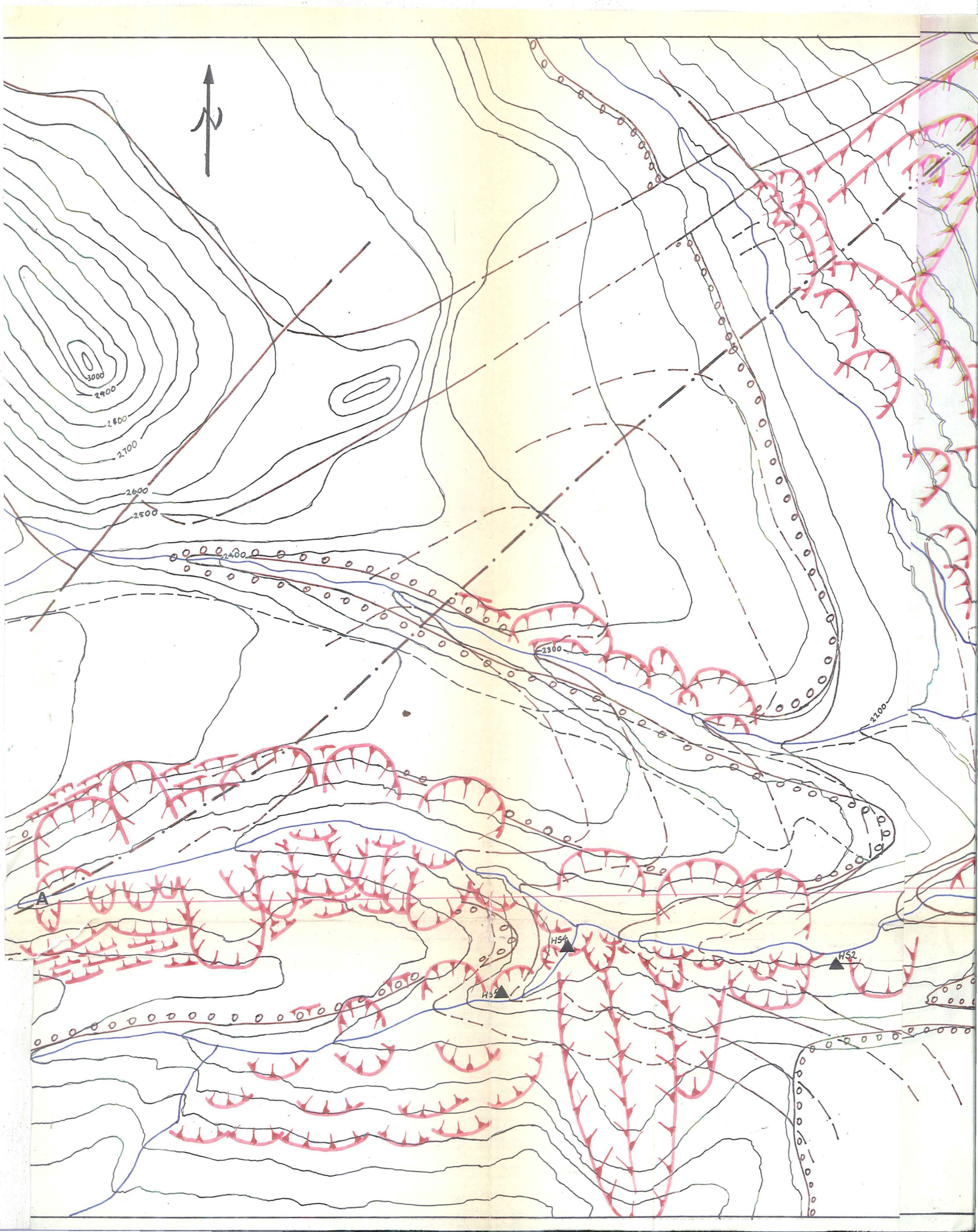
FIG. 9

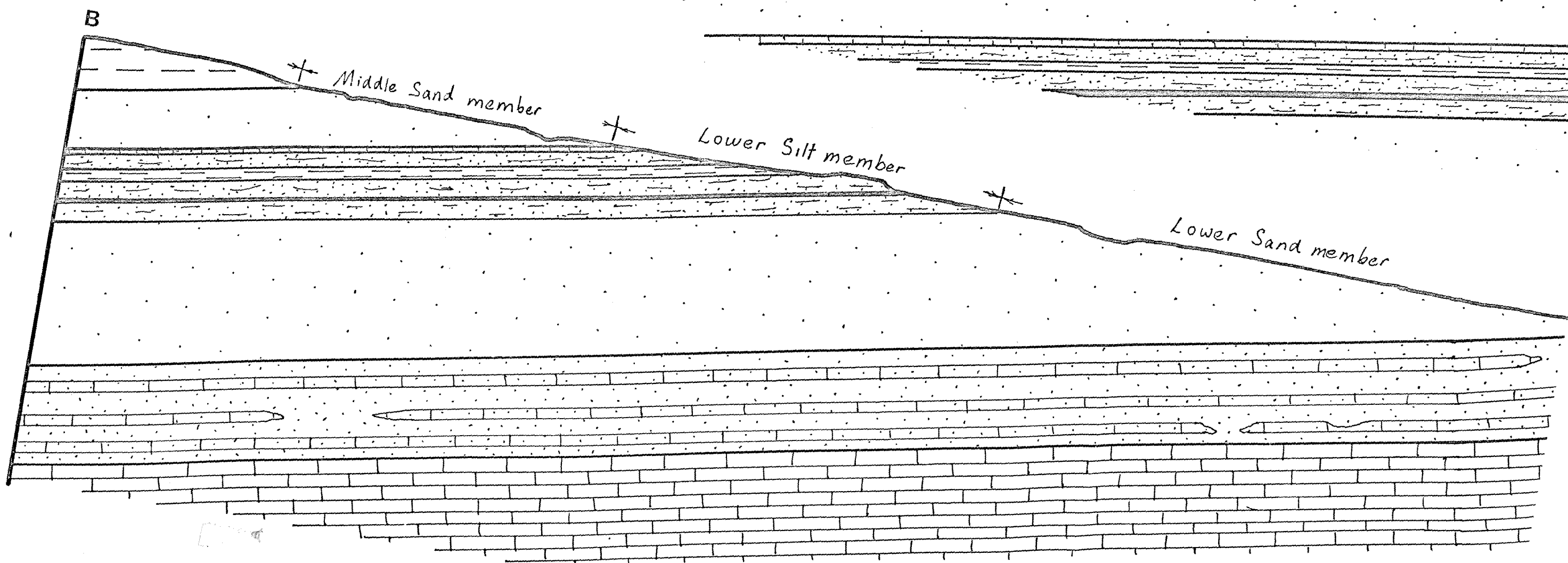
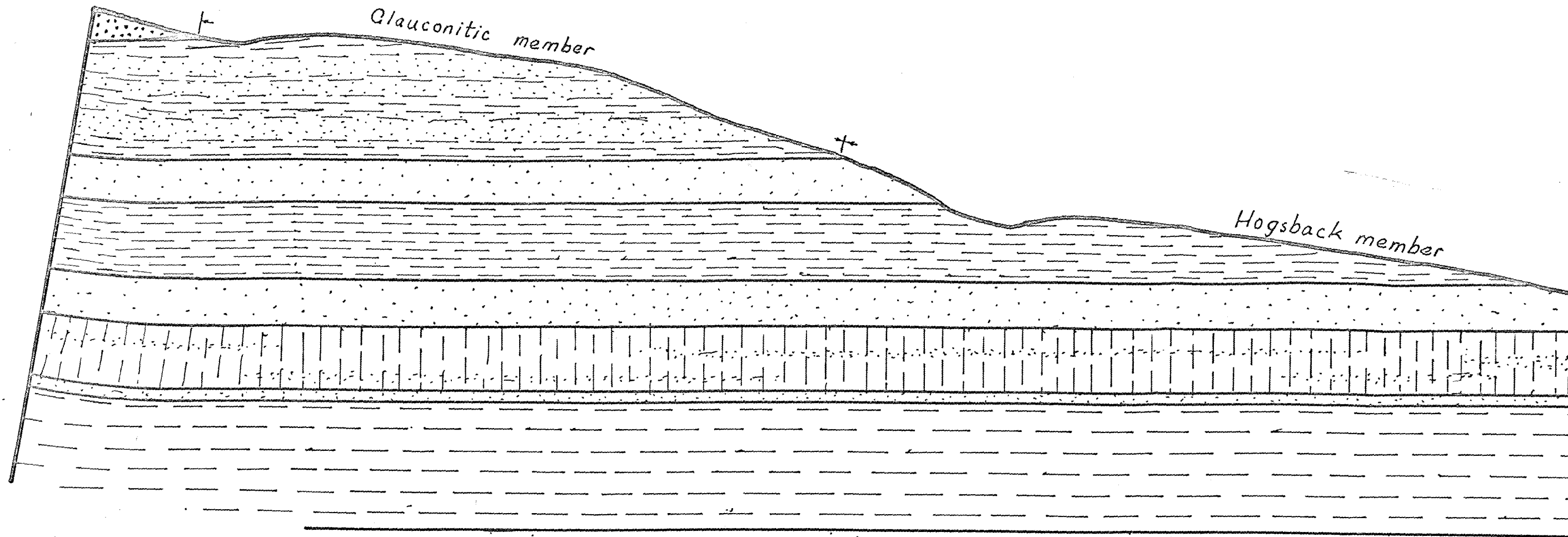
For location see fig 2

ENGINEERING GEOLOGY OF PART OF BROKEN RIVER

-  Mapped geological boundary; or as inferred beneath a thin cover of soil or gravel
-  Assumed geological boundary beneath thick terrace gravels or landslide debris
-  Limit of thick gravels
-  Syncline axis
-  Fault trace
-  Outline of landslide areas
-  Position of sample
-  Position of borehole







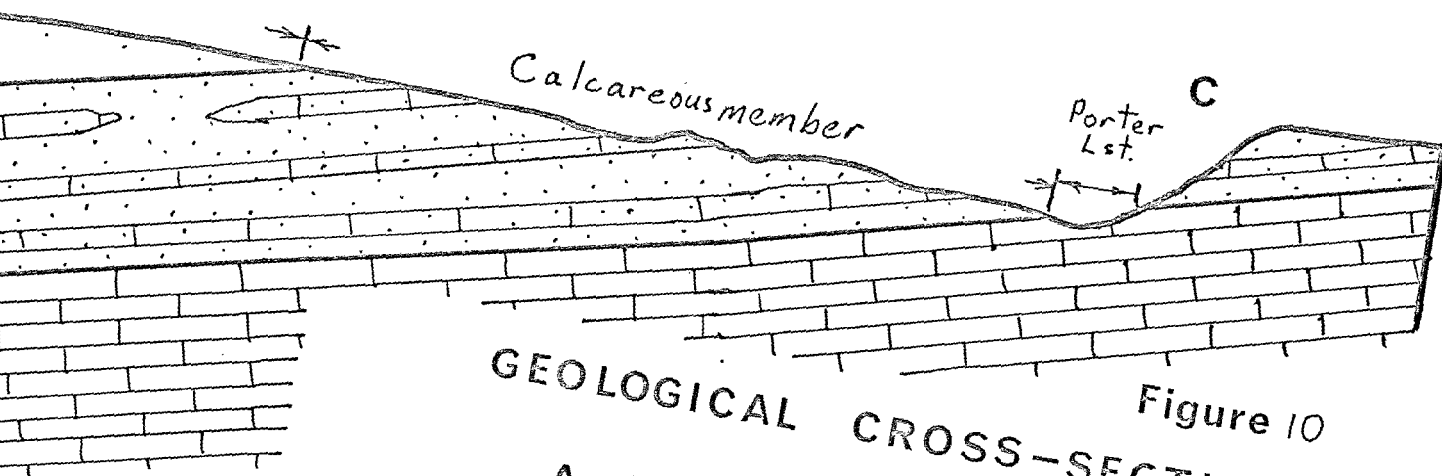
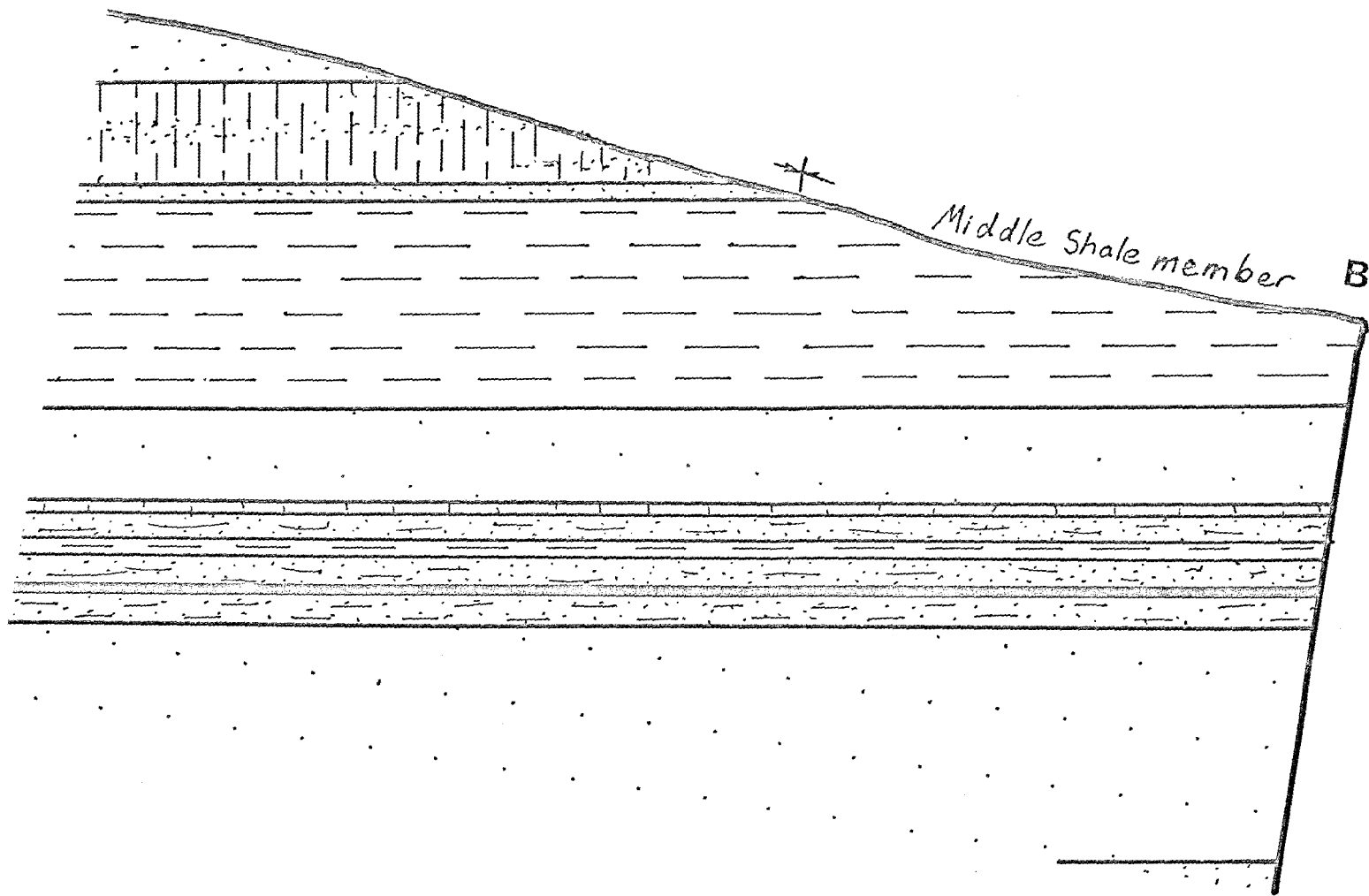
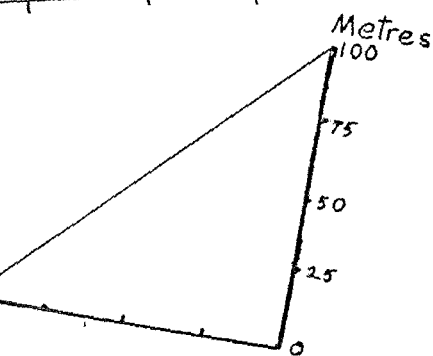


Figure 10

GEOLOGICAL CROSS-SECTIONS

A-B HOGSBACK TRAVERSE
(for details see fig ||b)

B-C BROKEN RIVER TRAVERSE
(for details see fig ||a)



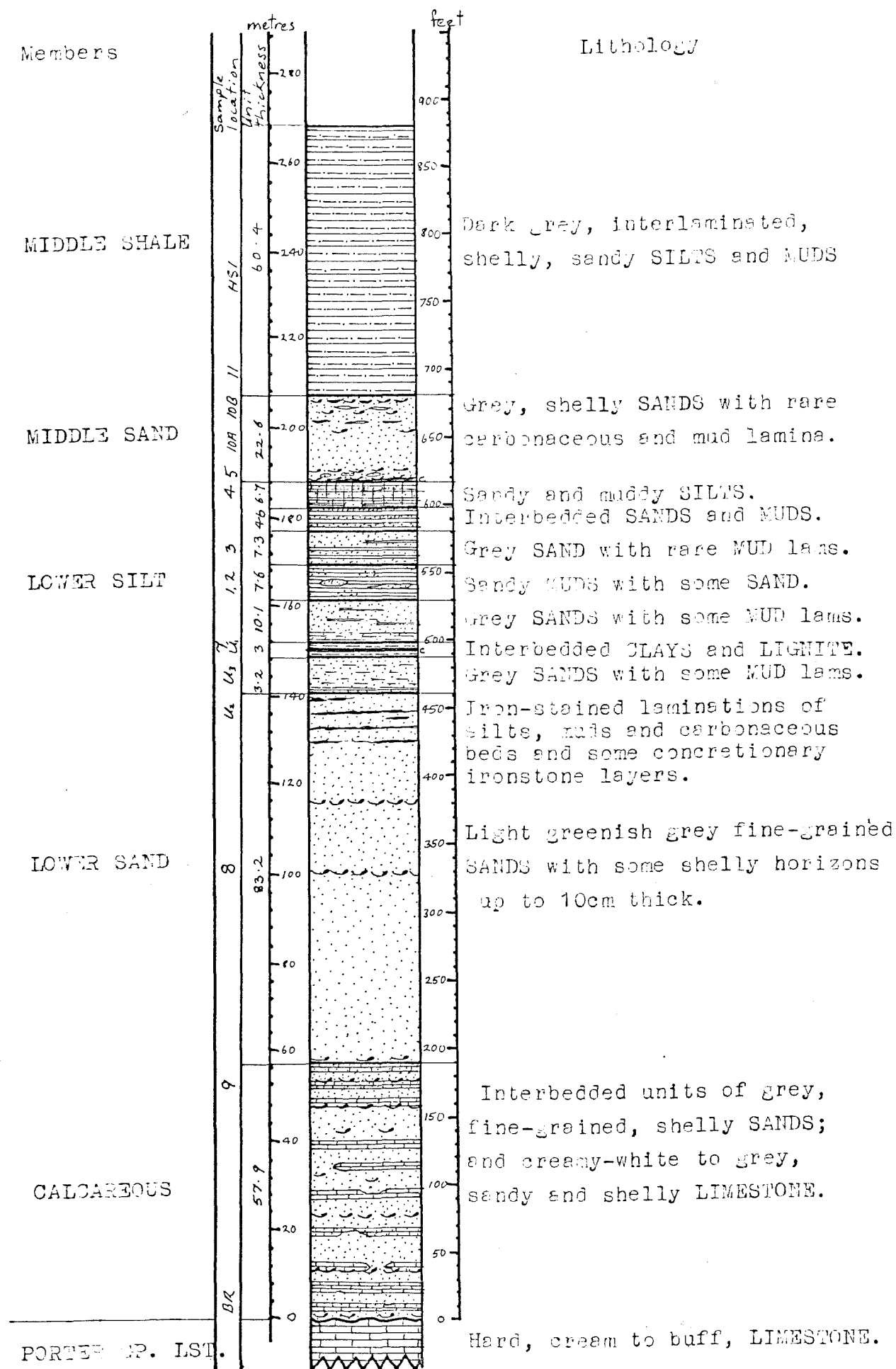


FIGURE 1A: STRATIGRAPHIC COLUMN OF ENYS FORMATION.

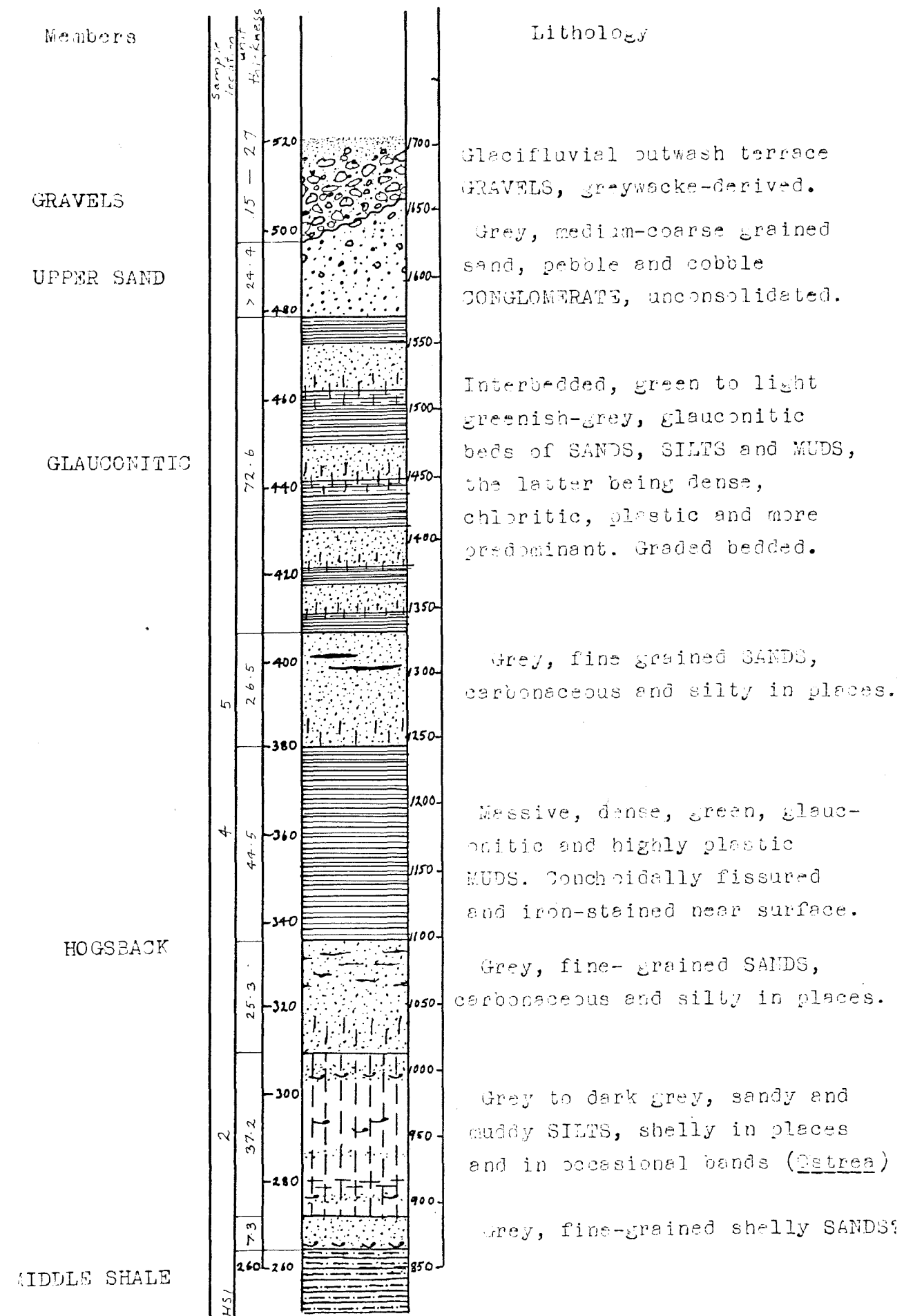


FIGURE 1B: STRATIGRAPHIC COLUMN OF ENYS FORMATION.

4.2 LITHOLOGIES OF THE ENYS FORMATION AT BROKEN RIVER

The geology was mapped by the author using conventional tape and compass techniques. Traverses were made up Broken River and its tributaries, and occasionally up terrace risers where in situ material was exposed. A soil auger was also used on the terrace risers to determine lithologies and boundaries. Because strikes of low-angle beds (see section 4.3.1) are often difficult to determine from apparent dips, a shovel was used to expose bedding planes. Thus a reasonably confident picture of the geology has been built up despite the ubiquitous landslide deposits.

An engineering geological map showing topography, geology and landslide boundaries is shown in figure 9. A cross-section along Hogsback Stream-Broken River (A-B-C of figure 9) is shown in figure 10 and a geological column showing thicknesses is shown in figure 11. A brief description of the members distinguished by the author is given below.

4.2.1 Calcareous Member:

Overlying the Porter Group is a succession of interbedded massive sands and thinly-bedded, impure limestones. The sands are grey, uncompacted to slightly calcified, current bedded in places, with a few scattered carbonaceous and mud laminae. The limestone beds are creamy white to grey (with increasing sand content), commonly sandy and contain abundant molluscan fragments.

4.2.2 Lower Sand Member:

The Lower Sand member forms a uniform sequence of greenish-grey to brownish-grey, fine-grained sands. The sands are glauconitic, massive and uncompacted with local current bedding where associated with shell bands. Towards the top of this member, a few iron-stained carbonaceous layers and concretionary ironstone layers appear. To the north, these extend laterally into interlaminated beds (up to 75 cm) of sand, silt and ferruginous muds.

4.2.3 Lower Silt Member:

The Lower Silt member is of highly variable nature and consists of at least 7 units:

(a) A sharp contact with the Lower Sand member leads to a bed of interlaminated muds and fine sands with increasing sand towards the top.

(b) Above unit (a) lie three, 1 m thick beds consisting of a dense, glauconitic mud at the base; an impure bed of extensively fissured, muddy lignite in the middle; and a dark, brownish-grey laminated, organic mud at the top.

(c) A gradational change leads to an identical bed to unit (a).

(d) Overlying unit (c) is a massive bed of interlaminated muds and fine silts that contain occasional lenses of fine sand.

(e) A well-defined contact leads to bedded, medium-grained sands with local mud laminae and shell layers.

(f) Another unit of interlaminated muds and sands overlies the sand unit and is characterised by the laminae thickening locally to elongated lenses of sand and mud.

(g) The upper unit of this member consists of sandy muds at the base followed by muddy silts, sands, very stiff muds, shelly silts and finally capped by a lense of impure, muddy lignite.

4.2.4 Middle Sand Member:

Above the Lower Silt member a shelly layer grades upwards into a massive bed of light grey, laminated to current bedded, fine-grained sands. The sands contain occasional shell beds, mud laminations and rare sandy concretions.

4.2.5 Middle Shale Member:

The Middle Shale member is characterised by massive interlaminated, very fine-grained sands, silts and muds displaying various shades of grey where fresh, and brown where weathered. The laminae are lensoidal with thicknesses ranging from 1 to 10 mm. Differences in grain size usually show a distinct parting between laminae but sometimes the contact is transitional. Overall, the mud laminae are thicker and more numerous than the silt and sand laminae.

4.2.6 Hogsback Member:

The Hogsback member consists of five units comprising three similar sand beds, intercalated with a bed of silt near the base and a greenmud higher up. The sand units are characterised by grey, fine-grained, quartz sands with occasional beds of laminated muds and sands, local shell horizons and rare carbonaceous laminae. Above the first

sand unit, a gradational change leads to a silt-dominated unit which is massive in places and locally interbedded with sands, muds and shell beds (predominantly Ostrea sp.). The fourth unit is a blue-green to grey-green, glauconitic, stiff-fissured mud.

4.2.7 Glauconitic Member:

Overlying the Hogsback member is a similar sequence of interbedded muds, silts and sands, all with varying hues of green, indicating a high glauconitic content. The beds range from 1 to 3 m thick, with the greenmud beds being thickest and more numerous. The transition from sand to silt to mud is often gradational but sharp contacts are not uncommon. Exposure of this member is discontinuous as the highly plastic nature of the greenmuds (see section 4.6.1(e)) is most favourable to slope failure by earthflow.

4.2.8 Upper Sand Member:

The Enys Formation at Hogsback Stream culminates with a greenish-grey, fine to coarse-grained, glauconitic, sand-dominated member. The sands are locally current-bedded as shown by small blebs of carbonaceous laminae and mud clasts, and are occasionally interbedded with a pebble and cobble conglomerate. The latter is greywacke-derived and forms irregular beds or lenses. Unfortunately, limited exposures allow only approximations to the frequency of these conglomerate bands but it appears they are more numerous towards the top of the member.

4.3 STRUCTURE

4.3.1 Intraformational structures:

(a) Bedding: Fieldwork has shown that the sediments at Broken River and Hogsback Stream have a reasonably uniform dip and strike. A prominent lignite band belonging to the Lower Silt member is a continuous marker bed exposed on both sides of Broken River and recorded in a core from borehole 8E8 (see figure 9) in the toe of the Broken River bridge slide. By using the "three borehole problem" method of determining dip and strike, a reliable dip of 11° and dip direction of 250° has been obtained. Boundary positions have also been determined from soil auger sampling. Although of lower accuracy, the dips and strikes obtained by the same method concur with those obtained from the coal marker bed.

The beds steepen slightly where they lap onto the limestone beds of the Porter Group. Gage (1970) reports an unconformity between the lower Enys sediments and the Porter limestone but the presence of impure limestone beds amongst shelly and sandy beds in the basal Calcareous member suggests a more or less continuous sequence of sedimentation, in Broken River at least.

Bedding is reasonably planar except where the strata are thinly bedded to laminated. In such cases they are more often undulatory or lensoidal in nature. Within the more massive sand beds, small carbonaceous and mud laminae indicate extensive current bedding.

(b) Chemical weathering: Superficial iron-staining and leaching of the sediments extends to depths of up to 0.5 m on terrace risers. Discolouration due to weathering seems to preferentially effect the finer-grained sediments. A possible reason is the more impermeable nature of the former being more favourable for deposition of iron oxidation products or it may just point to a greater proportion of iron minerals present.

Deep, extensive weathering does not seem to have developed in the Enys Formation, possibly due to the rapid degradation of the basin during glacial and periglacial times with subsequent blanketing by thick outwash gravels. The rate of degradation is such that only a superficial "skin" (less than 1 m) of weathered products has time to develop before lateral river erosion removes it. Because of the limited thickness, weathering does not significantly influence landslide development. It may very well be an important factor in superficial mass movements, however.

4.3.2 Tectonic Structures:

(a) Folding and faulting: The tectonic structure is simple; the beds form the southern limb of a south-easterly plunging syncline which descends from a point just north of Flock Hill. The only prominent fault is a normal fault which runs parallel to and northwest of Cave Stream (Bradshaw, 1975). This fault displaces limestone beds in the gorge at Broken River, halfway between the junction with the Porter River and Cave Stream. No evidence has been found to suggest that the fault has any effect on slope stability in the area studied.

A small fault has been mapped by the author at Broken River where the boundary of the Middle Sand member and the Middle Shale member is exposed in the river bank (see figure 9). This fault can be tentatively correlated with another small displacement seen in an exposure on the large terrace riser to the southwest. If this correlation is correct, an extrapolation to the northwest places the fault on the upstream side of the Broken River bridge slide. Whether it could have affected the stability of the slide (for the reasons advanced in section 3.6.2) is uncertain but it seems likely that it could be one of many contributing factors to movement. It is probable that other such faults exist but are not exposed.

(b) Jointing: Joints are seen to have developed within the massive sand beds only. The joints are mainly oriented perpendicular to bedding, and parallel to and oblique to the strike. Most joints are closed, although some may be open (up to 5 mm) and infilled with clay in places. The influence of joints as planes of weakness is probably insignificant as the joints are not continuous across adjoining argillaceous strata.

4.4 GEOHYDROLOGY

The influence of groundwater is one of the important factors contributing to slope instability. Many of the Enys Formation sediments have high porosities (see section 4.5.3 and 4.6.3) and this is usually associated with high permeabilities. Although groundwater levels have not been measured, surficial seepages indicate that

they are most frequently found at the base of the terrace gravels.

The geologic column (see figure 11) shows a series of potential aquifers in the permeable sands and aquicludes in the impermeable muds (especially the lignite and mud seams in the Lower Silt member). However, because of the network of deeply incised rivers allowing drainage in several directions and the lack of Enys Formation beds elevated above the terraces, it is doubtful if pressurised artesian conditions exist.

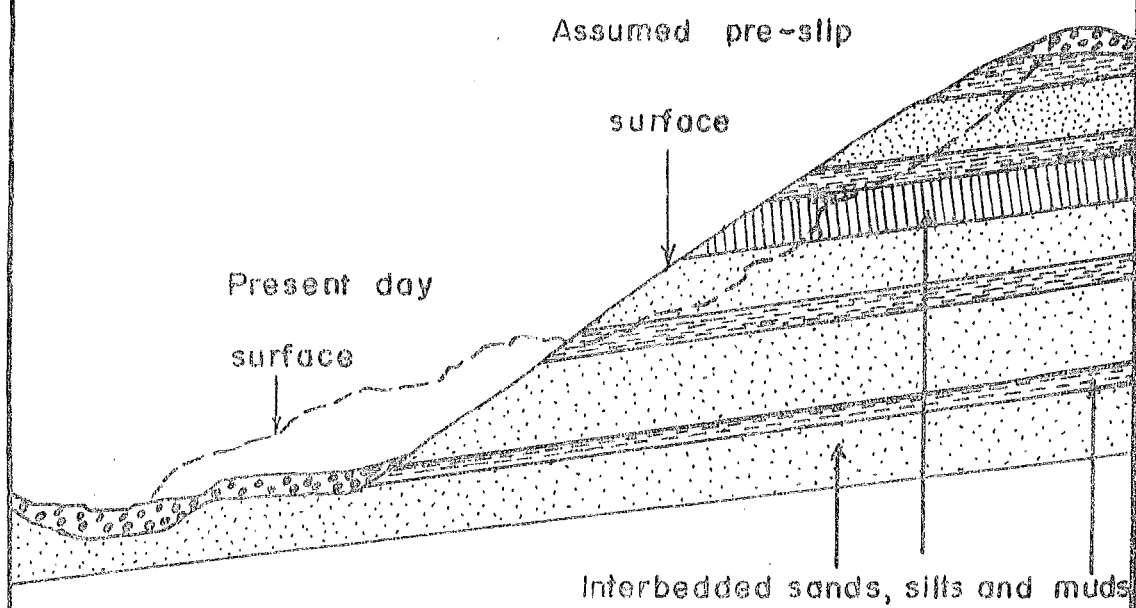
Where massive beds of sand are exposed, the almost continuous flow of ground water out towards the face flushes away any debris that may collect on the slope. The sand outcrops are quite common in the Broken River-Hogsback Stream area (see plate 10b) and revegetation of the exposure seems to be a slow process. Where sand beds are closely interbedded with muds or silts, differential erosion often leaves the more impermeable beds unsupported with subsequent collapse and deposition on the underlying sand bed. The softened debris tends to clog the outlet of the sand layer and it is possible that unstablizing pore pressures may develop. An example of landsliding in permeable and impermeable beds is shown in plate 29 with a possible cross-section shown in figure 12.

Superficial indications of prolonged over-saturation are usually reflected by the vegetation; a noticeably lush green growth with an abundance of silver tussock can be found growing in the marshy areas of many of the slides (as in plate 14).



Plate 29: Suite of slides in upper reaches of Broken River - see below for cross section.

Figure 12



SCHEMATIC PROFILE ACROSS PART OF BROKEN RIVER,
JUST UPSTREAM FROM HOGSBACK STREAM.

4.5 SAMPLING AND TESTING OF THE ENYS FORMATION

4.5.1 Introduction:

A sampling and geotechnical testing programme was carried out to try to determine the relationship between the geotechnical properties of the Enys Formation and mass movement. Geotechnical properties include classification, index, hydraulic and mechanical properties. A series of tests aimed at determining the first two types of properties were chosen for their minimal sample preparation, speed and simplicity of testing, ease of data reduction and ease of interpretation. Although the last two properties described above have more relevance in slope stability analyses their tests require specialised equipment and knowledge. As these resources were not readily available to the author in the time available, only a few undrained, unconsolidated triaxial tests were carried out to give an indication of mechanical properties.

The following classification and index properties were determined:

Natural water content, (w) = $\frac{\text{weight of water in natural sample}}{\text{weight of dry solids}}$

Saturation water content (i_s) = $\frac{\text{weight of water in saturated sample}}{\text{weight of dry solids}}$

Porosity (n) = $\frac{\text{pore volume}}{\text{bulk volume}}$

Dry bulk density (ρ_d) = $\frac{\text{weight of dry solids}}{\text{bulk volume}}$

Saturated bulk density (ρ_s) = $\frac{\text{saturated weight}}{\text{bulk volume}}$

Solid density (ρ_g) = $\frac{\text{weight of dry solids}}{\text{volume of solid fraction}}$

Uniaxial swelling strain
coefficient (ϵ_s)

= $\frac{\text{increase in height}}{\text{original height}}$

Slake durability indices
(Id_1 , Id_2 , Id_3)

= percentage of material retained
after each slaking cycle

Atterberg limits:

Plastic limit (PL)

= water content at plastic limit

Liquid limit (LL)

= water content at liquid limit

Plasticity index (PI)

= LL - PL

Liquidity index (LI)

= $\frac{w - PL}{PI}$

The objective of the testing programme was to identify any exceptional geotechnical properties of the sediments that would give some insight into the observed poor slope stability behaviour. Additionally, the property values could be used to infer values of the mechanical properties of cohesion and friction angle.

It was not the intention of the testing programme to obtain the complete and representative range of property values for each lithology of each member of the Enys Formation. Nor was it the intention to examine in any detail the variation of results and the significance of exceptional values. The difficulties associated with sampling (see section 4.5.2) and the long time required for testing and interpretation of data made such an approach impracticable.

4.5.2 Sampling:

Ideally, a systematic statistical survey based on a large number of data points from each bed would result in more representative values for that bed.

The correct type of sampling for such a survey is stratified random sampling (Krumbein & Graybill, 1964) where each member of a stratum in a stratified population has an equal chance of being selected. Note that the statistical use of strata is identical to the geological term in so far as the population (geologic column) is divided into discrete stratum for the purpose of identification. Because each stratum is only represented by a miniscule amount exposed in only a few outcrops, random sampling can only be limited to the superficial sheet of limited depth that is accessible. Furthermore, random sampling cannot be applied where ordering results in a trend or where cyclic variations exist (Blalock, 1960). To overcome the first difficulty would require drilling and the second difficulty would require closely spaced clusters of random sampling within each stratum that showed variation. As the number of samples created would involve a disproportional amount of time and effort for the amount of information gained, the idea of probability sampling was not adopted.

Instead samples were purposefully selected using judgement and geological intuition. The advantages of this method are that samples may be chosen which are in especially good positions to supply information or may represent extreme cases which would provide the most striking differences. As the samples are obtained by a non-probability method of sampling the use of statistical inference is not legitimate (Blalock, 1960). The properties are representative of the sample tested and only indicative of the bed or member from which it was taken. The following discussion on the geotechnical properties of the Enys Formation are thus generalisations based on the selected samples.

A policy was adopted of collecting one sample from different beds at each undisturbed outcrop. As many of the beds have similar lithologies it was not necessary to sample every bed at each outcrop. To obtain an indication of differences in properties with depth and lateral variation, the same lithology was sampled at various locations. In general, the argillaceous beds were sampled more frequently than the sands as it was thought that the former would have more influence on landslide development. Outcrops in the vicinity of landslides were examined more closely for critical beds or layers which may give some information on reasons for failure. Because of the limited amount of outcrops it is possible that a bed displaying potentially unstabilising characteristics was not exposed and hence not sampled.

The sample was chosen as being visually representative of the lithology from which it was collected and the amount varied between two and four kilograms. Each sample was wrapped and sealed in heavy-grade polythene bags immediately after collection to prevent moisture loss. Block samples were collected "undisturbed" and oriented with respect to bedding.

A number of problems were encountered when sampling the sediments. Difficulties arose when excavating a block of sediments - not only was access often difficult but many lithologies (particularly sands and lignite) had a tendency to disintegrate on sampling. Transportation from the sample site to the laboratory (part of the journey by foot) also caused sample disturbance, as well as limiting the amount of material able to be carried back.

4.5.3 Testing:

Testing of many of the properties was difficult due to the weak nature of the materials. Oven-dried specimens with a significant silt and sand content tended to collapse on immersion in water, and specimens with a significant clay content tended to swell with subsequent disintegration. Because of this loss of integrity, a method using toluol instead of water was developed (see Appendix 3). It is thought that toluol does not react with the sediments for two reasons. Firstly, the grain structure acts as a molecular "sieve" allowing the smaller water molecules in to react physically and chemically and not the larger toluol molecules. Secondly, the toluol molecules are not dipolar (whereas water is) and thus do not align themselves in monolayer thickness (this phenomenon is known as adsorbtion, see for example Grim, 1962).

The test methods that have been used for determining natural water content, saturation water content, porosity, density and Atterberg limits are well documented (see for example Akroyd, 1957). The New Zealand Standards Association is at present drafting standards for many geotechnical tests but this was not available at the time of testing.

The methods for determining the uniaxial swelling strain coefficient and the slake durability index were carried out in accordance with I.S.R.M. (1972) recommended standards.

The uniaxial swelling strain test consists of saturating an oven-dried, unconfined sample and measuring expansion in one direction (usually perpendicular to bedding). The apparatus used is shown in plate 30 and some typical specimens,

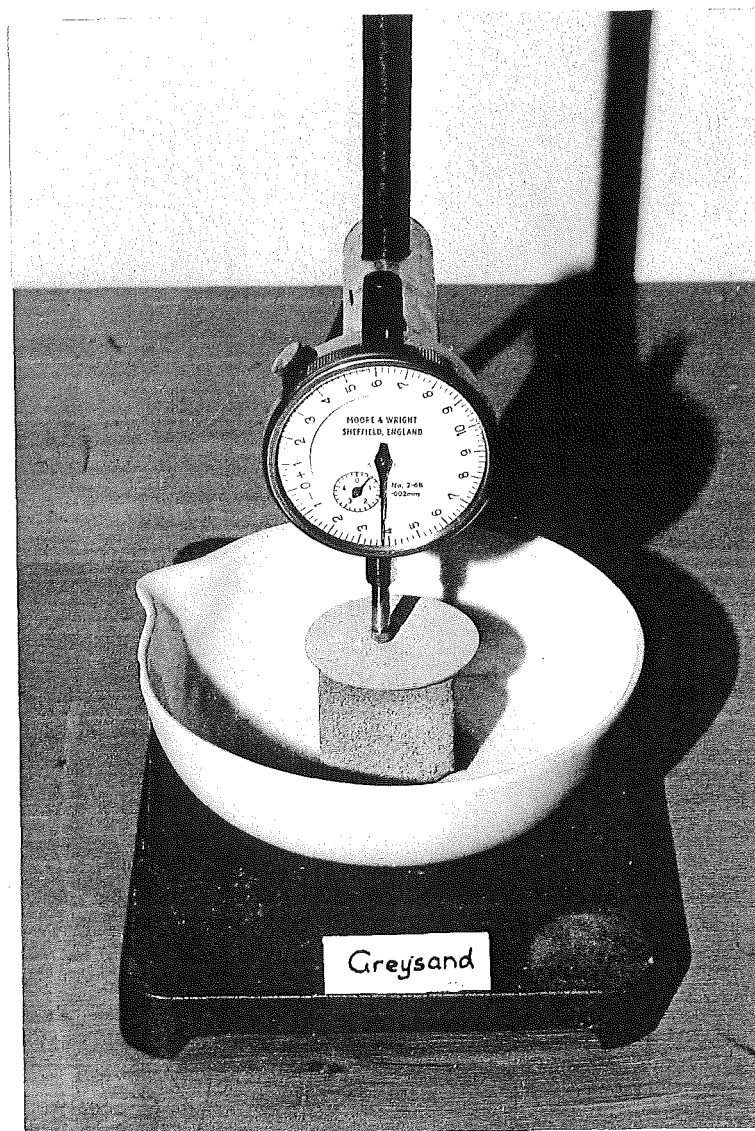


Plate 30: Uniaxial swelling strain testing apparatus. Sample is held between two porous plates in flat-bottomed dish and then immersed in water up to top porous plate.

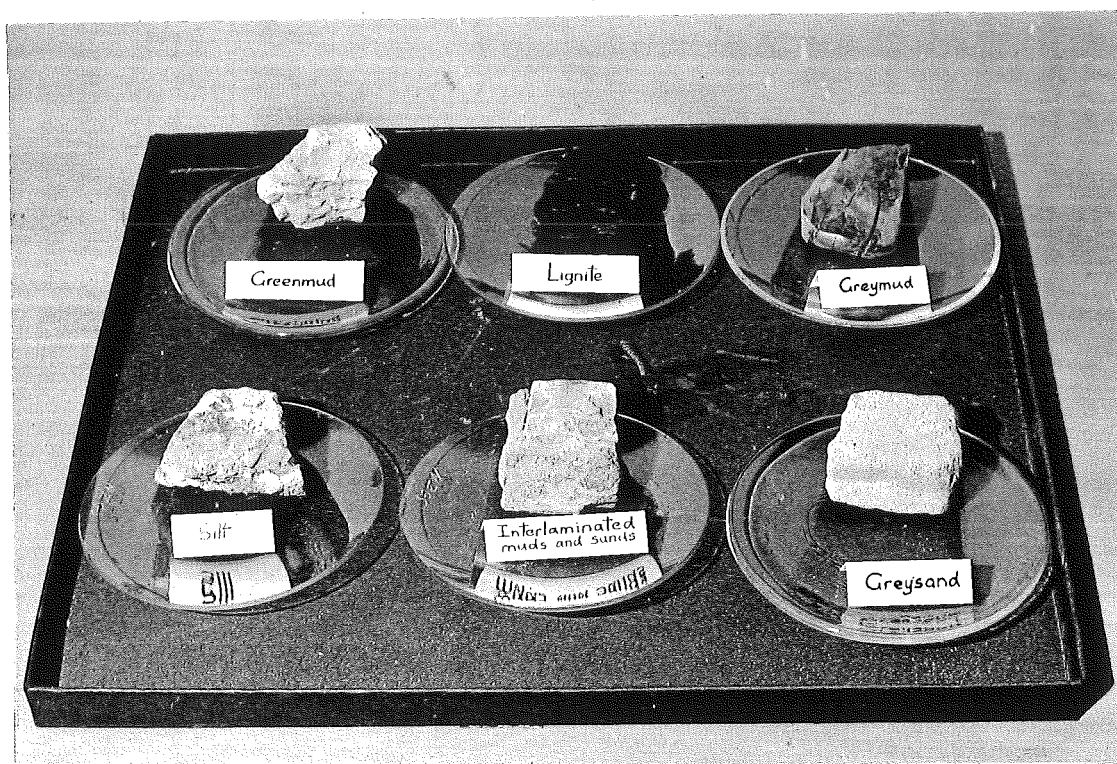


Plate 31a: Typical specimens selected for uniaxial swelling strain test.

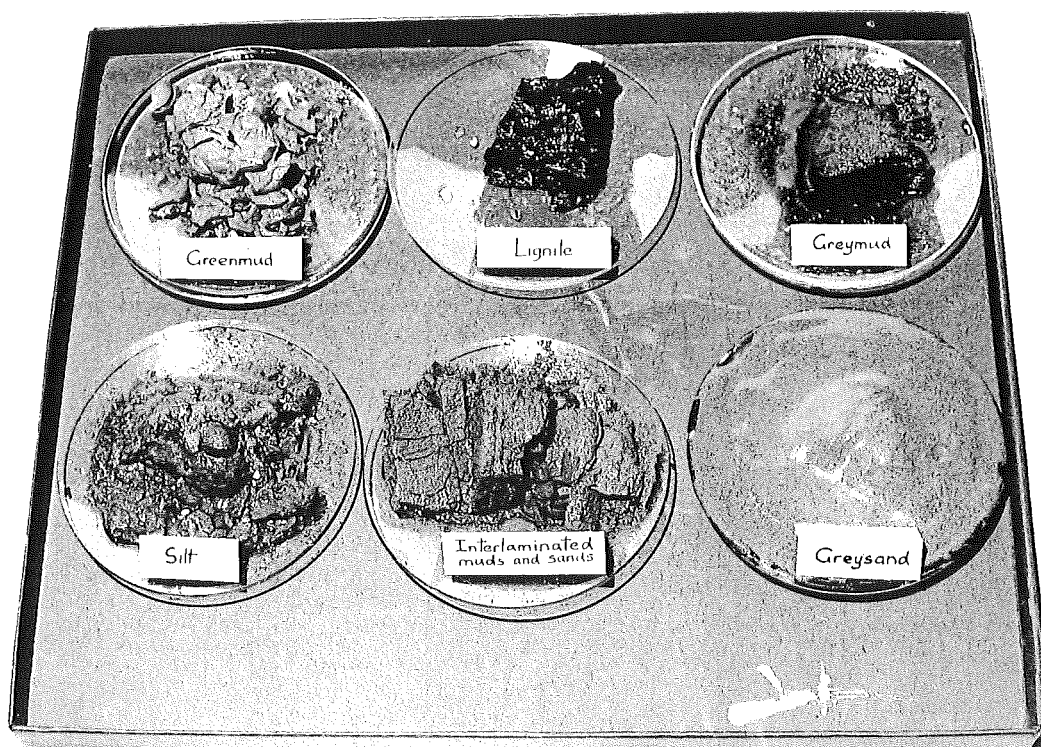


Plate 31b: Same specimens after testing.

before and after testing are shown in plates 31a and 31b. Expansion due to swelling was measured with time to relate rates of swelling with other properties. The total amount of expansion observed was used to calculate the uniaxial swelling strain coefficient, ϵ_s .

The slake durability index test is intended to assess the resistance offered by a rock sample to weakening and disintegration when subjected to changes in water content due to a standard drying and wetting cycle. The cycle consists of placing 10, roughly spherical, oven-dried lumps of material in a standard mesh cylinder then rotating the cylinder in a trough of water for 10 minutes. The amount retained within the cylinder after the slaking cycle is oven-dried and related to the original dry weight. The percentage retained after the first drying-wetting cycle is termed the slake durability index for cycle one (I_{d1}). The test required a special apparatus and this was constructed in the Geology Department, University of Canterbury, after Franklin's design (I.S.R.M., 1970). Some typical specimens are shown before and after testing in plates 32a and 32b.

Where practicable, groups of subsamples were tested, or several tests were run on the same sample and average values determined to reduce the effect of procedural irregularities. Such irregularities inevitably arose when several tests were being run in conjunction. It was often necessary to take more than one reading or continue with another phase of testing at the same time as another test reading was being made. The geotechnical property values are presented in Table 5.



Plate 32a: Typical specimens selected for slake durability testing.

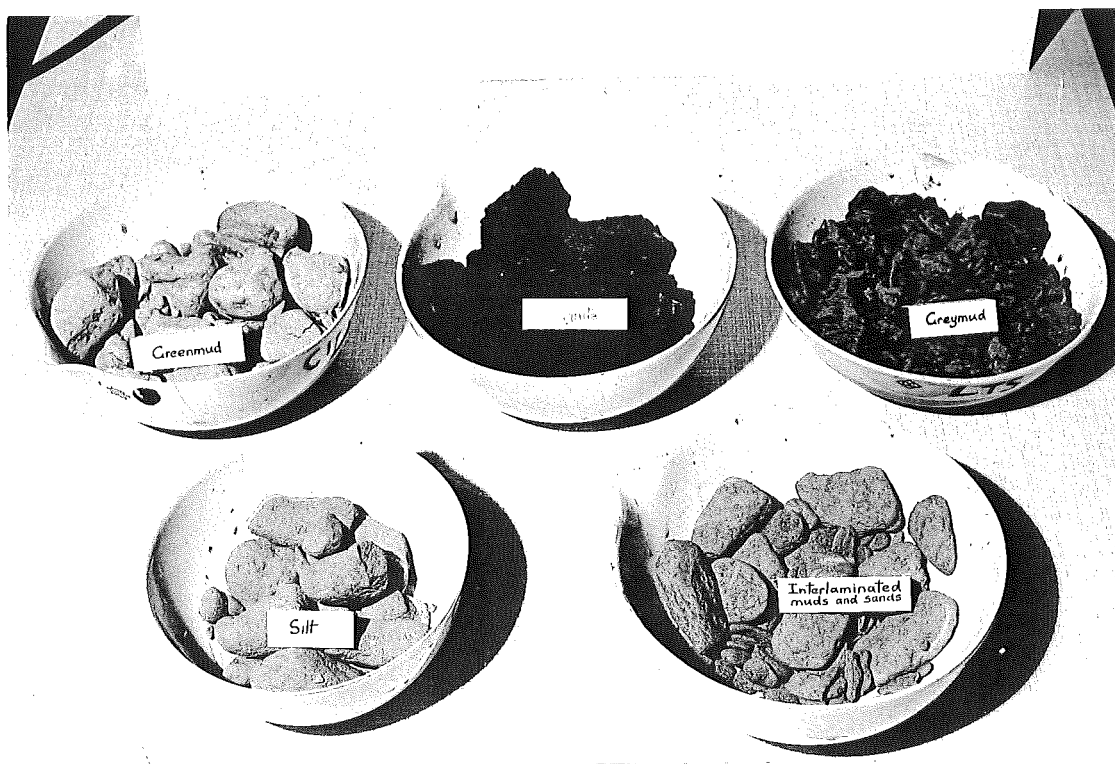


Plate 32b: Same specimens as above after one slaking cycle.

TABLE 5 GEOTECHNICAL PROPERTY VALUES FOR THE VARIOUS LITHOLOGICAL GROUPS

MPLE	W %	is %	n %	pg gm/cc	pd gm/cc	ps gm/cc	es %	Id ₁ %	Id ₂ %	Id ₃ %	LL %	PL %	PI %	LI %	CLAY %	SILT %	SAND %
OUP 1 SANDS																	
5	20.5	13.9	40.0	2.66	1.60	2.00									1.6	16.7	81.7
	16.5	11.5	43.2	2.67	1.52	1.95	0.01								1.8	18.8	79.4
	5.9	14.7	38.4	2.65	1.63	2.01	0.14								1.7	11.9	86.4
	7.6	17.9	42.9	2.66	1.52	1.95									5.3	38.6	56.1
	15.2	22.5	42.1	2.67	1.55	1.97									16.6	35.2	48.2
	13.1	16.1	41.3	2.66	1.56	1.98	0.08								5.4	24.2	70.4
	6.18	4.25	2.06	0.01	0.05	0.03									6.5	11.9	17.0
%	47	26	45	4	3	2									119	49	24
OUP 2 SILTY SANDS																	
(A)	15.0	15.8	38.8	2.67	1.63	2.02	0.04								3.5	33.1	63.4
(A)	13.0	15.3	39.0	2.67	1.63	2.02	1.1								3.6	33.1	63.4
	12.0	13.4	35.7	2.66	1.71	2.07	.35								3.7	56.0	40.3
	12.1	15.7	40.2	2.68	1.60	2.00	.39								5.8	41.4	52.8
A	14.9	14.3	38.2	2.66	1.66	2.04	.32								7.8	37.9	54.3
	13.4	14.9	38.4	2.67	1.65	2.03	0.44								4.9	42.7	52.4
	1.15	1.0	1.7	0.01	0.04	0.03	0.39								1.9	8.7	8.3
%	11	7	4	.4	3	1	90								39	20	16

Table 5 - Cont'd

SAMPLE	W	is	n	pg	pd	ps	es	Id ₁	Id ₂	Id ₃	LL	PL	PI	LL	CLAY	SILT	SAND
GROUP 3 SILTS																	
3(A)	15.0	13.5	36.1	2.66	1.68	2.04											
3A(B)	14.1	13.6	37.2	2.68	1.68	2.05	0.7										
3	9.9	13.3	36.9	2.66	1.68	2.05	0.2										
3A	27.0	16.2	40.3	2.67	1.59	1.48	1.0	51.6	46.4	30.1	49.8	25.4	24.4	- 0.02	1.2	98.3	0.5
3	25.0	18.9	42.9	2.66	1.52	1.95	1.7										
3S	20.5	15.6	36.5	2.66	1.69	2.05	.96	5.6	1.5	0	47.1	25.2	21.9	- .21	20.0	79.6	0.4
3B	10.7	10.1	32.1	2.68	1.82	2.14	0.3				21.9	21.3	0.6	-17.7	10.7	44.5	44.8
32	10.8	8.0	30.1	2.66	1.86	2.16	4.	52.5	29.5	13.2	50.7	23.7	27.1	- .50			
	16.6	13.6	36.5	2.67	1.69	1.99	1.27	36.6	25.8	14.4	42.4	23.9	18.5	- 4.6	11.6	69.4	19.0
	6.7	3.4	4.1	0.04	0.11	0.22	1.30				13.7	1.8	12.1		7.7	24.2	22.2
%	40	25	11	2	7	11	103				32	8	66		68	35	117
GROUP 4 INTERLAMINATED MUDS, SILTS AND SANDS																	
3A(B)	12.0	12.0	34.9	2.68	1.74	2.09	15.1	45.8	25.14	20.1	41.2	20.2	21.1	- .39	22.5	72.14	5.1
3(B)	13.1	10.4	32.5	2.67	1.80	2.13	11.3	44.2	17.7	5.4	37.5	20.8	16.7	- .47	19.6	68.3	12.1
3	15.9	11.5	22.8	2.67	1.77	2.11	8.0	46.8	9.9	0.2	46.2	20.1	26.1	- .16	14.3	75.2	10.5
3	16.5	9.5	31.4	2.66	1.82	2.13	13.0	29.2	14.9	8.0	36.7	19.8	17.3	- .34	15.5	12.9	11.6

Table 5 - Cont'd

SAMPLE	W	is	n	pg	pd	ps	es	Id ₁	Id ₂	Id ₃	LL	PL	PI	LI	CLAY	SILT	SAND	
GROUP 4 - Continued																		
3A	13.5	9.7	32.7	2.67	1.80	2.13	6.3	59.9	41.4	25.7	52.5	26.0	26.5	-	.47	14.4	83.8	1.8
4B	20.0	11.0	25.8	2.67	1.98	2.24	0.9				52.5	32.4	20.0	-	.62	4.1	95.2	0.7
11	15.2	10.6	33.2	2.68	1.79	2.12	13.6	29.4	13.8	4.3	45.9	24.4	21.5	-	.40	18.5	72.2	9.3
HS1	15.1	13.1	35.8	2.67	1.73	2.09	7.7	54.3	29.4	16.1	29.3	20.9	8.4	-	.70	19.8	77.5	2.7
\bar{x}	15.2	11.0	31.2	2.67	1.82	2.13	9.5	44.2	21.8	11.4	42.7	20.6	19.7	-0.1	16.1	69.7	6.7	
s	2.5	1.2	4.5	0.01	0.07	0.05	4.7	11.6	11.0	9.4	8.1	9.07	5.8	-	.49	5.6	24.4	4.7
V%	16	11	15	4	4	2	49	26	50	82	19	44	29	490	35	35	70	
GROUP 5 - MUDS																		
7C	18.7	8.2	31.0	2.72	1.88	2.17	13.5	88.5	78.8	52.8	59.1	31.7	27.4	-	.45	32.0	67.8	0.2
7A	7.3	7.8	30.1	2.73	1.88	2.19	10.6	72.5	58.3	44.9	51.3	23.1	28.2	-	.61	31.8	67.8	0.4
11	10.6	13.9	37.1	2.71	1.70	2.07	18.9	56.8	26.0	0	56.8	26.0	30.0	-	.52	12.7	87.2	0.1
4A	13.5	9.4	31.7	2.70	1.84	2.16	4.0	65.5	34.0	3.2	50.3	35.1	15.2	-	.10	19.4	80.2	0.4
HS4	15.8	10.1	39.2	2.75	1.67	2.06	3.5	69.3	64.8	64.3	61.3	27.0	34.3	-	.71	36.3	63.6	0.1
\bar{x}	13.2	9.9	33.8	2.72	1.79	2.13	10.1	70.5	52.4	33.0	55.8	28.6	27.0	-	.48	26.4	73.3	0.24
s	4.4	2.4	4.1	0.02	0.1	0.06	6.5	11.6	21.9	29.5	4.8	4.8	7.1		.23	9.9	9.9	0.15
V%	34	25	12	1	6	3	65	17	42	89	9	17	26		49	38	14	63

The grain size analyses and sand grain mineralogy determination were carried out in accordance with the Geology Department's recommended procedures for undergraduates. The grain size analyses are summarised briefly as sand, silt and clay fractions in table 5 and a more complete picture of the grain size distribution is given in the gradation curves in Appendix 4. The sand grain mineralogy percentages are shown in Table 6. The clay fractions of a limited number of specimens were analysed by Messrs D. Bell and R. Thompson using the X-ray diffraction technique and these are shown at the bottom of Table 6.

A few unconsolidated undrained triaxial tests were carried out in the School of Engineering's Soil Mechanics Laboratory following the laboratory's recommended procedures for undergraduates. The results are presented in Table 7.

TABLE 6

Sand grain mineral percentages for
the various lithology groups

A-spar P-spar clay agg	alkali feldspar plagioclase feldspar clay aggregates	heavys micas glauc.	heavy minerals (mostly magnetite mostly biotite glauc. glauconite)				
	QUARTZ	A-SPAR.	P-SPAR	CLAY	HEAVYS	MICAS	GLAUC. AGG.
<u>Group 1</u>	<u>Sands</u>						
HS5	79	4	4	7	5	1	-
9C	69	5	6	5	9	-	6
8	51	10	16	4	9	4	4
U2	62	9	3	5	11	-	10
U3	78	5	5	4	5	-	2

Table 6 - Cont'd

	QUARTZ	A-SPAR	P-SPAR	CLAY AGG.	HEAVYS	MICAS	GLAUC.
<hr/>							
<u>Group 2</u> Silty Sands							
1A(a)	70	3	4	4	10	1	7
2A(a)	69	2	4	15	5	-	5
5A	55	5	10	7	14	-	9
5B	60	2	9	7	10	2	10
10A	59	4	9	6	11	1	10
 <u>Group 3</u> Silts							
1B(A)	65	7	5	4	8	-	11
2A(b)	64	12	8	7	5	-	4
3B	48	13	4	9	22	-	5
10B	60	10	10	5	7	-	8
HS2*	45	8	10	29	2	-	6
 <u>Group 4</u> Interlaminated Muds, Silts and Sands							
1A(b)*	50	3	5	37	2	-	3
1B(b)*	36	4	4	31	5	-	20
1C	32	6	7	47	5	-	3
3A	27	14	9	29	13	-	8
4B*	26	1	4	64	3	-	2
11	49	3	3	37	7	-	1
HS1*	37	2	2	33	16	-	12
 <u>Group 5</u> Muds							
7C*	10	7	5	64	3	-	11
7A*	38	4	5	27	10	-	16
4A*	35	9	3	56	9	-	3

*The following minerals were identified in the clay fraction by X-ray diffraction: Quartz, mica (illite?) kaolinite and montmorillonite.

TABLE 7

Cohesion intercepts from unconsolidated undrained triaxial tests ($\phi = 0^\circ$) on some Enys Formation sediments

<u>Lithology</u>	<u>Location</u>	<u>Cohesion kPa</u>
Greenmud	Unit b, Lower Silt member, (sample BR7a, figure 9)	330
Greymud	Unit b, Lower Silt member (sample BR7c, figure 9)	449
Greysand	Middle Sand member (sample BR10a, figure 9)	395

4.6 INTERPRETATION AND SIGNIFICANCE OF GEOTECHNICAL TESTING

4.6.1 Reliability of Results:

(a) Natural water content: The values obtained depend on such factors as: time of day of sampling, proximity to water table, proximity to ground surface, and type of ground cover. The samples were all collected in late summer and mostly from outcrops which required only minor excavation to expose fresh, unweathered material. Some samples had to be collected from stream beds (below the water table) as they provided the only outcrops least affected by weathering. Some slight moisture loss is to be expected between the time of sampling and the time of testing.

(b) Saturation water content and porosity: In some samples the saturation water content value is less than the natural water content value. By definition this should never happen, but the discrepancy can perhaps be explained by the use of the toluol saturation method in determining the

former value. In this method, less fluid is absorbed into the sample because of the possible reasons advanced in section 4.5.3. As a result, the values for saturation water content and porosity are expected to be slightly less than their true values.

(c) Densities: For the same reasons as those mentioned in section 4.6.1(b) above, the densities are also expected to have slightly lower values than from tests using water as the saturating fluid.

(d) Uniaxial swelling strain and slake durability: The uniaxial swelling strain test is a particularly simple and easily repeatable index test. Although a small but finite swelling strain can be obtained from a sand it is debateable whether this is indicative of the presence of swelling clays (see section 4.6.3(d) and hence a true swelling strain.

The slake durability testing apparatus was built with a gearing ratio giving a slightly higher, final drive speed than that recommended by the I.S.R.M. procedures. The effects of the higher drive speed were minimised by allowing a shorter period of wetting and rotation. The reliability of the index values thus derived are believed to be close to values which would be obtained using a commercially made apparatus.

(e) Atterberg limits: The procedural difficulties associated with this method are such that no precise value of liquid or plastic limit can be obtained for a particular soil, but rather a range of values is more representative.

Irregularities arose due to the variable amounts of dehydration, rehydration and curing the specimen underwent. It was almost impossible to replicate these conditions from test to test and variation in values results. For a more complete description of the problems associated with Atterberg limit determination the reader is referred to the ASTM Symposium on soil specimen preparation for laboratory testing (1975).

(f) Grain size analysis: Naturally-occurring clay aggregates, incomplete sample disaggregation and floc formation in the settling tube are all thought to result in grain size distribution curves weighted towards the coarser fractions. The sand grain mineralogy study revealed a large proportion (up to two-thirds) of clay aggregates, especially within the more argillaceous sediments. Also, some samples (for example Br6A, Br6B) displayed properties which were inconsistent with their low clay fraction (see Table 5), suggesting that clay aggregates were responsible for the lower clay fraction. Thus, when studying the geotechnical property values interpretation may be aided if a higher clay fraction is assumed.

(g) Grain mineralogy: The staining of the sand fraction did not differentiate between quartz and feldspars as clearly as had hoped, possibly due to a grain coating of either clay, iron, or superficial feldspar weathering not allowing the stain to react with the mineral. The quartz percentages and the relative feldspar percentages are thought to be reliable to within $\pm 10\%$.

4.6.2 Variation of Results and Significance to Properties:

As would be expected from the considerable lithological variation (see section 4.2), the geotechnical properties also vary greatly. The range of values for all the samples tested is seen to reduce when the samples are arranged into the following groups:

- Group (1) Sands
- " (2) Silty sands
- " (3) Silts
- " (4) Interlaminated muds, silts and sands
- " (5) Mud

Group 3 consists of silts and other similar materials which are less suited to any other group.

The amount of variation within these groups can be expressed by the coefficient of variation (V), which is defined as the quotient of the mean and the standard deviation. The amount of variation deemed to be unacceptable has been arbitrarily set at 50% and those properties with V values over 50% can be considered unsuitable for interpretation.

Variation of properties mostly arose due to the variability of the lithologies within each group and the variability of the bed from which the sample was taken.

The mapping of the Broken River-Hogsback Stream-Trout Stream exposures revealed a marked lateral diversity within each member. Road cuttings and outcrops in the Lower Sand member at Broken River near the highway bridge provide a good example of lateral variation within a short distance. Similarly, outcrops in Hogsback Stream, Trout Stream and Broken River are difficult to correlate because of the variation.

A quick reconnaissance in Thomas River showed that correlation of the sandy members was easiest but individual beds could not be traced. Whether this variation represents a lateral facies change or is a reflection of changing patterns in sedimentation is difficult to say. The most common variations are the local increase in cementation in sand beds, and lenses or channels of fine sand, carbonaceous sediments or lignite in the argillaceous sediments.

The limitations of the sampling and retrieval procedures (see section 4.5.2) and the reliability of the testing procedures also give rise to property variation.

Referring to table 5, it can be seen that the properties associated with the more argillaceous sediments (for example e_s , I_d , LL and PL) are the most variable. The variation can most likely be explained by the variable nature of the clay fraction, clay mineralogy, structure and texture. More pertinent reasons for variability can be found for each property.

Values for water content (w) are highly variable, mainly due to the difficulties in gaining a sample typical of the in situ water content (see section 4.5.4(a)). The main criterion in sampling was gaining a specimen representative of lithology and a characteristic water content was usually not possible at the same time. Saturation water content (i_s) values are determined from fully-saturated samples. This condition is found naturally in sediments located beneath the water table and can be easily and repeatably obtained in the laboratory. For this reason, the i_s values are not as variable

as the water content values. However the porosity (n) values are significantly less variable than the i_s values. The difference is difficult to reconcile as the two properties express essentially the same relationship between voids and bulk; the saturation water content in terms of weight and porosity in terms of volume. Both properties display increasing values with decreasing depth in the lithologic column. This implies that part of the variation in i_s and n can be accounted for by the varying amount of consolidation the sediments have undergone.

Densities are highly consistent, not only within each group but throughout the entire range of lithologies tested. The relatively similar mineral assemblages (see table 6) within each group and the similar solid densities (ρ_g) of the minerals (see table 8) give rise to the consistent results. Dry and saturated bulk densities are more variable than solid densities because the volumetric relationship between voids and bulk is dependent on the amount of consolidation the sediment has undergone.

Values for swelling strain are extremely variable and very little information can be interpreted from the results. The reason may be due to swelling being measured in varying directions. Where possible, samples were oriented so that swelling was measured in a direction perpendicular to bedding. However only the interlaminated muds and sands displayed distinct bedding in laboratory samples and it is significant that Group 4 has the lowest coefficient of variation for this property.

The slake durability indices display varying V values. In general the amount of variation increases with the number of slaking cycles suggesting that the variation is due in part to the testing procedure. It is not clear at this stage what facet of the testing procedure is responsible for the variation. The Atterberg limits require an experienced operator to gain repeatable values and part of the variation encountered is probably due to the author's lack of experience in these tests. Accuracy of results is affected by the variable testing procedures mentioned in section 4.6.1.(e). The properties of plasticity index and liquidity index are derived from liquid limit, plastic limit and natural water content and the coefficients of variation are a combination of each individual property.

The clay, silt and sand fractions display large amounts of variation within each group which reinforces the author's earlier opinion, derived from field mapping, about the diversity of the Enys Formation sediments (see section 4.2).

4.6.3 Discussion of geotechnical properties and significance on slope stability:

(a) Natural and saturation water content: Natural water contents can range from 0% in exceptionally dry situations to the saturation water content (is) below the water table.

Table 5 shows that most of the specimens have values close to the saturation water content indicating that the water table is not far below the surface. Some New Zealand volcanic ash soils containing the clay minerals halloysite and allophane have been found to have water contents as high as 200% (A. Olsen* Pers. comm.). The Enys Formation

sediments do not display any exceptional values and indeed the range shown in table 5 is typical for most soils.

Because of their age and induration, the Enys Formation sediments have relatively high i_s values and on the basis of Duncan's (1962) classification system, they can be described as weakly cemented - weakly compact rocks.

Wilun and Starzewski (volume 1, 1975) deduced that the strength parameter, cohesion, was dependent on the number of particle contacts within a unit volume of soil. The number of particle contacts was in turn dependent on the water content. Their deductions have been confirmed by the experimental evidence of Bjerrum (vide 1954) presented in figure 13.

(b) Porosity: The Enys sediments have relatively high porosity values, generally between 30% and 40% although a calcite-cemented sand from the Calcareous member was found to have the low value of 24% and a lignite sample (unit b Lower Silt member) had the high porosity value of 88%.

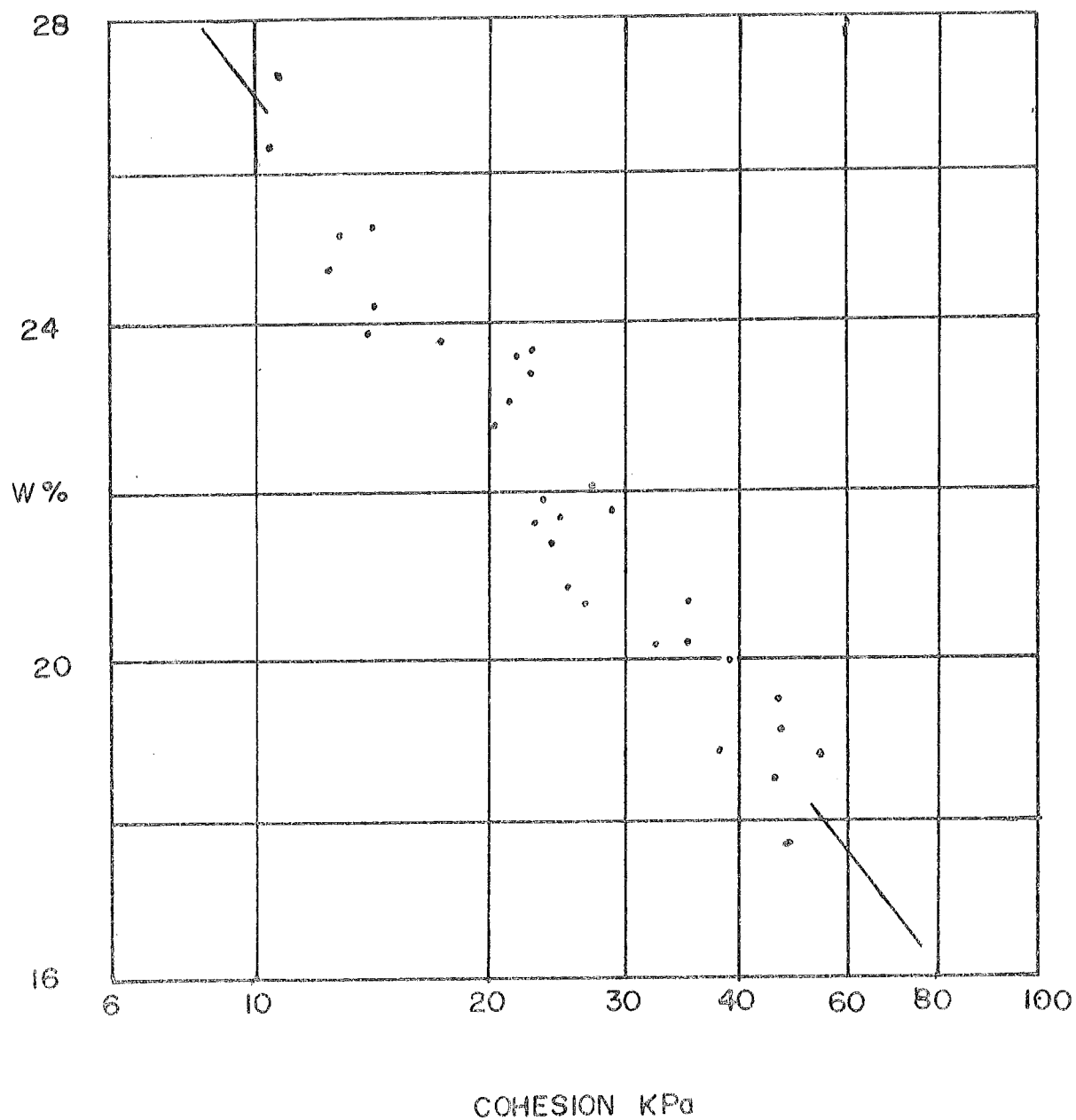
In general, soils of low porosity are considered to be of low permeability, however the presence of joints and other structural discontinuities in the ground would considerably raise the coefficient of permeability (k).

The presence of pores in the fabric of a soil significantly decreases the strength parameters and increases its deformability (Duncan, 1962).

FIGURE 13

RELATIONSHIP BETWEEN WATER CONTENT W AND COHESION

(WILUN AND STAŹZEWSKI 1975 vide BJERRUM 1954)



(c) Densities: Densities are useful for deriving other physical properties, and for comparing and correlating with the index properties. Physical properties may be related to each other by the following interdependence equations (Duncan, 1962):

$$\rho_n = (1+w) \rho_d$$

$$\rho_g = \frac{\rho_d}{1-n}$$

$$\rho_d = \frac{\rho_s}{1+is}$$

$$n = is \rho_d$$

where

ρ = mass density

subscripts; s, n and d refer to the weights and bulk volumes in a saturated, natural and dry condition respectively

subscript w; refers to water

subscript g; refers to the solid mineral grain fraction

In slope stability analyses the unit weight γ is commonly used in calculating forces and is proportional to the bulk density by the simple relationship:

$$\gamma = \rho g$$

where g is the acceleration due to gravity (9.81 m/s^2).

Because the solid density of all the common constituent minerals is much the same (see table 8), the ρ values of the different lithologies are also generally consistent.

TABLE 8

Solid Grain Specific Gravities for
Mineral Constituents
(after Terzaghi & Peck, 1967)

Quartz	2.66	Kaolinite	2.60 - 2.63
Orthoclase	2.57	Illite	2.60
Plagioclase	2.62 - 2.76	Montmorillonite	2.40
Augite	3.20 - 3.40	Chlorite	2.60 - 3.00
Hornblende	3.20 - 3.50	Micas	2.70 - 3.10
Magnetite	5.17	Calcite	2.72

(d) Uniaxial swelling strain index: Sediments with a predominant sand content show only a slight volume change on soaking followed by rapid disintegration. Sediments with an appreciable clay content, swell on wetting; the amount of expansion being dependent on many factors. Of most importance are the types and amount of clay minerals present and their structure within the soil.

Soils which have an oriented structure (i.e. platy minerals with parallel alignment) would be expected to show greater swelling than soils with a random structure. The laminated silts and muds (Group 4) are known to have an oriented structure and thus have a higher uniaxial swelling strain index (ϵ_s) than some of the massive muds like the greenmud (sample HS4) of Hogsback Stream.

Mitchell (1976) relates an increase in swelling with increasing surface area of the clay particles so that potential expansion of the clay minerals decreases in the following order: montmorillonite, illite, halloysite

and kaolinite. It is probable that the swelling muds in Groups 4 and 5 contain at least some proportions of these minerals in the clay fraction.

The uniaxial swelling strain index has been found to be related to the original dry bulk density for the Enys Formation sediments. A plot of the two properties is shown in figure 14 and it can be seen that ϵ_s increases with ρ_d .

The rate of expansion may be indicative of the specimen's permeability as table 9 shows.

TABLE 9

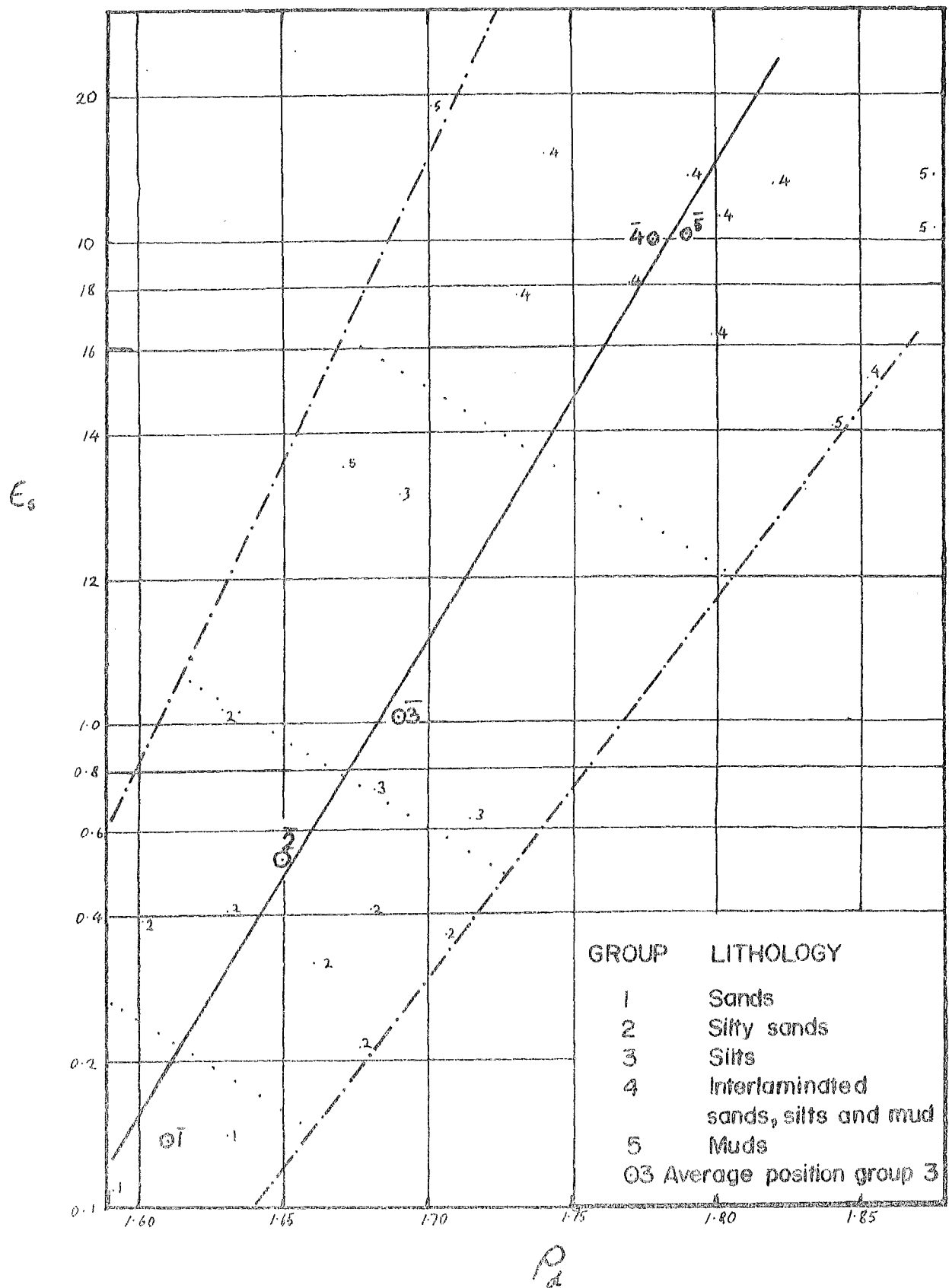
Relation between rate of expansion
and permeability
(k values from Terzaghi & Peck, 1967)

Group	Rate of Expansion (cm/sec)	Soil Description	Degree of Permeability	k cm/sec
1	$10^{-1} - 10^{-2}$	Fine Sands	Medium	$10^{-2} - 10^{-3}$
2	10^{-2}	Silty Sands		$\approx 10^{-3}$
3	$10^{-3} - 10^{-4}$	Silts	Low	$10^{-3} - 10^{-5}$
4	10^{-4}	Interlaminated Muds & Silts		$\approx 10^{-4}$
5	$10^{-5} - 10^{-6}$	Muds	Very Low	10^{-5}

A lignite sample gave the highest ϵ_s values (24%) and could be expected to have a medium to low permeability on the basis of its rate of expansion. The lignite's exceptional value does not seem to be due to an appreciable clay content but is more likely the result of an unusual structure. The very low dry bulk density and exceptionally high porosity indicate

Figure 14:

PLOT OF SWELLING INDEX AGAINST DRY DENSITY



that the carbonaceous matter could have a loose 'honeycomb' structure which contracts markedly on drying.

The behaviour of the samples in laboratory unconfined swelling tests must not be confused with the likely behaviour of the same material in the ground, for two reasons. Firstly, the ϵ_s values were determined by saturating oven-dried specimens; a condition that is unlikely to arise in the field. Secondly, Grim (1962) reports that confining pressures, due to overburden, increase with depth so that at a level not far below the surface, the confining pressure overcomes any swelling stress likely to develop. Thus, no swelling strain would manifest itself except, perhaps, where joints and fissures were available to take up any expansion.

A number of specimens sampled in the vicinity of landslides showed above-average values for swelling strain index. For instance, specimens BrU, Br7A, Br7C and the lignite sample were all from unit b in the Lower Silt member (see section 4.2.3). The beds in unit b lie beneath a very large landslide in Broken River at a depth where it is suspected they form part of the failure surface (see Chapter 5). It is possible that a high swelling strain may affect slope stability indirectly through its relation to permeability, structure and dry bulk density. However testing has not been carried out to the extent where conclusive results can be drawn.

(e) Slake durability index: As with the swelling strain index, the slake-durability index of a laboratory specimen cannot necessarily be indicative of in situ conditions.

Field observations show that the sand outcrops do not deteriorate as rapidly as their slake durability index ($I_{dl} = 0 - 1\%$) would suggest. Exposed greysand tends to weather to a light yellow brown due to the coating of grains by such weathering products as oxides and clay minerals. These products form weak bonds between grains which help resist deterioration by cyclic wetting and drying. For the argillaceous soils the slake durability index gives a good indication of comparative deterioration, and susceptibility to superficial mass movement.

The slake durability test is similar to the uniaxial swelling strain test in that values are indicative of the sample's permeability. Highly permeable sediments, such as those in Groups 1 and 2 allow water to penetrate so quickly that they seldom last one slaking cycle. Dense and impermeable muds, on the other hand, can last three wetting and drying cycles without serious deterioration. With the common factor of permeability affecting both the slake durability test and the swelling strain test a relation between the two properties would be expected to exist. However only an approximate trend (I_d increases with increasing e_s) is apparent for the values obtained and more results will be required if a definite relationship is to emerge. Alternatively, no definite relationship may exist and different controlling factors may be responsible for each property. Unfortunately, the swelling strain test and the slake durability test are seldom performed in New Zealand and no values were obtained for comparison with the results in this study.

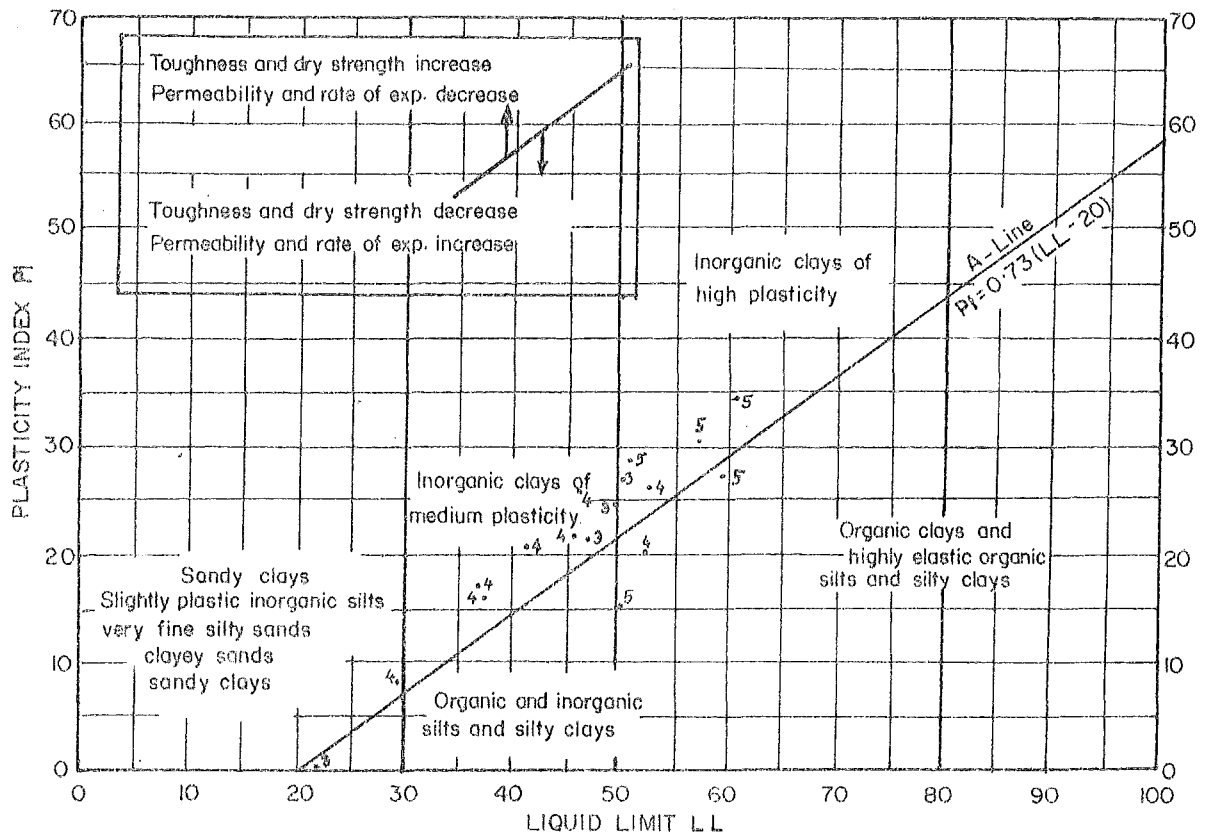
(f) Atterberg limits: For the purposes of classification, each soil can be plotted on the plasticity chart (see figure 15) as a function of its plasticity index and liquid limit. The chart gives a comparative indication of the quantity of clay minerals present in relation to its Atterberg limits.

Grim (1962) has found that a liquid limit value of over 50% usually indicates the presence of montmorillonite. Liquid limits below 50% occur for sediments with kaolinite, illite and chlorite as the predominant clay minerals and for sediments with increasing amounts of coarser fractions or non-clay minerals. None of the Enys Formation soils display exceptional properties although the greenmuds of the Glauconitic, Hogsback and the Lower Silt members do show appreciable plasticity. It can be seen from Table 5 that Atterberg limits increase with increasing clay content and it is safe to assume that they also increase with increasing clay mineral content.

Remoulding a sample has the effect of decreasing its shear strength (Terzaghi and Peck, 1967) so that material disturbed by a landslide suffers a significant loss of strength. This strength decrease is shown by many of the landslides at Broken River which have small slumps developed within the landslide material. An increase in water content from the plastic limit through to the liquid limit also decreases the shear strength (Terzaghi and Peck, 1967).

The range of 20-60% for the liquid limits of Enys Formation sediments is not unusual for soils. Natural soils

FIGURE 15
PLASTICITY CHART
(after A. Casagrande)



- Group 3 Silts
Group 4 Interlaminated silts and muds
Group 5 Muds

with LL values over 100% are not uncommon and LL values between 100 and 900% are possible for the clay mineral montmorillonite (Mitchell, 1976). Similar high values exist for other clay minerals and their plastic limits are also very much higher than the samples tested.

From theoretical concepts, Grim (1962) predicted that the cohesion would increase with increasing plasticity index and that the coefficient of internal friction would decrease. From results of drained triaxial tests, Kanji (1974) relates the plasticity index to the angle of shearing resistance, ϕ with figure 16. A similar relationship has been found for plasticity index, liquid limit and the residual friction angle (Mitchell, 1976) - see figure 17.

As the water content of any remoulded, cohesive soil is increased from the plastic limit to the liquid limit, an increase in volume must accompany the moisture increase. Thus the plasticity index may be related to the swelling strain index by table 10.

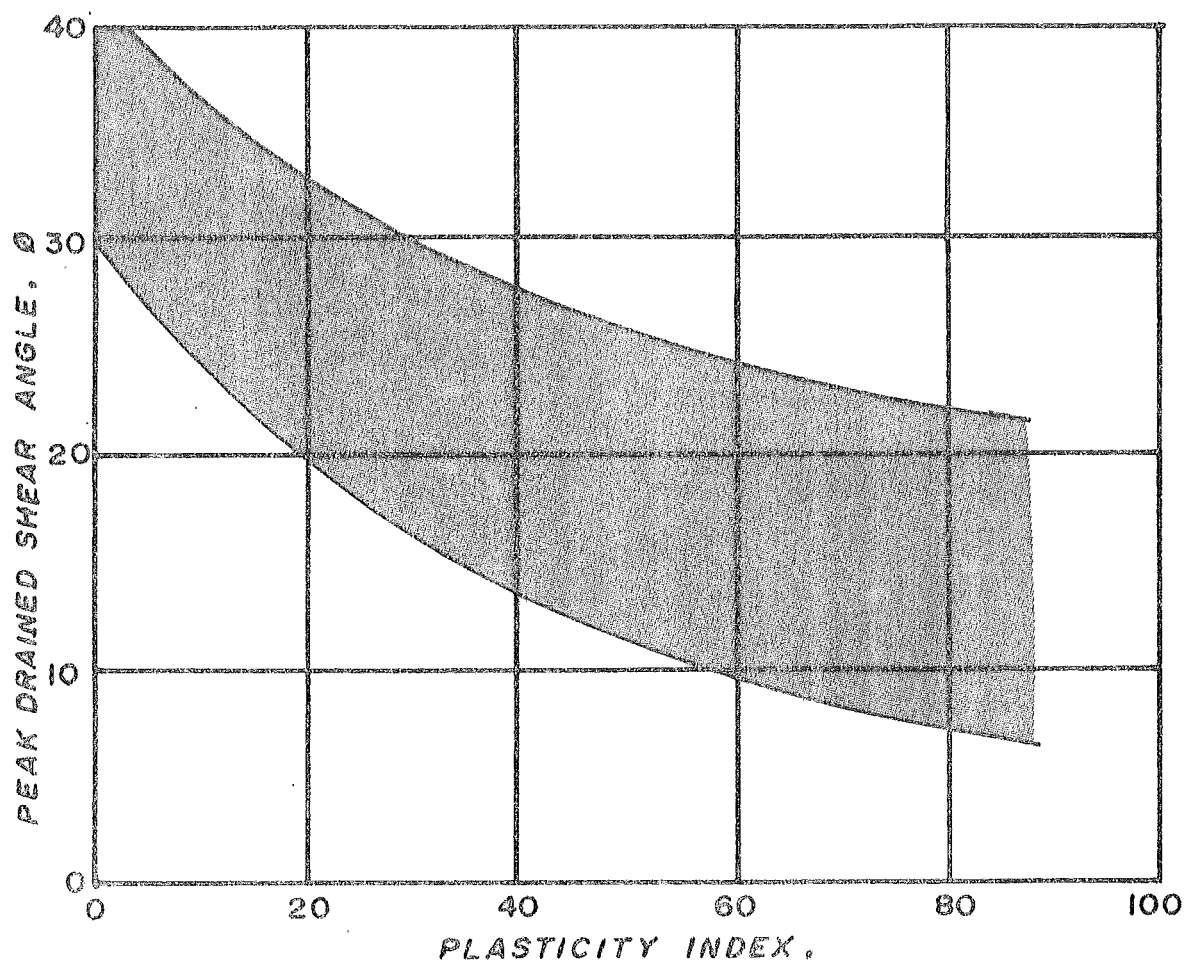
TABLE 10

Approximate relation between plasticity
Index and Swelling Strain Index ϵ_s

PI %	Example	Swelling Capacity	ϵ_s %
0-15	Br10B	Low	0-1
10-35	HS2, Br1C, 2B, 3A	Medium	1-10
20-55	Br1A(B), 11, 7C, U1	High	10-25
35+		Very high	25+

FIGURE 16

(After . Kanji, 1974)

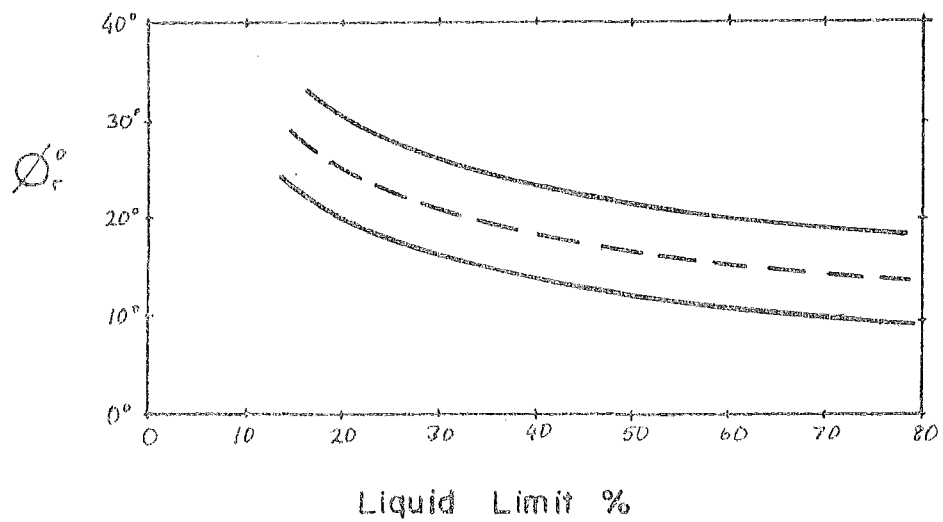
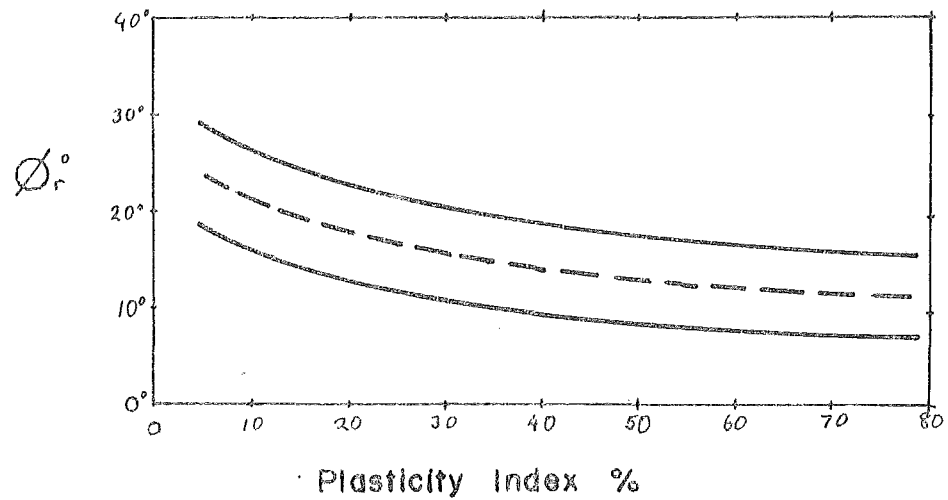


ϕ_{peak} IS DEPENDENT ON CONFINING STRESS
AND SOIL STRUCTURE ; HENCE VERTICAL SPREAD.

FIGURE 17

RELATIONSHIP BETWEEN PLASTICITY INDEX, LIQUID
LIMIT AND RESIDUAL FRICTION ANGLE, (ϕ_r).

(MITCHELL, 1976)



The liquidity index LI is an expression of the natural water content of a soil in relation to its limit values. Soils with a liquidity index greater than unity have a natural water content greater than the liquid limit and (according to Terzaghi and Peck, 1967) may be transformed into a thick viscous slurry on remoulding (for example by mass movement).

For cohesive soils, the LI value is indicative of the stress history of the soil (Mitchell, 1976). Normally consolidated clays may have liquidity indices of about unity, while overconsolidated clays may have LI values approaching zero. The negative values of LI obtained for the Enys Formation muds represent a heavily overconsolidated state, a condition supported by the dense packing of the sands.

Atterberg limits for cohesionless, granular soils are meaningless even though values may be found using the liquid limit device and the plasticity test. In such cases, the plasticity is due to an apparent cohesion from capillary pressures.

(g) Grain size analysis: It was originally thought that most of the geotechnical properties of the Enys sediments could be related to the grain size distribution (or gradation). However, the testing has shown that very little correlation could be found between gradation and the other properties. It is thought that factors such as mineralogy, grain shape, fabric, and stress history of the soil directly influence the geotechnical properties more than the grain size distribution.

For sands, Lambe and Whitman (1969) have related the effect of grain shape, grading and degrees of consolidation to the friction angle by way of table 11.

TABLE 11
Effect of angularity and grading on peak
friction angle ϕ
(Lambe and Whitman, 1969)

Shape and grading	Loose	Dense
Rounded, uniform	30°	37°
Rounded, well graded	39°	40°
Angular, uniform	35°	43°
Angular, well graded	39°	45°

A broad relationship (Mitchell, 1976) exists between the shear strength parameters and the percentage clay fraction, but a wide and complex range of factors affecting the mode of failure makes this a tentative relationship only. In general, the angle of shearing resistance ϕ , decreases with increasing clay content. For a given effective pressure of about 5 kg/cm², Terzaghi and Peck, (1967) give the relationship presented in table 12.

TABLE 12
Representative values of ϕ
for dense sands and silts
(Terzaghi & Peck, 1967)

Material	ϕ degrees
Sandy gravels	50
Sand, angular grains, well graded	45
Silty sand	30-34

Mitchell (1970) also describes how the cohesion decreases with decreasing clay content, for any given clay type of similar structure and carrying the same exchangeable cations. Sands are normally regarded as a cohesionless material but local cementation or capillary pressures may give rise to an apparent cohesion. This type of cohesion may also be found in silts and clays (Mitchell, 1976).

(h) Grain mineralogy: The coarser fraction of the Enys Formation sediments consists mostly of grains of quartz, feldspar and minor amounts of other stable minerals (see table 6) which in themselves do not contribute to slope failures. Quartz, mica (illite?), kaolinite and montmorillonite were found in the clay fractions of all the specimens tested by the X-ray diffraction technique and in particular specimens Br 7c and HS4 (greenmuds). There is abundant evidence of slope instability (particularly in Hogsback Stream - see figure 9) in sediments associated with these greenmuds. Mitchell (1976) relates strength to composition by the use of failure envelopes. The curves show that the friction angle is greatest for the non-clay mineral quartz followed, in descending order, by kaolinite, illite and montmorillonite.

The presence of clay minerals, even in very small quantities gives rise to the cohesive nature of fine grained soils.

4.6.4 Conclusions from Geotechnical Testing:

A large amount of variation in most property values was found - a common feature of geotechnical testing. Much of this variation reflects the variable nature of the Enys Formation

although variability due to the sampling and testing procedures cannot be discounted.

For the purposes of classification, the sediments can be described as weakly cemented - weakly compact rocks or heavily overconsolidated soils.

The testing did not reveal the presence of any sediments with exceptional properties, although it is possible that a critical layer was not exposed and hence not sampled. A similar layer is known to exist, unit b in the Lower Silt member (see section 4.2.3), and the three sampled beds do exhibit above average values (specimens Br 7a, 7b and 7c). It is thought that this layer forms part of the failure plane of a large landslide in Broken River (see Chapter 5).

The geotechnical properties can be used to indirectly infer the magnitude of the strength parameters. For this purpose, the sediments can be considered as either cohesive soils or cohesionless soils. Cohesive soils (sediments from Groups 2, 3, 4 and 5) are estimated to have a low friction angle of between 15° and 30° (from figure 16) and can rely on a significant amount of cohesion for strength. The cohesionless soils (sediments from Groups 1 and 2) are mostly frictional materials; a range of friction angles between 30° and 55° being possible for sediments ranging from silts to gravels (tables 11 and 12). Cohesion is usually small or non-existent although it may be a significant part of strength where local capillary pressures or cementation gives rise to an apparent cohesion.

When considering values of strength parameters the conditions under which a soil is likely to fail must be considered. Cohesion and friction angle are affected by rates of loading (time to failure) and changes in water content (drainage).

With very slow rates of loading (such as gradual increase in slope height through river erosion) there is no change in the original strength parameters. On the other hand, faster rates of loading such as construction of a batter or embankment often leaves the groundwater elevated and high porewater pressures may develop in the short-term case. With granular cohesionless soils the groundwater is able to drain away rapidly, but with the more impermeable cohesive soils, porewater pressures will develop. With very fast rates of loading (for example: a prolonged rainstorm rapidly raising the groundwater level, dynamic loading by an earthquake, or sudden shearing through landslide movement), porewater pressures may increase rapidly. Terzaghi and Peck (1967) explain how the effect of positive porewater pressures is to decrease the friction angle. Cohesive soils are particularly likely to suffer a loss of frictional strength but cohesionless soils may actually increase frictional strength through dilation. When a saturated granular soil dilates or expands, water is drawn into the pores with resulting negative porewater pressures. Negative pressures increase the normal stress across the grain boundaries and hence increase the frictional component of strength according to the Mohr-Coulomb relationship (Terzaghi and Peck, 1967):

$$\tau = c + \{p-u\} \tan \phi \quad (\text{positive pore pressure})$$

$$\tau = c + \{p(-u)\} \tan \phi \quad (\text{negative pore pressure})$$

where τ = shear strength or shearing resistance

c = cohesion

p = total normal stress

u = porewater pressure

ϕ = angle of friction

The term $(p-u)$ is often called the effective normal stress and where porewater pressures are taken into consideration the strength parameters are denoted by a dash, hence

$$\tau = c' + p' \tan \phi'$$

Thus it can be seen that under similar rates of loading, the fine-grained cohesive soils are more likely to fail than the coarser cohesionless soils.

CHAPTER 5

SLOPE STABILITY ANALYSIS OF THE
BROKEN RIVER BRIDGE SLIDE5.1 INTRODUCTION

In this chapter an attempt will be made to analyse the stability of the Broken River Bridge slide, a large landslide located just upstream from where the State Highway crosses Broken River (see plate 33 and figure 9 for location). To analyse the stability of a soil mass, driving forces (those trying to cause motion) and resisting forces (those opposing motion) are determined. The ratio of resisting forces to driving forces is called the safety factor. When the driving forces equal the resisting forces the safety factor is unity, the slope is said to be in a state of limiting equilibrium and is on the point of failure. When the resisting forces are greater than the driving forces the safety factor is greater than one and the slope is considered to be stable. Just how stable the slope is can be quantitatively judged from the value of the safety factor.

The main forces acting on the material within slopes are the internal forces governed by the weight of the sliding mass and the strength of the soil at the failure surface.



Plate 33: Broken River bridge slide.

The weight of the sliding mass is governed by the unit weight of the soil, the geometry of the sliding mass and the position and nature of the groundwater table. The strength of the soil is governed by the strength parameters, cohesion and friction angle. External forces may sometimes be taken into account; for example: surcharge, earthquake loading, or some form of ground reinforcement. Obviously it is not possible to determine forces with a high degree of accuracy mainly due to the difficulties in determining the geometry of a sliding mass before it has failed and in relating laboratory-determined strength parameters to field conditions.

The theoretical analyses available for evaluating stability also require that some assumptions be made in order to derive a working solution. A discussion of the various methods and their limitations, advantages and disadvantages will not be attempted here. Despite the shortcomings of stability analyses, they have been successfully applied in numerous cases for many years. When designing cut slopes or embankments it is normal practice to consider the worst possible case, i.e., when the driving forces are highest and the resisting forces are lowest. This leads to a conservative safety factor.

One way in which the validity of the assumptions made may be verified is to perform a back-analysis on an actual landslide. As the slope has failed, the geometry of the failed material can be more accurately determined and the safety factor can be assigned the value of one. In this chapter, stability analyses will be attempted by various methods. It is hoped that the analyses will help verify assumptions made about the strength parameters.

5.2 FIELD CONDITIONS

The Broken River Bridge slide has developed in Enys Formation sediments on one of the highest stretches of terrace riser to be found in the basin. A large-scale map of the landslide is given in figure 18, and a vertical cross-section showing the geology is given in figure 19. From the discussion of the geotechnical properties (sections 4.6.3 and 4.6.4) and a comparison of the geometry of the slide with the cross-section, it seems highly likely that the brownmud lignite-greenmud strata form a major part of the failure surface.

5.3 MECHANISMS OF MOVEMENT

A combination of permeable and impermeable sediments dipping with an apparent dip of 7° out towards a 60 m high slope of 23° are known to exist. An extensively fissured lignite seam interbedded between two plastic mud seams provides the overlying material with a possible, deep-seated zone of failure. As the lignite seam is extensively fissured, highly porous and hence of high permeability, seepage pressures may arise when ground water levels are high. The adjacent mud beds might swell on saturation and, over a period of time, the sediments at the interfaces would soften and deteriorate in strength. Finally, some triggering factor, possibly a rapid rise in ground water level above a critical height or perhaps an earthquake, would set the mass in motion.

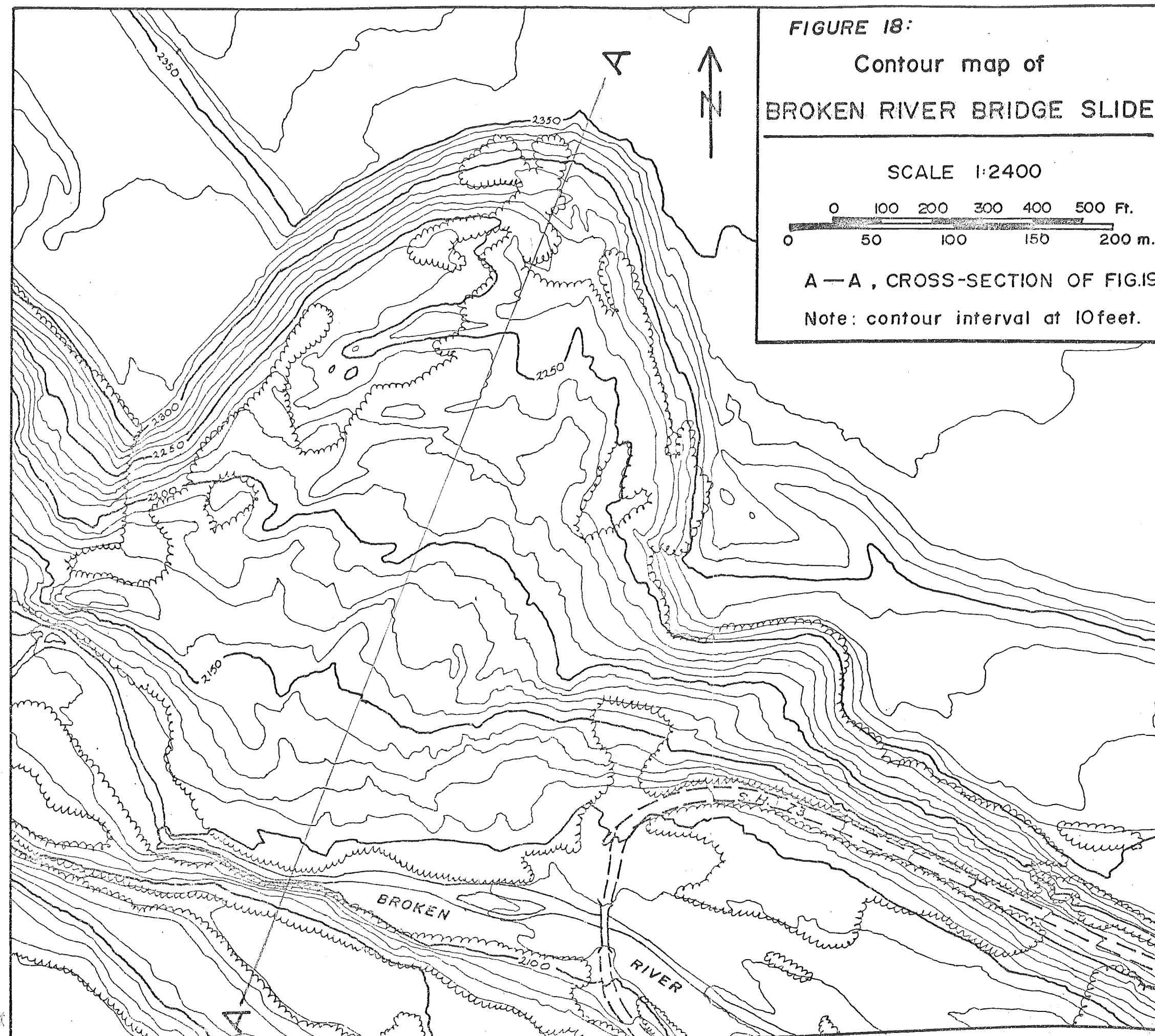
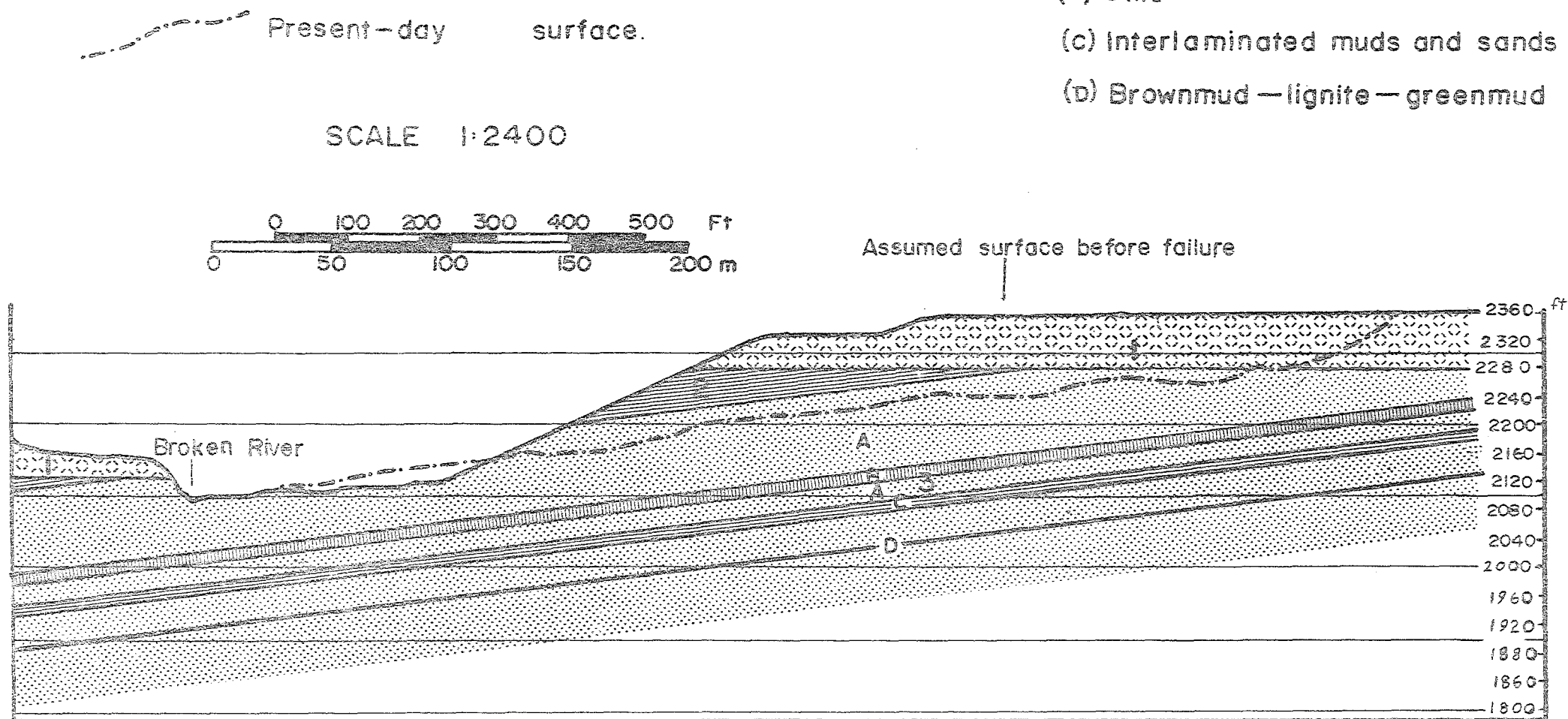


FIGURE 19:
VERTICAL CROSS-SECTION OF THE
BROKEN RIVER BRIDGE SLIDE (A-A OF FIG 18),
showing geology and present-day surface.

KEY:

- 1 TERRACE GRAVELS
- 2 MIDDLE SHALE MEMBER
- 3 MIDDLE SILT MEMBER
- (A) Sands
- (B) Silts
- (c) Interlaminated muds and sands
- (d) Brownmud — lignite — greenmud



5.4 STABILITY ANALYSES

5.4.1 Initial Assumptions:

For the purpose of a stability analysis it will be assumed that the landslide developed in previously intact sediments and that one major movement was responsible for the present form of the landslide. This assumption implies that there was no pre-existing slip surfaces and that the stability can be analysed in terms of peak strength and not the considerably lower residual strength. Pre-existing slip surfaces may develop through glacial advances distorting sediments, tectonic movements, stress release from weathering, or the effects of an older landslide (Skempton and Hutchinson, 1969).

Castle Hill Basin is known to have been glaciated, but according to Breed (1958) the only time there was glacial ice in the basin was during the Porika Glaciation (see section 2.6.2). The surface corresponding to this Glaciation is now some 300 m above the Broken River Bridge area so it is improbable that a slip surface was generated at this depth. Similarly, a series of tectonic movements is known to have effected the Castle Hill Basin sediments (see section 2.4) but the undeformed nature of the Broken River section and the general absence of low-angle thrust planes within the basin suggest that the slip surface is not along a fault or shear zone. A small fault has been mapped (see section 4.3) and tentatively extended to pass along the northwestern boundary of the landslide (see figure 9) but this is more likely to cut the slip surface rather than form a significant part of it. The effects of stress relief from weathering can be neglected as outcrops and borehole cores show that weathering is only

superficial (section 4.3.1(b)). The possibility of the landslide suffering retrogressive failure has been examined and rejected. As the landslide debris and rear scarp show an equal amount of defacement and revegetation the debris is considered to have moved en masse. The stability analyses that follow show that it is the large volume of material involved that is an important contributing factor.

There is abundant evidence (for example, Skempton and Hutchinson, 1969) that in overconsolidated sediments, the cohesion at the time of failure has a very small but finite value. In fact, the shear strength is predominantly composed of the frictional component.

From figure 16, ϕ values are likely to range from 17° - 28° for average plasticity index values. We can narrow this range down to 24° - 28° on the basis of residual ϕ data presented in figure 17.

An estimate of the cohesion may be made by doing a back-analysis on an idealised slump of typical height and slope angle that is commonly found in the Broken River - Hogsback Stream area. A number of workers (see for example Hoek and Bray, 1970) have produced failure charts which calculate factors of safety for a given slope geometry, strength parameters and ground water level and assuming a circular arc failure. As the factor of safety for a slope at failure is known to be unity (the condition for limiting equilibrium), values for peak cohesion may be obtained through knowing the height, slope angle, peak friction angle and estimating likely positions of the ground water surface (see table 13).

TABLE 13

Effective cohesion values for varying
 ϕ values and groundwater levels

ϕ	Cohesion for fully saturated slope	Cohesion for partially saturated slope
24°	49 kPa	33 kPa
26°	35	19
28°	29	16

5.4.2 Analysis Assuming Rotational Failure:

A relatively quick back-analysis can be made using the computer program LEASE*. LEASE-I is designed to perform stability analyses of arbitrary slopes by the method of slices assuming circular arc failure surfaces (Bailey and Christian, 1969). The program will locate the radius of a circular failure surface having minimum factor of safety at each of a specified set of trial centres. Alternatively, an arc may be defined in part, or explicitly, and the program used to define factors of safety, circle centres and radii.

LEASE-I calculates factors of safety using the Simplified Bishop method and the Normal method (a variation of the Simplified Fellenius method). A comprehensive description of these methods and a discussion of their virtues and limitations is beyond the scope of this presentation but can be found in Bailey and Christian (1969) and Whitman and Bailey (1967). Briefly, the methods consist of subdividing a cross-section of unit width through the slide into a number of vertical slices and subsequently

TABLE 13

Effective cohesion values for varying
 ϕ values and groundwater levels

ϕ	Cohesion for fully saturated slope	Cohesion for partially saturated slope
24°	49 kPa	33 kPa
26°	35	19
28°	29	16

5.4.2 Analysis Assuming Rotational Failure:

A relatively quick back-analysis can be made using the computer program LEASE*. LEASE-I is designed to perform stability analyses of arbitrary slopes by the method of slices assuming circular arc failure surfaces (Bailey and Christian, 1969). The program will locate the radius of a circular failure surface having minimum factor of safety at each of a specified set of trial centres. Alternatively, an arc may be defined in part, or explicitly, and the program used to define factors of safety, circle centres and radii.

LEASE-I calculates factors of safety using the Simplified Bishop method and the Normal method (a variation of the Simplified Fellenius method). A comprehensive description of these methods and a discussion of their virtues and limitations is beyond the scope of this presentation but can be found in Bailey and Christian (1969) and Whitman and Bailey (1967). Briefly, the methods consist of subdividing a cross-section of unit width through the slide into a number of vertical slices and subsequently

*Limiting equilibrium analysis for soil engineers

considering the forces that act on each slice at limiting equilibrium. Different assumptions are made about the normal forces acting on the failure surface for the two methods and in the Simplified Bishop method, the shear forces on the vertical sides of the slices are assumed to be zero. Neither method satisfies statics but the Simplified Bishop method is reported by Bailey and Christian (1969) to give factors of safety which compare closely with solutions that do satisfy statics, for simple cross-sections. On the other hand, Whitman and Bailey (1967) have shown that the Normal method will sometimes compute factors of safety lower than the lowest values that could be obtained with a method that satisfies statics.

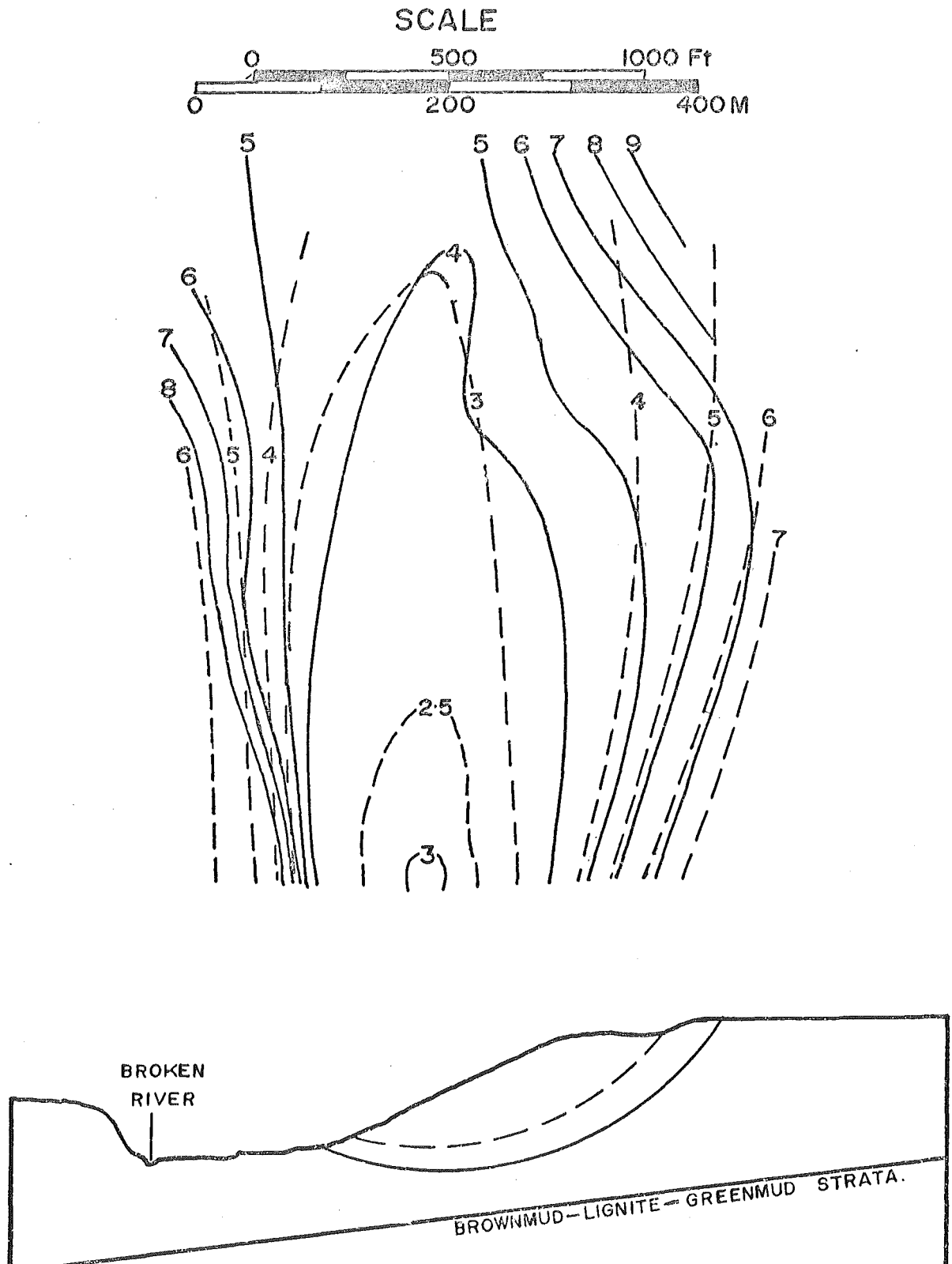
The input parameters required to solve the stability problem are unit weight of water (to inform the computer whether the following units are metric or imperial), unit weight of soil, effective strength parameters (c' and ϕ'), slope geometry and ground water surface. The last two are described in terms of an arbitrary co-ordinate system and an imaginary grid of trial centres is also specified so that the program can compute safety factors for a range of possible radii. LEASE-I also has a routine which searches for the circular arc failure surface having the minimum safety factor by the Simplified Bishop method.

The results for the Broken River Bridge slide are shown in figure 20 where the minimum safety factors are contoured for two different strength criteria. The minimum safety factor is seen to be associated with a small volume of material near the terrace riser which is inconsistent with the well-

FIGURE 20:
CONTOURED POSITIONS OF SAFETY FACTORS
FOR THE BROKEN RIVER BRIDGE SLIDE.



Failure surfaces drawn for the lowest safety factor found.



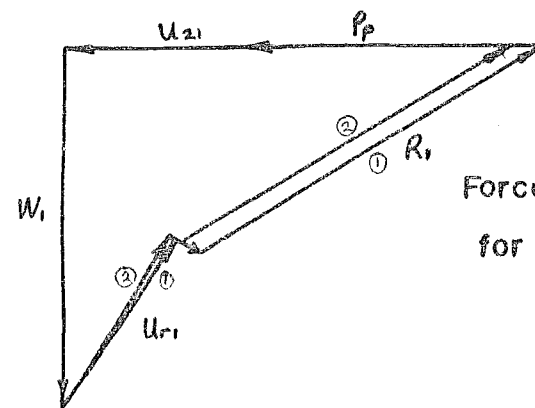
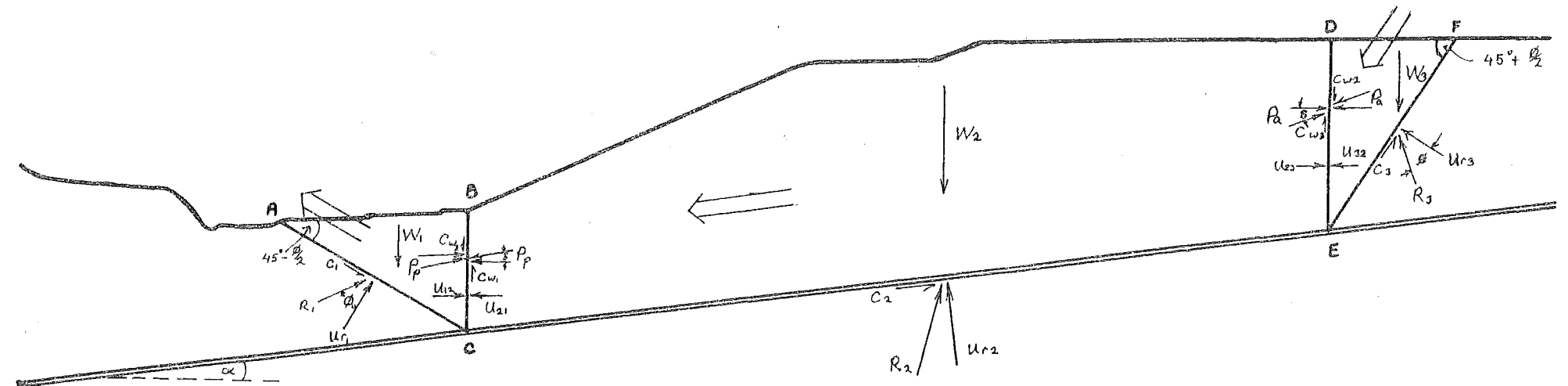
defined rear scarp (see figure 20). It is possible to specify a fixed point on the failure arc (in this case, the point where the rear scarp meets the terrace) and program LEASE-I to calculate safety factors and radii. However, in this case, the safety factors were unrealistically high (between 3 and 15).

From the LEASE-I analyses it is concluded that the failure surface was not a circular arc as it is unlikely the input parameters are significantly in error. The assumption that the failure surface is a circular arc is necessary for analysis by the LEASE program but it is a basic limitation. It is well established (Skempton and Hutchinson, 1969) that circular arc failure surfaces are applicable to homogeneous, isotropic soils. However, in strongly stratified soils, failure is likely to be influenced by the presence of weak layers and impermeable beds hindering drainage. Hence a method which takes into account the most likely failure surface is more applicable.

5.4.3 Analysis Assuming Translational Failure:

As previously mentioned, it is thought that the greenmud-lignite-brownmud strata form a likely failure surface. By assuming a major portion of the failed material slid as a block along these strata, then movement would be resisted in front by a passive wedge and assisted at the rear by an active wedge (figure 21). The stability of the block can be found by considering the driving and resisting forces acting at peak shear strength (see equation, figure 21). There are two methods available for determining the passive and active earth pressures acting on the block from the wedges. The first involves determining earth pressures

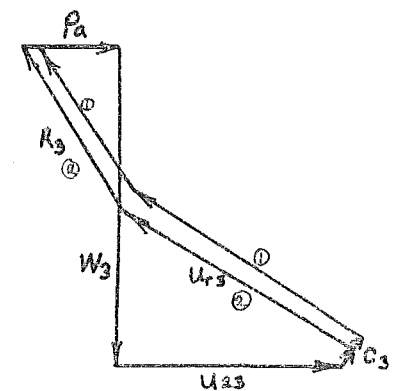
FIGURE 21: CROSS-SECTION THROUGH BROKEN RIVER BRIDGE SLIDE SHOWING ROTATIONAL-TRANSLATIONAL MODE OF FAILURE, POSSIBLE SLIP SURFACES, DIRECTIONS OF MOVEMENT (\Rightarrow) AND FORCES.



Force polygons for wedges ABC (left) and DEF (right) for determination of Rankine earth pressures.

Approximate scale:

1mm=1000KN



The sum of the driving forces, D.F. and resisting forces, R.F. is:

Smooth Interface

$$\Sigma D.F. = W_2 \sin \alpha + P_a \cos \alpha + U_{32} \cos \alpha$$

$$\Sigma R.F. = C_2 l_2 + \{W_2 \cos \alpha + P_p \sin \alpha - P_a \sin \alpha - U_{r2}\} \tan \phi' + P_p \cos \alpha + U_{12} \cos \alpha$$

Rough Interface

$$\Sigma D.F. = W_2 \sin \alpha + Cw_2 \sin \alpha + P_a \cos (\delta - \alpha) + U_{32} \cos \alpha$$

$$\Sigma R.F. = C_2 l_2 + \{W_2 \cos \alpha + P_a \sin (\delta - \alpha) - P_p (\delta - \alpha) + (Cw_2 - Cw_1) \cos \alpha - U_{r2}\} \tan \phi' + P_p \cos (\delta - \alpha) + U_{12} \cos \alpha + Cw_1 \sin \alpha$$

Figure 21 - Cont'd

Areas (A) ABC = 1855 m² BCED = 27360 m² DEF = 2106 m²

Lengths (l) AC = 88 m CE = 350 m EF = 95 m

Heights (h) BC = 50 m DE = 78 m

$\gamma_s = 20.2$ kPa $\gamma_w = 9.8$ kPa

strength parameters

Case (1) $\phi' = 24^\circ$ $c' = 49$ kPa

Case (2) $\phi' = 28^\circ$ $c' = 29$ kPa

$W = \gamma_s A$ $U_r = \frac{1}{2} \gamma_w h \cdot l$ $U = \frac{1}{2} \gamma_w h^2$ $C = c' l$
(x unit width to give forces in newtons)

$P_p = \frac{1}{2} \gamma_s h^2 N\phi + 2c'h \sqrt{N\phi}$) Rankine earth pressures
 $P_a = \frac{\gamma_s h^2}{2N\phi} - \frac{2c'h}{\sqrt{N\phi}} + \frac{2c'^2}{\gamma_s}$) (Terzaghi and Peck, 1967
p. 198 and 199)

where $N\phi = \tan^2 (45 + \phi/2)$

$P_p = \frac{1}{\cos \alpha} \{ \frac{1}{2} K_p \gamma_s h^2 + c'h K_{pc} \}$) Coulomb earth pressures
 $P_a = \frac{1}{\cos \alpha} \{ \frac{1}{2} K_a \gamma_s (h^2 - z_o^2) - c' (h - z_o) K_{ac} \}$) Wilun & Starzewski: vol 12,
1972, p 112&114

where $z_o = \frac{2c'}{\gamma_s \sqrt{N\phi}}$

$K_p = 2.50$ (1) $K_p = 3.62$ (2)) Wilun & Starzewski
 $K_{pc} = 4.81$ (1) $K_{pc} = 5.87$ (2)) vol. 2, 1972
 $K_a = 0.42$ (1) $K_a = 0.31$ (2)) p 112 & p 114
 $K_{ac} = 1.62$ (1) $K_{ac} = 1.47$ (2))

	Passive earth pressures P_p		Active earth pressures P	
	CASE (1)	CASE (2)	CASE (1)	CASE (2)
Graphical sol. (smooth interface)	36400 kN	35000 kN	10200 kN	12300 kN
Rankine solution (smooth interface)	67386 kN	74686 kN	21200 kN	19593 kN
Graphical sol. (rough interface)	67000 kN	65900 kN	6150 kN	10150 kN
Coulomb solution (rough interface)	78345 kN	105622 kN	7457 kN	6284 kN

graphically from a polygon of forces (see figure 21) and assumes the material is a rigid body whose peak shear strength is mobilised without any deformation. On the other hand, if the material is allowed to deform till it is just on the verge of failure then it is said to be in a "Rankine state of plastic equilibrium" (Terzaghi and Peck, 1967). The earth pressures associated with such a state may be obtained from the following equations (in Terzaghi and Peck, 1967, p 198 & p 199, for example):

$$\text{Active earth pressure: } P_a = \frac{\gamma s h^2}{2N\phi} - \frac{2c'h}{\sqrt{N\phi}} + \frac{2c'^2}{\gamma s}$$

$$\text{Passive earth pressure: } P_p = \frac{1}{2}\gamma s h^2 N\phi + 2hc' \sqrt{N\phi}$$

$$\text{where } N\phi = \tan^2 \left(45 + \frac{\phi'}{2} \right)$$

γs = unit weight of soil

h = height of wedge

c' = cohesion

ϕ' = friction angle

In triaxial tests of soils and rocks there is always some strain before peak strength is reached suggesting that the Rankine theory is more relevant.

However, as the active and passive earth pressures act in opposite directions, their effect on stability is lessened somewhat with only a small change in safety factor as a result.

A further condition that must be considered is the influence of friction between the sides of the block and wedges. As the Rankine theory requires smooth boundary conditions, the existence of rough sides can lead to appreciable error in earth-pressure computations (Terzaghi and Peck, 1967). This error can be avoided by using

Coulomb's theory or by graphical methods. As the actual surface of failure is more closely approximated by a curved slip surface, the graphical method involves laborious computations such as by the logarithmic spiral method or friction circle method (Terzaghi and Peck, 1967). A simplified graphical method may be used without appreciable error if planar boundaries are assumed. Wilun and Starzewski (1972) offer the following analytical equations based on the friction circle method which appear in the British Civil Engineering Code of Practice No.2 (1951):

$$\text{Active earth pressure } P_a = \frac{1}{2\cos\delta} K_a \gamma s \left(h^2 - \frac{4c'^2 N\phi}{\gamma s} \right) - c' K_{ac} \left(h - \frac{2c' \sqrt{N\phi}}{\gamma s} \right)$$

$$\text{Passive earth pressure } P_p = \frac{1}{2\cos\delta} K_p \gamma s h^2 + c' h K_{pc}$$

where the coefficients K_a , K_p , K_{ac} , K_{pc} are given in tables 4.6, 4.8 Wilun and Starzewski (1972)

δ = angle between earth pressure resultant and the perpendicular to block-wedge interface taken as equal to $\phi/2$

The factors of safety that have been calculated by the various methods for two different strength criteria are shown in table 14.

5.5 DISCUSSION OF RESULTS

5.5.1 Some Additional Factors Responsible for Movement:

So far no suitable method has been found which gives an answer consistent with the fact that failure has occurred. A translational mode of failure gives the lowest safety factors for a failed mass agreeing with the well defined scarp in the field. Some possible factors which have not been accounted for and would give rise to higher driving forces

TABLE 14

Computed forces and safety factors for
block and wedge analyses

$$\text{Safety Factor} = \frac{\text{Sum of resisting forces}}{\text{Sum of driving forces}} = \frac{\sum RF}{\sum DF}$$

Method	Case (1) $\phi=24^\circ$ C = 49 kPa		Case (2) $\phi=28^\circ$ C = 29 kPa	
Graphical solution (smooth interface)	RF = 301126kN		RF = 338103kN	
	S.F. = 2.4		S.F. = 2.6	
	DF = 125976kN		DF = 128051kN	
Rankine solution (smooth interface)	RF = 333122kN		RF = 379994kN	
	S.F. = 2.4		S.F. = 2.8	
	DF = 136841kN		DF = 135253kN	
Graphical solution (rough interface)	RF = 329562kN		RF = 365353kN	
	S.F. = 2.7		S.F. = 2.9	
	DF = 123947kN		DF = 126361kN	
Coulomb solution (rough interface)	RF = 340922kN		RF = 402904kN	
	S.F. = 2.7		S.F. = 3.3	
	DF = 123947kN		DF = 122510kN	

or lower resisting forces are listed below.

(a) The strength parameters are considered to be uniform throughout the soil even though the material is known to be strongly stratified and anisotropic. The parameters are average values based on the performance of typical slopes in the Enys Formation nearby. The presence of the weak greenmud-lignite-brownmud strata probably warrants the adoption of lower strength parameters for the block in the stability analyses. The extent to which this weakening effect is counteracted by diagonal shearing through the strata at the wedge boundaries is unknown and hence adoption of properties for each stratum is difficult.

100

(b) When analysing the Broken River Bridge slide, a central strip of unit width was considered to have moved along a dip component of the strata oriented perpendicular to the terrace riser. From an inspection of the scarps, troughs and tension cracks on the landslide surface, a sliding direction perpendicular to the slope face seemed the most likely. The true direction of dip is oriented upstream so that the landslide mass seated on the greenmud-lignite-brownmud strata would involve a larger volume of material upstream and a smaller volume downstream than the central strip shown in the section of figure 21. The effect of this asymmetry on the direction of sliding assumed in the stability analysis is difficult if not impossible to determine. If the direction of sliding was oriented in the true down dip direction, the effect of increasing the plane of sliding to 11° (using existing data) would be to decrease the safety factor to 1.65 for the smooth interface, Rankine solution (case 1).

(c) The position of the passive wedge resisting movement is an estimate based on the knowledge that most slope failures tend to pass through the toe of the slope where stress concentrations exist. A passive wedge located underneath the existing valley floor (see figure 21) would reduce the passive resistance and increase the driving force of the block. However the present day valley morphology supplies no evidence to support the possibility that a portion of the stream bed was once upheaved a considerable distance.

(d) The groundwater levels were chosen as being level with the ground surface at failure. This condition gives the highest static porewater pressures that are structurally

possible and result in the lowest safety factor. What has not been considered is the situation where groundwater levels have been at ground surface for some time through prolonged rainfall and steady seepage has developed. Draining water would create seepage pressures within the slope due to the downward drag on the sediments. The effect of including seepage pressures in a stability analysis is to lower the safety factor. Seepage pressures would be higher in the sandy layers and may even be a critical factor in the porous lignite layer. Calculation of seepage pressures has not been attempted due to the stratified nature of the sediments complicating calculations.

(e) Earthquake loading is another factor that has not been included in the analyses. As the landslide has been estimated to be over 150 years old (see section 3.5.2) it is not possible to draw on accurate seismic records to prove or disprove the influence of an earthquake shock. The only evidence to suggest that a high magnitude earthquake may have been responsible for initiating the Broken River Bridge slide is the appearance of other landslides in the Broken River - Hogsback Stream vicinity. These landslides visually appear to be of a similar age to the Broken River Bridge slide but it must be emphasised that this is merely an opinion of the author.

The adoption of a lateral force proportional to the seismic coefficient (see section 2.5.2) is a simplified procedure for ease of stability calculations. The actual effect of seismic shock waves on a soil-water-air system is very complex and probably warrants the adoption of dynamic strength parameters. An indication of the driving

force due to an earthquake acting on the central block in the above example can be found by multiplying the seismic coefficient by $W \cos \gamma$ ($=126,000 \text{ kN}$). Despite the cursory analysis, it can be immediately seen that this force is very large compared to the other driving forces (see figure 21).

If included with the driving forces in the smooth interface, Rankine solution, the safety factor is reduced from 2.4 to 1.3. If dynamic strength parameters are used to calculate resisting forces instead of static parameters then no doubt the conditions for limiting equilibrium can be attained.

Felt intensity is only weakly correlated with acceleration, the former being a function not only of maximum ground motion but also of the duration of that motion and its frequency spectrum (Smith, 1976). Intensity may be locally increased for a number of reasons. Adams et al (1974) report the following soil amplification effects for the Dunedin, 1974 earthquake:

- (a) Unconsolidated recent alluvium causing amplification of the incident earthquake waves.
- (b) Amplitude of the waves increasing with change in physical properties (unspecified).
- (c) Increased intensity at the bedrock - Tertiary sediments interface.
- (d) Slight focussing effect along ridges.
- (e) Resonance effects amplifying vibrations of certain frequencies depending on the size and thickness of the layers involved and on the direction of incident earthquake waves.

Seed (1970) also reports a focussing of earthquake vibrations where a terrace and the uphill part of a terrace riser meet. It is possible that the effects outlined in (b) and (c) above may have been responsible for landslide development but the main influence is undoubtedly the lateral force acting outwards.

5.5.2 Degree of Influence of Slope Stability Characteristics:

The five factors mentioned above are the most obvious ones to the author. It is possible that other factors may have been operating. The following characteristics (listed in decreasing order of importance) are considered to be the most important in slope stability analyses:

(a) Choosing a suitable mode of failure. The different assumptions involved with different methods of analysis result in widely varying safety factors. For the Broken River Bridge slide a much lower safety factor could be obtained for a translational failure than could be obtained for a rotational failure assuming the same strength parameters and water table conditions.

(b) Determining the geometry and volume of material that has failed. The weight of the material is one of the larger forces that has to be taken into consideration. The weight has two components; the driving force component acting down the failure plane and the resisting force component acting normal to the failure plane. The relative proportion of these two components is governed by the inclination of the failure plane. Thus a detailed knowledge of the landslide boundaries and failure plane is critical for the evaluation of slope stability.

(c) The strength properties play an important part in determining the shear resistance of the material, but note

that they do not appear in the calculation of driving forces. The cohesion contributes only a small amount to the resisting forces whereas the frictional component accounts for about 75% of the resisting force. In the block and wedge analysis an increase in the friction angle from 24° to 28° resulted in an increase of resisting forces between 12% and 18%.

(d) The groundwater conditions are perhaps the most difficult to evaluate and account for in slope stability analyses. Pore pressures may act as driving forces (thrust of water in tension cracks and saturated active wedge) or resisting forces (reduction of normal stress across failure plane and thrust of saturated passive wedge). As the pore pressures are dependent on the height of the hydraulic head a knowledge of the position of the ground water table is needed. When designing cut slopes or embankments against the worst possible conditions a ground water table coincident with the ground surface may be used. When monitoring the performance of a slope, instruments (piezometers) may be installed to determine the ground water table position. In a back analysis such as the exercise just carried out the water level can only be estimated.

(e) The saturated bulk density is used for determining the weight of the block and wedges. Because the constitutive minerals of clastic sediments are much the same, the bulk density shows little variation, despite varying grain sizes. Wilun and Starzewski (1972) report that a saturated bulk density value of 2.1 gm/cc may safely be assumed for most calculations. The geotechnical testing (section 4.6) showed a slight variation in density values and an average value may be used without too much loss in accuracy.

Finally, in reviewing the original intentions of this chapter, viz., to verify assumptions made about the strength parameters, it is seen that only partial success has been obtained. Moderately low safety factors have been obtained, however these are inconsistent with the fact that the slope has failed. The very nature of stability analyses ensures that this discrepancy cannot be attributed to any particular factor. Only the obvious factors have been considered in the analyses. Whether the discrepancy lies with an obvious factor such as strength or whether it can be attributed to an unconfirmed factor such as an earthquake is impossible to say.

CHAPTER 6

REASONS FOR SLOPE FAILURE
IN CASTLE HILL BASIN6.1 INTRODUCTION

In this concluding chapter the processes and contributing factors to mass movement in Castle Hill Basin are summarised and the results are used in the presentation of a landslide susceptibility map. No attempt will be made to give individual reasons for each slide as rarely does any single factor account for mass movement, but rather, a combination of factors is responsible. Similarly, no remedial or preventive measures will be put forward as such measures would be as variable as the causes.

The combination of factors that leads to the development of a slide begins with the deposition of the materials themselves, is developed during the diagenetic and tectonic processes involved and includes the subsequent events of erosion and weathering. Finally, some factor, whether large or small, sets the mass in motion downhill. This final factor is thus not necessarily the cause of the landslide but merely the last of many processes that have been acting on the slope for a very long time.

According to Terzaghi (1950), the causes of landslides can be of either external or internal origin. External causes are those which produce an increase of the shearing stresses whilst shearing resistance of the slope material remains unaltered. Internal causes are those which lead to a decrease in shearing resistance without any change in surface conditions.

In both cases, the causes may be peculiar to a localised area, or to the whole basin itself, or alternatively to soils and rocks of a similar age and geological history. The processes may have been operating since the original uplift of the sediments or since some particular phase in the development of the geomorphology or they may only have come into operation since the advent of man. With such a diversity of processes and causes involved, it is possible to classify them into several categories.

6.2 CLASSIFICATION OF LANDSLIDE PROCESSES AND CAUSES

6.2.1 External Processes:

(a) Removal of lateral support: Erosion by streams and rivers, especially at the downstream side of meanders and at the toes of landslides, is responsible for many landslides (see section 2.1.3).

Because of the high precipitation, lateral erosion is probably most active in the northwestern part of the basin. During glacial times, lateral widening by glaciers of the greywacke slopes in some of the larger valleys on the Craigieburn Range would have occurred. Glaciers are only

considered to have reached the basin floor during the Avoca Advance (see section 2.6.2). However, the surface associated with this advance is now some 250-300 m higher than the present-day Tertiary sediments so that glaciation would not have been responsible (by the process of removing lateral support) for the landslides visible today.

New slopes may be created by rockfall, landslide, subsidence, or large-scale faulting which all effectively remove lateral support. Many of the larger landslides, in particular the Broken River Bridge slide have increased the risk of slope failure by leaving an unsupported scarp.

Human activities, such as the creation of road cuts and quarries, locally remove lateral support. As yet, no road cuts (the highest of which are near the Thomas and Broken Rivers) have failed; probably due to the cuts being made in the relatively stable, sandy sediments. The limestone quarries are also stable at their present depth. However, the possible land slide just north of Castle Hill homestead (see figure 7) could reactivate movement if quarrying operations went deeper.

(b) Surcharge: The accumulation of talus or landslide material over ground susceptible to failure is a possible process. No evidence has been found in Castle Hill Basin to support this, mostly because the bulk of the landslide debris ends up in the river bed. A surcharge of groundwater is an ever present factor in slope instability. A weight increase of up to 28% has been found for samples of Enys Formation sediments passing from a dry to a saturated condition (see table 5). A surcharge of rain and snow

is thought to have been a major contributing factor with the fossil landslides.

(c) Removal of underlying support: Of minor importance is the undercutting of banks by rivers which results in unstable conditions in a few localised areas. Of more significance is weathering by slaking and frost heave which can undermine resistant strata to a point where they collapse or fall. Undermining is common around the limestone escarpments where the underlying tuffs are gradually being removed.

Removal of soluble carbonates in the limestone strata sometimes leads to cavern collapse especially around the southern end of Flock Hill.

(d) Tectonism: Castle Hill Basin does not appear to be a tectonically-active region at present, but it is influenced by events outside the region (see section 2.5.2). No faults are thought to have moved within the last century (see sections 2.5.1 and 2.5.2) but there is evidence to suggest that faulting has played a role in landslide development at some stage in the past (see section 3.6.2). Regional tilting could lead to a progressive increase in slope angle in some areas which may lead to unstable slopes. Tilting is very slow compared to man's activities so that proof of this mechanism is difficult to substantiate. Four earthquakes with an intensity of MM8 or greater have been estimated to have been felt in Castle Hill Basin over the last century (table 3) and there is a strong likelihood that these have been responsible for triggering some of the larger landslides (see section 5.5.1).

(e) Topography: Slope stability is effected by topography in two ways; the slope angle and the slope height. The slope angle of the terrace risers lies consistently around 23° ($\pm 3^{\circ}$) and for many lithologies this angle is stable. For the finer-grained sediments however, slope failures are common and for a diverse range of materials this angle represents a critical angle at or near limiting equilibrium. The critical slope height at which mass movement occurs for the Enys Formation in Hogsback Stream and Trout Stream (see figure 9) appears to be between 45 m and 60 m; the variation being due to the differing gravel thicknesses. At this height the slope seems to be close to limiting equilibrium and incipient scarps can be seen on the terrace behind the slope (see plates 35, 34a and 34b). Upstream from this point, the slope height lessens and the valley sides are stable (see plate 35). Downstream, the rivers have deepened their courses, a greater height of Tertiary material is exposed and slope failures are common.

(f) Vegetation: Vegetation acts more as a controlling factor in the mode of failure rather than as a direct cause. Vegetation's influence on the frequency and mode of failure is best demonstrated in Hogsback Stream (see section 2.1.2) where slope failures occur on both sides of the valley in the weak materials. Repeated burnings during Polynesian and European times severely reduced the forest cover (see section 2.1.2) which in turn would have led to accelerated erosion.



Plates 34a and 34b: Incipient scarplets on valley sides of Hogsback Stream around about where terrace risers reach a critical height .

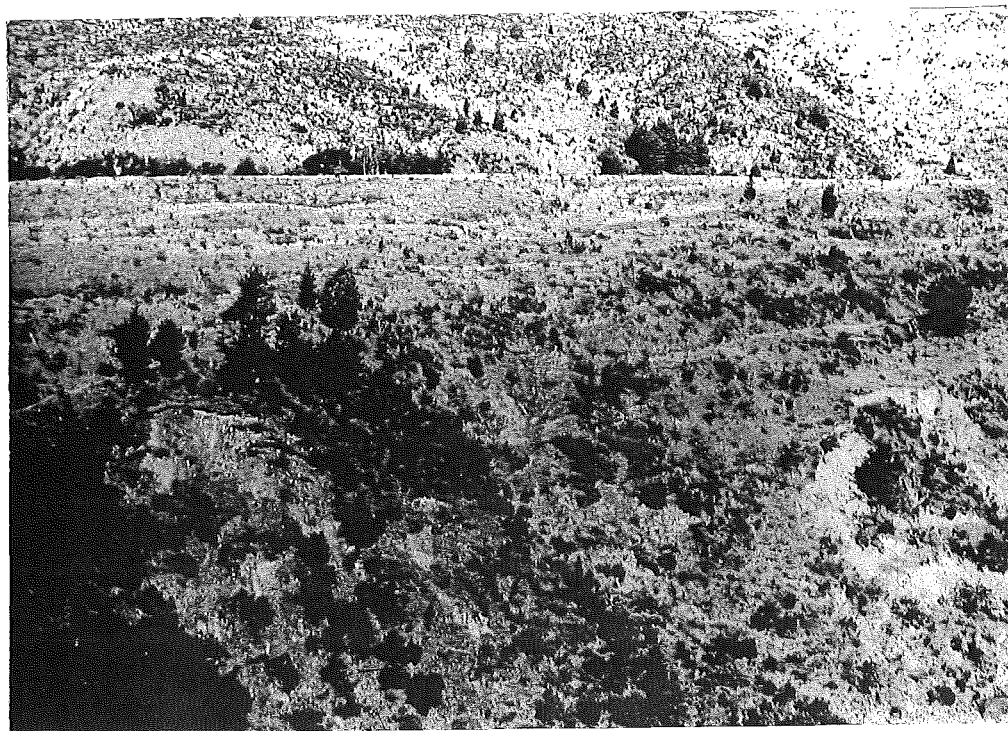




Plate 35: Stable slopes in upper Trout Stream. Note matagouri shrubs growing on Enys Formation sediments on lower slopes and tussock covering overlying gravels and stream alluvium.

6.2.2. Internal Causes:

(a) Geotechnical properties of the soils and rocks: Sixty landslides in a relatively small area such as Castle Hill Basin (see figure 23) suggests that the local geology is a prime factor. The geotechnical properties, in particular the strength parameters, are the main geological factors in landslide development in soils. The young sediments are mostly unindurated and uncemented. Geotechnical testing of the Enys Formation sediments (see sections 4.5 and 4.6) classified them in general, as weakly cemented-weakly compact and heavily overconsolidated soils with low shear strength.

(b) Structural weaknesses: Inherently weak strata interbedded with stronger materials usually form zones of failure in unstable areas. Of equal importance is the interbedding of strata with widely differing geotechnical properties such as permeable and impermeable beds, plastic and non-plastic beds, swelling and non-swelling beds.

The gross structure (see section 2.4) varies from place to place and locally gives rise to unstabilising conditions (see section 3.6.2). On a small scale, the presence of discontinuities such as bedding planes and joints may have a minor weakening effect. Unfavourable bedding plane orientation and faults in the vicinity of terrace risers can also lead to slope failures.

(c) Changes due to weathering and other physico-chemical reactions: Argillaceous sediments often experience a gradual decrease in shear strength with time.

The loss in strength is attributed by Grim (1962) to a decrease in cohesion due to the cyclic adsorption and dessication of water by clay minerals. The influence of differing exchangeable cations on clays is also attributed by Grim (1962) as being able to alter the physical properties. However no investigations have been carried out into such time-dependent effects at Castle Hill Basin. Wetting and drying of argillaceous sediments disintegrates near-surface materials (see section 4.6.3(e)) resulting in fissuring and eventual ingress of rainwater. Slaking readily assists the superficial mass wasting processes but is an insignificant factor in deep-seated failures.

(d) Changes in intergranular forces due to pore water: After prolonged rainfall, high groundwater levels can lower shear strength by buoyancy decreasing effective intergranular pressure and friction, loss of capillary tension (or apparent cohesion) on saturation and seepage pressures of percolating groundwater. The above factors are particularly important when concentrated along a highly porous stratum or a thin bed in the vicinity of a likely zone of failure.

(e) Subterranean erosion by removal of soluble carbonates: Subterranean erosion in the limestone strata sometimes leads to cavern collapse and the best example of this is seen at Cave Stream where a line of sinkholes can be distinguished above where the stream flows underground (see section 2.6.3).

(f) Lateral pressure: An outward thrust from water in tension cracks and caverns is conducive to unstable conditions.

especially if the water freezes.

6.3 PRESENTATION OF LANDSLIDE SUSCEPTIBILITY MAP

6.3.1 Preparation:

For an approximate guide to the likelihood of future movement, it is possible, on the basis of a knowledge of the causes and processes involved, to present a landslide susceptibility map. Such a map would depend heavily on the major, regional factors with an application of the local factors to give the necessary detail. Most of the information can be conveyed in three maps (in pocket at back).

- (a) Base map of part of NZMS 1 map S66/8, showing contours, drainage patterns, terrace and escarpment edges, roads and forested areas (see figure 22).
- (b) Geological map showing the stratigraphic units, fold axes, faults and landslides. The significance of the geotechnical properties is implied in the lithologies (see figure 23).
- (c) Slope-angle map, derived from the contour map, showing slope angle zones; (0° - 10°) (10° - 20°) (20° - 30°) and ($<30^{\circ}$) (see figure 24). Spacing for the boundaries of these zones is ascertained from the following formula:

$$\text{zone width} = \frac{\text{contour interval} \times \text{scale}}{\tan \theta}$$

where θ is the angle of the upper boundary.

From these three maps the landslide susceptibility map (figure 25) can then be prepared.

6.3.2 The Concept of Landslide Susceptibility:

The concept of susceptibility to landsliding is difficult to define but can be thought of as involving:

- (a) A scale of future movement,
- (b) A time span in which the likelihood of movement is expected to take place,
- (c) A probability of future movement.

It is convenient here to relate the above-mentioned factors in terms of man's activities. The first factor, which concerns the size and importance of the landslide, would involve only those landslides large enough to influence or disrupt man's activities. Thus most of the mass-wasting forms can be conveniently neglected, as can some of the smaller slumps, rockfalls and translational slides.

A time span of interest can be arbitrarily set at 100 years. Although it is not possible to predict the extent of man's activities in that period, no large-scale influences on slope stability can be envisaged. Climate and possibly other factors vary slowly with time but it is doubtful if the change would be significant in 100 years time. As all slopes flatten or degrade as a response to gravity and other agencies, the degree of susceptibility will be based on the past performance of slopes over the last century.

Slope failures are influenced by so many factors that it is extremely difficult to interpret these phenomena in terms of the statistical concept of the probability of an event occurring. Therefore, a qualitative approach has been adopted of classifying or zoning the area in terms of a three-fold classification; namely, zones of high, medium or low degree of susceptibility to mass movement. As the bounds of these zones (apart from the upper bound) cannot be

quantitatively fixed by analytical methods, their definition is obviously open to interpretation.

The classification is necessarily simple in the hope that other workers in the same area would arrive at the same conclusions. It is not expected that this classification can be applied to similarly unstable ground elsewhere. For instance, what may be considered an unstable situation in an urban area on greywacke may not receive the same classification rating as a similarly unstable situation in Castle Hill Basin. However it is hoped that the classification remains internally consistent throughout Castle Hill Basin. More experience is needed in relating field conditions to degrees of susceptibility in other areas before criteria suitable for universal application can be suggested. The following criteria have been used for defining the three degrees of susceptibility in Castle Hill Basin.

Zone one of the classification represents the highest degree of landslide susceptibility. The zone is defined as areas of probable slope failure in which some movement, whether slight or catastrophic, is expected to occur within the next century. Included in this category are all recent landslides, reactivated portions of older landslides and other areas of known instability. Some speculations are drawn as to the probability of movement in areas that have not previously moved and which are deemed to be unstable. Such areas include oversteepened terrace risers, particularly in the younger, argillaceous sediments, which are being actively eroded at the base. It should not be too difficult for other

engineering geologists to recognise oversteepened, undercut slopes comprising unfavourably structurally oriented beds of plastic impermeable muds and non-plastic, permeable sands as having a high degree of susceptibility. Where coincidence of all these factors does not occur then obviously a certain amount of subjective opinion is required to determine where the lower bound of zone one should lie. The upper bound may be considered as those slopes that are just on the point of failure; i.e. those slopes having a safety factor of one.

The intermediate zone of susceptibility, zone two, covers areas of possible slope failure. In zone two there are fewer factors coinciding than in zone one but there are enough to warrant a moderate degree of risk of mass movement. The most likely areas are still on steep terrace risers but the lithology and structure are more favourable for slope stability than in zone one. Some dormant and fossil landslides, where renewed movement is possible, are included in this category as are areas bordering zone one which may be left unsupported in the event of a landslide occurring.

The lowest degree of landslide susceptibility, zone three, is considered to consist of essentially stable areas which have only a remote possibility of failing under present day conditions. Included in this zone are all terraces and other areas of low slope angles and dip slopes in limestone of moderate angle. The lower bound can be thought of as those slopes having a probability of moving within 100 years of zero.

6.3.3 Use of the Susceptibility Map:

A landslide susceptibility map is of possible use to planners and engineers who are involved with the development of Castle Hill Basin. Because of the empirical approach and the generalisations involved, the map is limited to a general guide. It is hoped that the preparation of similar maps by other workers will result in their recognition and eventual adoption as an investigatory tool. With more widespread use and acceptance it should be possible to develop the susceptibility classification to include more intermediary zones and to define more clearly the boundaries between zones.

Finally, it cannot be emphasised too strongly that, owing to the variability of conditions in Castle Hill Basin, it is almost impossible to predict when a landslide will occur. Even using analytical methods to determine how close a slope is to failing, the number of unknown factors and sources of error involved make this method of prediction useful as an indication only. Thus, no matter how detailed the field investigations, laboratory testing and numerical analysis is, it is still possible that several unknown or unpredictable factors exist which lead to the development of a large landslide without warning.

ACKNOWLEDGEMENTS

The help of the following people and organisations is acknowledged.

Staff of the Geology Department, Canterbury University,
in particular

J.K. Hill (Supervisor)

D.B. Bell (X-ray diffraction work)

R.D. Thompson (X-ray diffraction work)

A. Downing (Photographic developing & printing)

K. Swanson (Photographic developing & printing)

Dr M.J. Pender, M.W.D. (Critical evaluation of draft)

A.J. Olsen, M.W.D. (Critical evaluation of draft)

P.E. Bartlett, M.W.D. (Critical evaluation of draft)

Dr B.R. Riddolls, N.Z.G.S. (Critical evaluation of draft)

G.T. Hancox, N.Z.G.S. (Critical evaluation of draft)

T.L. Grant-Taylor, N.Z.G.S. (Critical evaluation of draft)

P. Liss (Photographic developing and printing)

REFERENCES

- ADAMS, R.D. & KEAN, R.J. (part 1); BISHOP, D.G. (Part 2) 1974
 "The Dunedin earthquake, 9 April, 1974, part 1:
 Seismological studies; part 2: Local effects".
 Bulletin of the New Zealand National Society for
 Earthquake Engineering, Vol 7, no.3, Sept. 1974.
- AKROYD, T.N.W. 1957 "Laboratory testing in soil engineering"
 Geotechnical monographs, no.1, Soil Mechanics Ltd.
- AMERICAN SOCIETY FOR TESTING & MATERIALS 1975 Symposium on
 "Soil specimen preparation for laboratory testing",
 ASTM STP 599.
- BAILEY, W.A. & CHRISTIAN, J.T. 1969 "ICES LEASE-I: A
 problem oriented language for slope stability analyses-
 users manual". Dept Civil Engineering, Massachusetts;
 Institute of Technology 02139.
- BLALOCK, H.M. 1960 "Social Statistics" McGraw-Hill.
- BRADSHAW, J.D. 1975 "The folds at Castle Hill (Canterbury)
 and their bearing on Kaikouran deformation style in
 the Canterbury basin". Journal of the Royal Society
 of N.Z., vol.5, no.2, pp209-217.
- BREED, W.J. 1958 "River Terraces and other geomorphic
 features of Castle Hill Basin, Canterbury, N.Z.".
 Unpublished M.Sc. thesis, Canterbury University.
- BROWN, I.R. 1974 "Stability of slopes in soft rock". Proc.
 Symp. on stability of slopes in natural ground, Nelson,
 N.Z. Geomechanics Society.
- CARSON, M.A. & KIRBY, M.M. 1972 "Hillslope form and
 process'. Cambridge University Press.
- CHIN, T.J.H. 1975 "Late Quaternary Snowlines and Cirque
 Moraines Within the Waimakariri Watershed".
 Unpublished M.Sc. thesis, Canterbury University.
- DUNCAN, N. 1969 "Engineering Geology and Rock Mechanics"
 Volume 1, Leonard Hill, London.
- FRANKLIN, J.A. & CHANDRA, R. 1972 "The slake-durability
 test". Int. Jour. Rock Mech. Min. Sci., vol.9,
 pp325-341.
- GAGE, M. 1958 "Late Pleistocene glaciation of the
 Waimakariri Valley, Canterbury, N.Z.". N.Z. Journal
 of Geology and Geophysics, vol.1 no.1, ppl23-155.
- GAGE, M. 1970 "Late Cretaceous and Tertiary rocks of
 Broken River, Canterbury, N.Z..
- GRIM, R.E. 1962 "Applied Clay Mineralogy" McGraw Hill.

- HABIB, P. 1975 "Production of gaseous pore pressure during rock slides" Rock Mechanics, vol.7, no.4, pp193-197.
- HAYWARD, J.A. 1967 "The Waimakariri catchment; a study of some aspects of the present systems of land use, with recommendations for the future". Tussock Grasslands and Mountain Lands Institute, special publication no.5.
- HAYWARD, J.A. & BOFFA, F.D. 1972 "Recreation in the Waimakariri Basin", Lincoln papers in resource management, no.3.
- HOEK, E. & BRAY, J. 1974 "Rock Slope Engineering" Institution of mining and metallurgy.
- INTERNATIONAL SOCIETY FOR ROCK MECHANICS, 1972 "Suggested Methods for Determining Water Content, Porosity, Density, Absorption and Related Properties and Swelling and Slake-Durability Index Properties", Committee on Laboratory Tests, document no.2.
- KANJI, M.A. 1974 "The relationship between drained friction angles and Atterberg limits of natural soils". Geotechnique, vol.24, no.4, pp671-674.
- KRUMBEIN, W.C. & GRAYBILL, F.A. 1968 "An introduction to statistical models in geology". McGraw-Hill.
- LAMBE, T.W. & WHITMAN, R.V. 1969 "Soil Mechanics", Wiley.
- MEANS, R.E. & PARCHER, J.V. 1963 "Physical properties of soil". Charles E. Merrill Books Inc..
- MITCHELL, J.J. 1976 "Fundamentals of soil behaviour" J. Wiley & Sons.
- SEED, H.B. 1970 "Earth slope stability during earthquakes" in Wiegel R.D. (ed) "Earthquake engineering" Chap 15, Prentice-Hall.
- SKEMPTON, A.W. & HUTCHINSON, J.N. 1969 "Stability of natural slopes and embankment foundations". State of the Art Report, Proc. 7th Intl. Conf. Soil Mech. and Foundation Eng, Mexico, vol.1, pp291-340.
- SMITH, W.D. 1974 "Statistical estimates of the likelihood of earthquake shaking throughout New Zealand" Bulletin of the New Zealand National Society for Earthquake Engineering, vol.9, no.4 Dec. 1976.
- TERZAGHI, K. 1950 "From theory to practice in soil mechanics". J. Wiley and Sons.
- TERZAGHI, K. & PECK, R.B. (2nd ed.) 1967, "Soil mechanics in engineering practice". Wiley and Sons.
- TOURTELOT, H.A. 1974 "Geologic origin and distribution of swelling clays". A.E.G. bull, vol.XI, no.4, pp259-275.

- VARNES, D.J. "Landslide types and processes" in Eckel E.B. et.al., (1958) "Landslide and engineering practice" Highway Research Board, spec. rep.29.
- VOIGHT, B. 1973 "Correlation between Atterberg plasticity limits and residual shear strength of natural soils", Geotechnique, vol.23, no.2., pp265-267.
- WHITMAN, R.V. & BAILEY, W.A. 1967 "Use of computers for slope stability analysis" Journal of the Soil Mechanics and Foundation Engineering Div. vol.93, SM4 pp475-498.
- WILUN, R.V. & STARZEWSKI, D.M. 1975 "Soil Mechanics in engineering practice" vols 1 & 2, Carson.
- YONG, R.N. & WARKENTIN, B.P. 1966 "Introduction to soil behaviour". Macmillan Company, New York.
- YOUNG, A. 1974 "The rate of slope retreat". Special publication no.7. Institute of British Geographers.

APPENDIX 1

GLOSSARY OF TERMS

- Adsorption** A process whereby electrostatically charged cations and anions carried in groundwater are attracted to the surfaces of clay minerals. The charged particles may become organised on the plane surfaces of clay minerals and form an expanded crystal lattice giving rise to the swelling phenomenon observed in clays.
- Aggradation** A process whereby a stream deposits transported sediment and so builds up its channel.
- Aquiclude** A relatively impermeable stratum which does not readily yield water to wells for man's use. Aquicludes usually act as an upper and lower boundary to an aquifer.
- Aquifer** A water-yielding permeable stratum.
- Atterberg limits** Arbitrary boundaries denoting degrees of consistency of a remoulded soil-water mixture. As the water content of a soil-water slurry decreases the mixture passes from a liquid state, through a plastic state and finally into a solid state. The water contents are known as the liquid limit and plastic limit for the liquid-plastic transition and the plastic-solid transition respectively. The difference in water contents within which a soil possesses plasticity is known as the plasticity index.
- Cirque** A concave basin that has been hollowed out by glaciation.
- Clay** A group of particles having a grain size finer than 0.002 mm. Clays are often composed of clay minerals (e.g. kaolinite, illite and montmorillonite) but may also include very fine particles of minerals which normally occur in the silt and sand range (e.g. quartz and feldspar).
- Cohesion** The amount of resistance to shearing a soil has when no normal load is applied.

Cretaceous Period	A period of time between 64 and 136 million years ago. The division of the period into lower and upper is at about 100 million years ago.
Dendritic Drainage	A very common drainage pattern characterised by irregular branching of tributary streams in a similar manner to that in which a tree branches.
Diagenetic Processes, Diagenesis	Those processes affecting a sediment at low temperature and pressure which result in the transformation of a loose sediment into a rock. Compaction (or consolidation) and cementation are the two most important processes.
Dilation	An increase in volume through grain re-arrangement while under loading.
Epicentre	The point on the earth's surface above the focus of an earthquake.
Estuarine	Referring to those sediments which have been deposited in an estuary or tidal river mouth.
Facies change, lateral	A change (laterally) in the sedimentary features (e.g. rock type, mineral content, sedimentary structures, fossil content, etc.) which characterise a sediment as having been deposited in a given environment.
Floc	A collection or aggregation of discrete particles which are capable of settling out from the dispersion medium.
Fluviatile	Referring to those sediments deposited in a river channel.
Focus, earthquake	The point of origin of an earthquake in the earth's crust.
Friction angle, angle of shearing resistance	The angle, ϕ between the axis of normal stress and the tangent to the Mohr envelope on a Mohr-Coulomb diagram. The coefficient of friction, $\tan \phi$ relates the normal stress to the corresponding shear stress at failure. If the material which is being stressed has not failed before then a peak friction angle value will be obtained. After failure, a surface of sliding forms and continued stressing will result in a decreasing

resistance to shear. Finally, after large displacements an ultimate shearing resistance is reached and a residual friction angle is obtained.

Glaciofluvial deposits	Sediments deposited from the outwash of a glacier which are characterised by being coarse, angular and heterogeneous in structure.
Gradation	The relationship between soil particle size and grain designation (e.g. sand, silt, clay). Particle size may be determined by sieving and wet analysis and gradation or particle size distribution curves prepared (see Appendix 4) which help classify the soil.
Indurated	A term to describe rocks which have been hardened by diagenesis.
Karst	A closely dissected topography developed in limestones. Mildly acidic rainwater and groundwater are responsible for dissolving the limestone along joints and bedding planes. Occasionally, the collapse of a cavern leads to the development of a sinkhole or swallowhole at the surface.
Lacustrine	Referring to those sediments deposited in a lake.
Landslide	A generic term referring to all forms of slope failures (falls, slides, flows, complex movements) except superficial mass wasting movements.
Mohr-Coulomb relationship	<p>A relationship between the applied stresses and shear stress operating on a soil at failure. The applied stresses can be graphically represented as a Mohr's circle. Where a number of triaxial strength tests are performed at different stress levels an envelope may be fitted to the corresponding Mohr's circles. All or parts of this envelope may often be approximated by a straight line with the equation</p> $\tau = c + p \tan \phi$ <p>This linear relationship is known as Coulomb's equation and it relates the shearing resistance or shear strength to the applied stresses at failure by the coefficients c and ϕ (see strength parameters).</p>

Moraine	An accumulation of rock material which has been transported and deposited by glaciers.
Mud	A fine-grained or argillaceous sediment comprised of silt and clay.
Neve	Permanent fields of compacted snow and ice which give rise to glaciers.
Orogeny	A period of mountain building. Orogenesis is the process leading to the formation of the intensely deformed belts which constitute mountain ranges.
Outlier	A limited area of younger rocks completely surrounded by older rocks.
Over-consolidation	A process whereby a sediment is subjected to a pressure in excess of its present overburden pressure. The excess pressure is often caused by overlying sediments which have since been eroded away.
Peneplanation	The destruction of relief by continual erosion and aggradation of broad river valleys. The resultant landform is known as a peneplain and is considered to be the final phase of the cycle of erosion.
Permafrost	Permanently frozen ground which may thaw and soften in summer or with a change in climate.
Permeability, coefficient of (k)	The capacity of a sediment to conduct groundwater. It is measured as the proportionality constant, k, between flow velocity, v, and hydraulic gradient, i. $v = k \cdot i$
Point load test	A method of loading an irregular sample in compression through conical platens. The point load index may be related to the unconfined compressive strength of a sample.
Pressure, capillary	A tensile pressure acting on moisture in a partially-saturated soil which effectively increases the particle-to-particle contact pressure.

Pressure, earth	The pressures acting on every part of a body of soil when it is on the verge of failure are known as earth pressures. If the body of soil is compressed to failure then it is exerting a passive earth pressure as a response. On the other hand, if the mass is stretched then active earth pressures are operating.												
Pressure, effective	<p>The effective pressure, p' is the resultant pressure acting solely on the solid phase of the soil. It is the combination of the total normal pressure, p, and the porewater pressure, u, such that</p> $p' = p - u$												
Pressure, seepage	Seepage pressure is the frictional drag of water flowing through voids or interstices causing an increase in the intergranular forces.												
Regression	The withdrawal of the sea from a large area of land.												
Safety factor, factor of safety	The ratio between potential resisting forces and driving forces acting on a body when peak strength is being mobilised. When the ratio equals unity the driving forces are on the point of overcoming the resisting forces and failure is imminent. The higher the resisting forces the higher the safety factor and hence the ratio may be used to express the degree of safety.												
Sand, silt, clay	<p>The predominant grain sizes with the following boundaries</p> <table> <tr> <td></td><td>2 mm</td></tr> <tr> <td>sand</td><td></td></tr> <tr> <td></td><td>0.06 mm</td></tr> <tr> <td>silt</td><td></td></tr> <tr> <td></td><td>0.002 mm</td></tr> <tr> <td>clay</td><td></td></tr> </table>		2 mm	sand			0.06 mm	silt			0.002 mm	clay	
	2 mm												
sand													
	0.06 mm												
silt													
	0.002 mm												
clay													
Seismic coefficient	The ratio between the horizontal component of an earthquake acceleration and the acceleration due to gravity. Usually taken as 0.1 in New Zealand engineering.												
Shear strength	<p>The maximum shear stress a soil can resist without failing for any given type of loading. Denoted by the Coulomb equation</p> $\tau = c + p \tan \phi$												

Solifluction	The slow downhill movement of a superficial soil or debris layer as a result of the alternate freezing and thawing of the contained water.
Strain	The deformation of a loaded sample with respect to its original dimension.
Stratigraphy	The study of stratified rocks, especially their sequence in time, the character of the rocks and the correlation of beds in different localities.
Strength parameters	Cohesion c , and friction angle, ϕ , are the two strength parameters which define the shear strength at failure for any given type of loading.
Talus creep	A creeping process similar to solifluction occurring in the heaps of coarse debris (talus or scree) that accumulate at the foot of steep slopes and cliffs.
Tectonic depression, tectonism	A depression or downwarp caused by compressional and tensional forces in the earth's crust (tectonism). Long-continued compressional forces in the crust and overlying sediments give rise to mountain chains being formed (see orogenesis).
Terrace riser	The inclined slope adjoining a terrace and formed by active downcutting of rivers.
Tertiary Period	The period of time which elapsed between 2.5 and 64 million years ago.
Tor	A residual limestone outcrop in the form of loose boulders, blocks or slabs often capping hills in a Karst landscape. Weathering and solution have often been operating on the tor for a very long time.
Transgression	The invasion of a large area of land by the sea. The reverse of a regression.
Triaxial test, drained- and undrained	A test whereby a cylindrical sample is loaded in compression along three mutually perpendicular axes. A pre-selected hydraulic confining pressure is applied

Triaxial test, Cont'd	laterally along the two horizontal axes and the sample is loaded to failure along the cylindrical axis in a testing machine. During testing, the sample may be totally enclosed so that no change in porewater volume is allowed. Such a test is known as an undrained test and significant pore pressures usually develop. On the other hand, provision may be made for draining the sample so that no pore pressures are allowed to develop. From a knowledge of the applied pressures, the appropriate Mohr's circles can be drawn and a Coulomb relationship fitted to the corresponding envelope. In this way the strength parameters of the soil sample tested can be obtained.
Type section	A locality chosen to be a standard for comparison of a stratigraphic unit.
Unconformity	A break or disruption in the assumed total sequence of sedimentation. The break may be a period of time, an interruption of deposition or an abrupt change in structure.
Weathering	The process by which rocks are broken down and decomposed by the action of external agencies such as wind, rain, temperature change plants and bacteria.
X-ray diffraction	A diagnostic tool for recognising minerals through their characteristic way of diffracting incident X-rays off their crystal lattices.

APPENDIX 2

NOTATION

w	natural water content
i_s	saturation water content
n	porosity
ρ_d	dry bulk density
ρ_s	saturated bulk density
ρ_g	saturated solid density
ϵ_s	uniaxial swelling strain coefficient
PL	plastic limit
LL	liquid limit
PI	plasticity index
LI	liquidity index
Id_1, Id_2, Id_3	slake durability indices for 1st, 2nd & 3rd cycle
γ	unit weight of soil
ϕ	friction angle, angle of shearing resistance
c	cohesion
p	pressure, stress
ϕ'	effective friction angle
c'	effective cohesion
p'	effective pressure
u	pore pressure
k	coefficient of permeability
cc	cubic centimetre
mm	millimetres
cm	centrimetres
m	metres
km	kilometres
kPa	kilopascals = 10^3 Newtons /m ²
MPa	megapascals = 10^6 Newtons /m ²
RF	resisting forces
DF	driving forces
S.F.	safety factor

APPENDIX 3

A METHOD SUITABLE FOR DETERMINING CERTAIN
INDEX PROPERTIES OF SOILS WHICH ARE APPRECIABLY
AFFECTED, BOTH CHEMICALLY AND PHYSICALLY, ON
SATURATION WITH WATER

Most of the soils investigated in the Enys Formation at Broken River were adversely affected when water-saturated in an unconfined condition. Swelling, spalling and disintegration resulted in the original bulk volumes (Bv) and the pore volumes (Pv) being substantially altered. Determination of volumes was often made impossible as a result. Both Bv and Pv are essential for determining many key index properties, including porosity and density.

An alternative to the saturation of samples in water is to substitute toluol or kerosene for water. Toluol and kerosene are members of the benzene group and are reasonably cheap, safe to handle and have the advantage of being non-dipolar, as water is. In using toluol, it is necessary to adjust for the difference in densities and thus the equations for Bv and Pv need to be divided by 0.8669 gm/cc.

The technique is to select a representative undisturbed, sample that is small enough to fit through the neck of a vacuum flask. A thin strand of copper wire or thread of negligible weight is tied to the material and labelled if necessary. The strand allows retrieval from the flask, the support of the sample during a submerged weighing, and in general, to minimise sample handling.

The sample is oven dried at $100^{\circ} - 110^{\circ}\text{C}$ for 24 hours, cooled to room temperature in a drying cabinet, weighed, and the grain weight recorded as G_w . The sample is then immersed in toluol and all air is evacuated under vacuum for at least two hours. An occasional shaking of the vacuum flask will free entrapped air and total expulsion is evident when no further bubbles arise.

On complete saturation, the sample is transferred to a toluol-filled beaker on a tared balance. The sample is suspended by the strand, taking care that neither the sides nor the bottom of the beaker are touched. The measured weight, W_{sub} is effectively the weight of the toluol displaced by the sample. The sample can then be placed directly on the balance and the weight of the saturated sample, W_{sat} , recorded. The reading should be taken with the sample surface-dry, a condition that soon occurs due to the rapid evaporation of toluol.

The values G_w , W_{sub} and W_{sat} are thus substituted into the following equations to give:

$$Pv = (W_{\text{sat}} - G_w) \div 0.8669 \text{ gm/cc}$$

$$Bv = (W_{\text{sat}} - W_{\text{sub}}) \div 0.8669 \text{ gm/cc}$$

APPENDIX 4

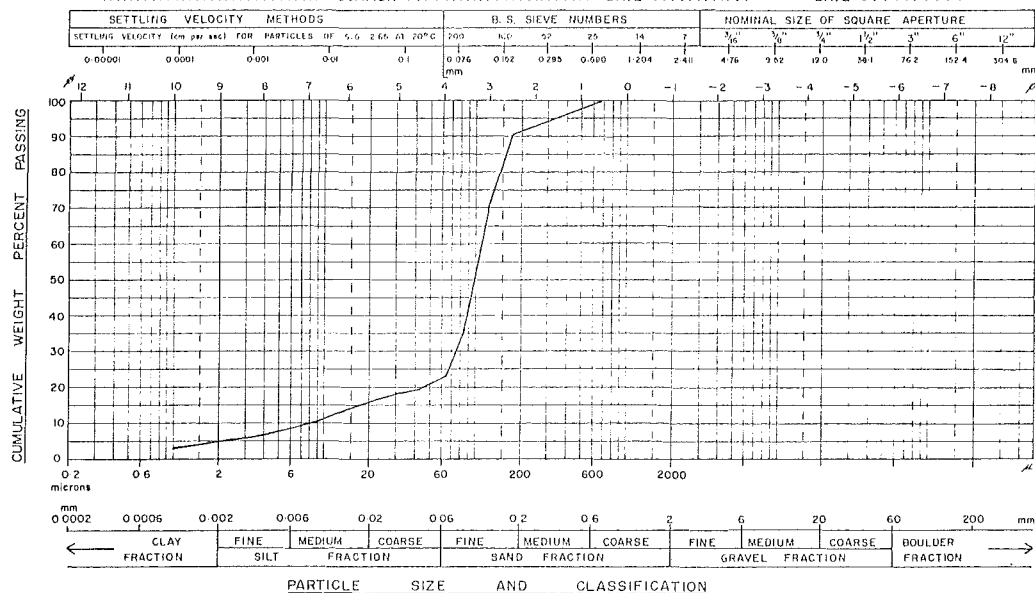
PARTICLE SIZE DISTRIBUTION CURVES

UNIVERSITY OF CANTERBURY

DEPARTMENT OF GEOLOGY

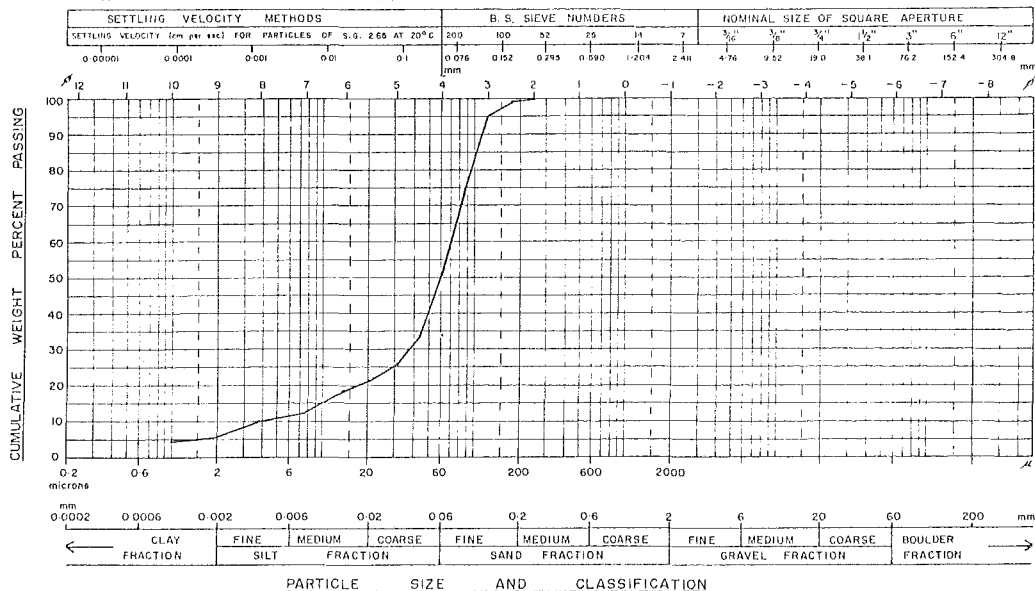
PARTICLE SIZE DISTRIBUTION — SEMI LOG PLOT

PROJECT M.Sc. thesis SAMPLE NO. SANDS SAMPLED BY JMB ANALYSED BY JMB
 Geotechnical investigations LOCATION Broken river DATE DATE



PARTICLE SIZE DISTRIBUTION — SEMI LOG PLOT

PROJECT M.Sc. thesis SAMPLE NO. SILTY SANDS SAMPLED BY JMB ANALYSED BY JMB
 Geotechnical investigations LOCATION Broken river DATE DATE



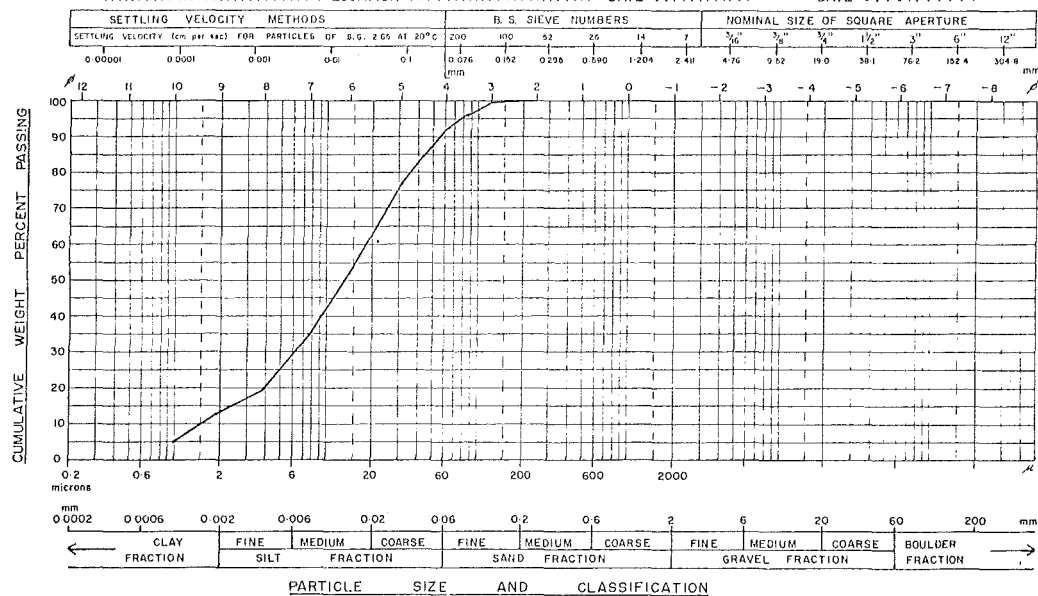
APPENDIX 4 - Cont'd

UNIVERSITY OF CANTERBURY

DEPARTMENT OF GEOLOGY

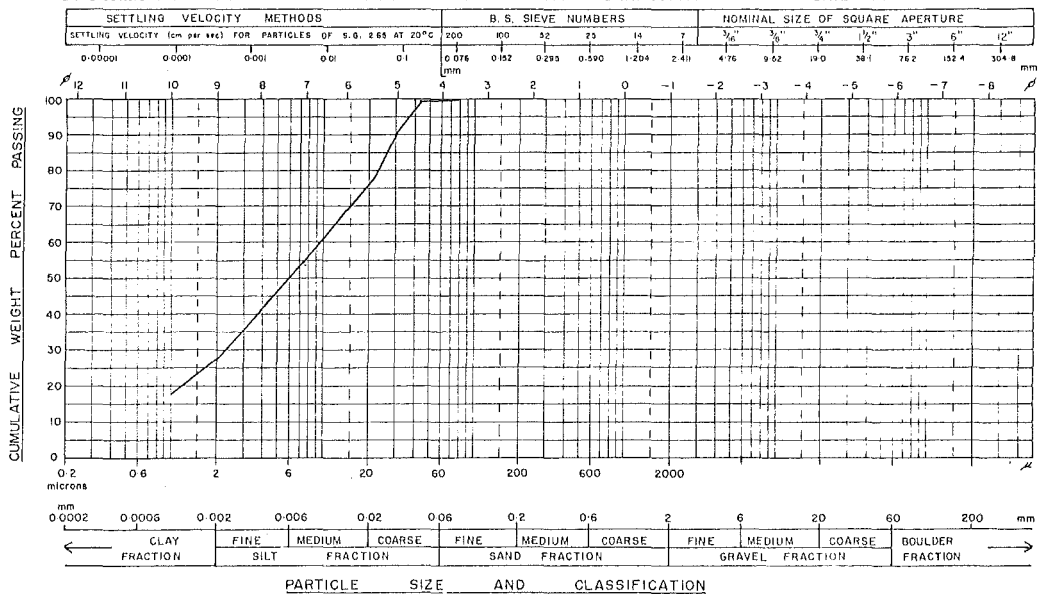
PARTICLE SIZE DISTRIBUTION - SEMI LOG PLOT

PROJECT M.G.C. Theria..... SAMPLE NO. SILTS..... SAMPLED BY JMB..... ANALYSED BY JMB.....
 Geotechnical Investigation LOCATION Broken River..... DATE DATE



PARTICLE SIZE DISTRIBUTION - SEMI LOG PLOT

PROJECT MSQ. TURSIS..... SAMPLE NO. MUDS..... SAMPLED BY JMB..... ANALYSED BY JMB.....
 Geotechnical Investigations LOCATION BROKEN RIVER..... DATE DATE



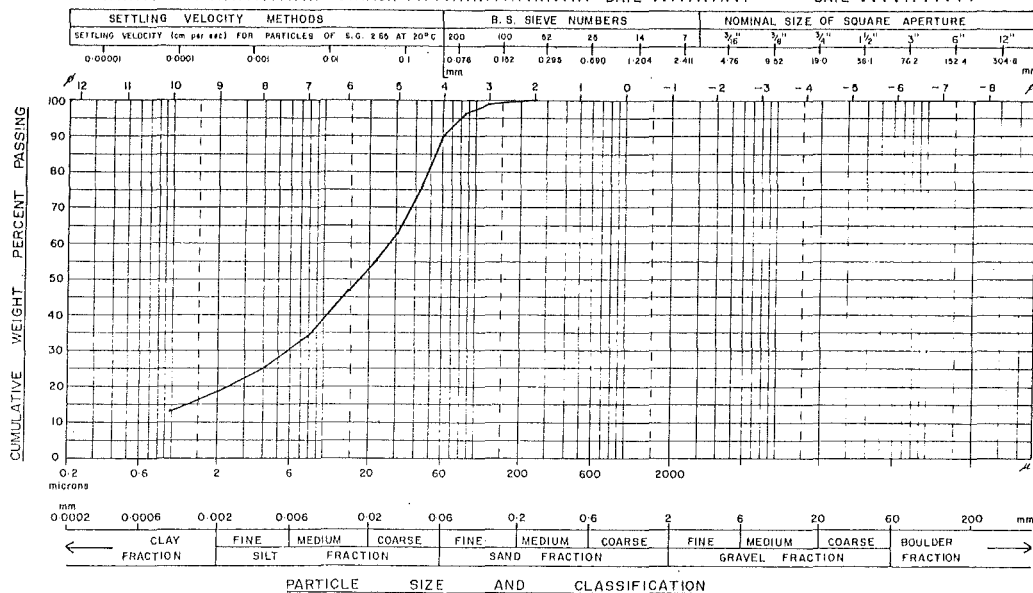
APPENDIX 4 - Cont'd

UNIVERSITY OF CANTERBURY

DEPARTMENT OF GEOLOGY

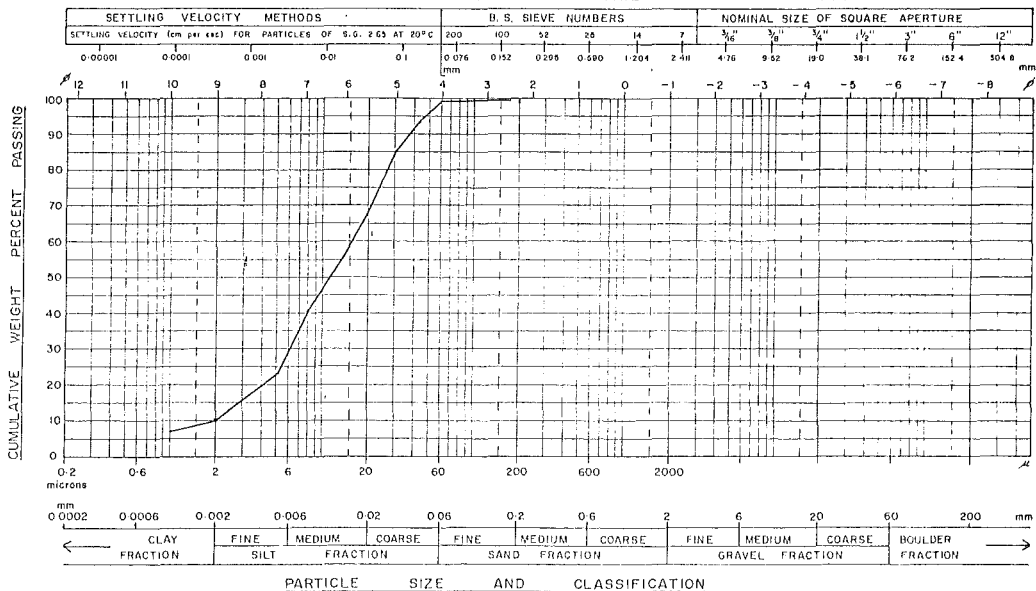
PARTICLE SIZE DISTRIBUTION - SEMI LOG PLOT

PROJECT M.Sc. thesis SAMPLE NO SITTS AND MUDS SAMPLED BY JMB ANALYSED BY JMB
 Geotechnical investigations LOCATION Broken river DATE DATE



PARTICLE SIZE DISTRIBUTION - SEMI LOG PLOT

PROJECT M.Sc. thesis SAMPLE NO SLIP MATERIAL SAMPLED BY JMB ANALYSED BY JMB
 Geotechnical investigations LOCATION Broken river DATE DATE



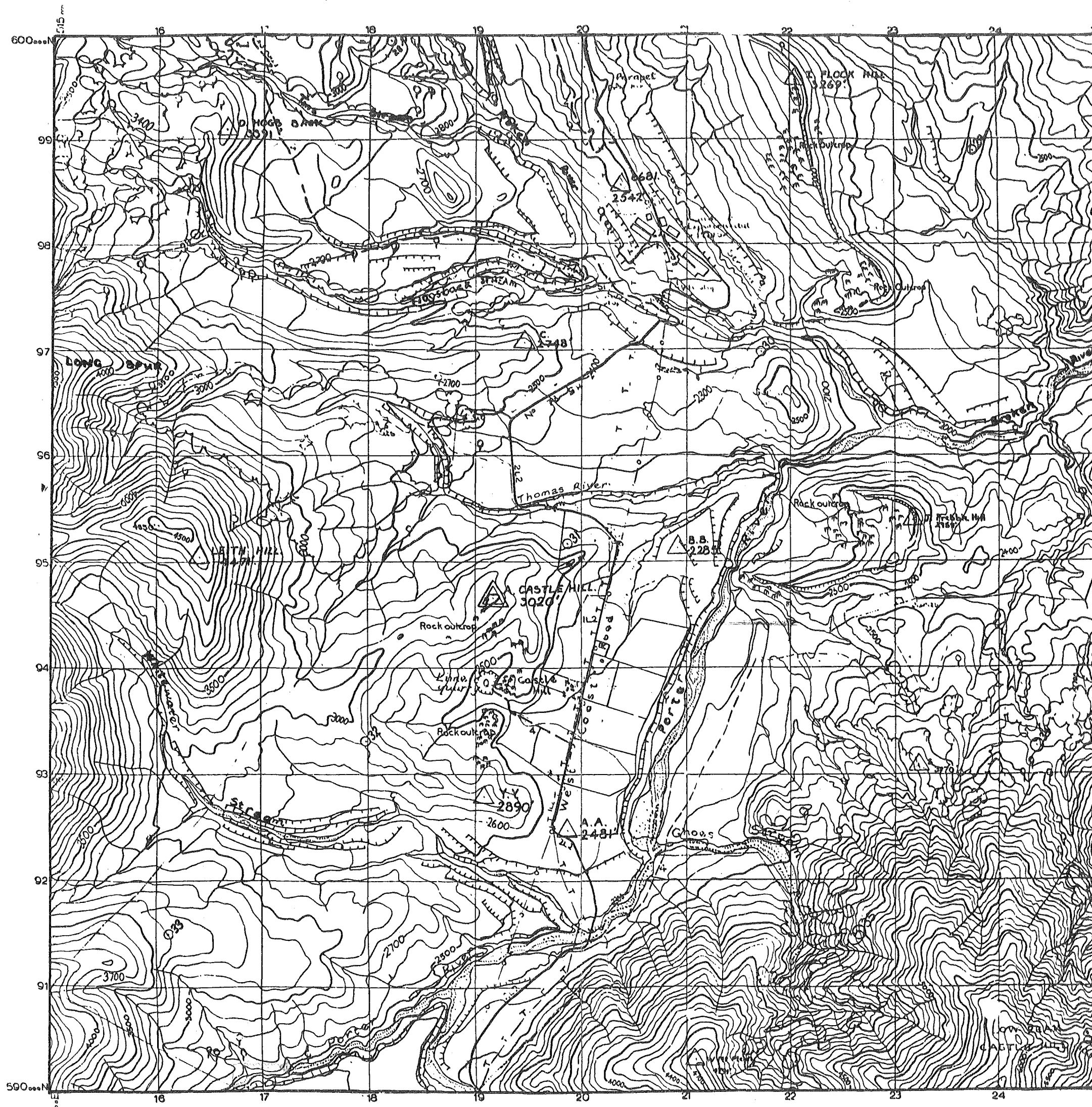


FIGURE 23

GEOLOGY AND LANDSLIDE DISTRIBUTION OF CASTLE HILL BASIN

Geology after Gage (1970) and Brodshaw (1975)

- CONTEMPORARY LANDSLIDES
- FOSSIL LANDSLIDES
- PRE-CRETACEOUS BASEMENT
- B BROKEN RIVER COAL MEASURES
- I IRON CREEK GREENSAND
- C COLERIDGE FORMATION
- T LIMESTONE AND TUFF MARKER BEDS OF THE THOMAS FORMATION
- E ENYS FORMATION
- G GLACIFLUVIAL GRAVELS
- A RECENT ALLUVIUM

FAULT FOLD AXIS

1: 52000

SCALE

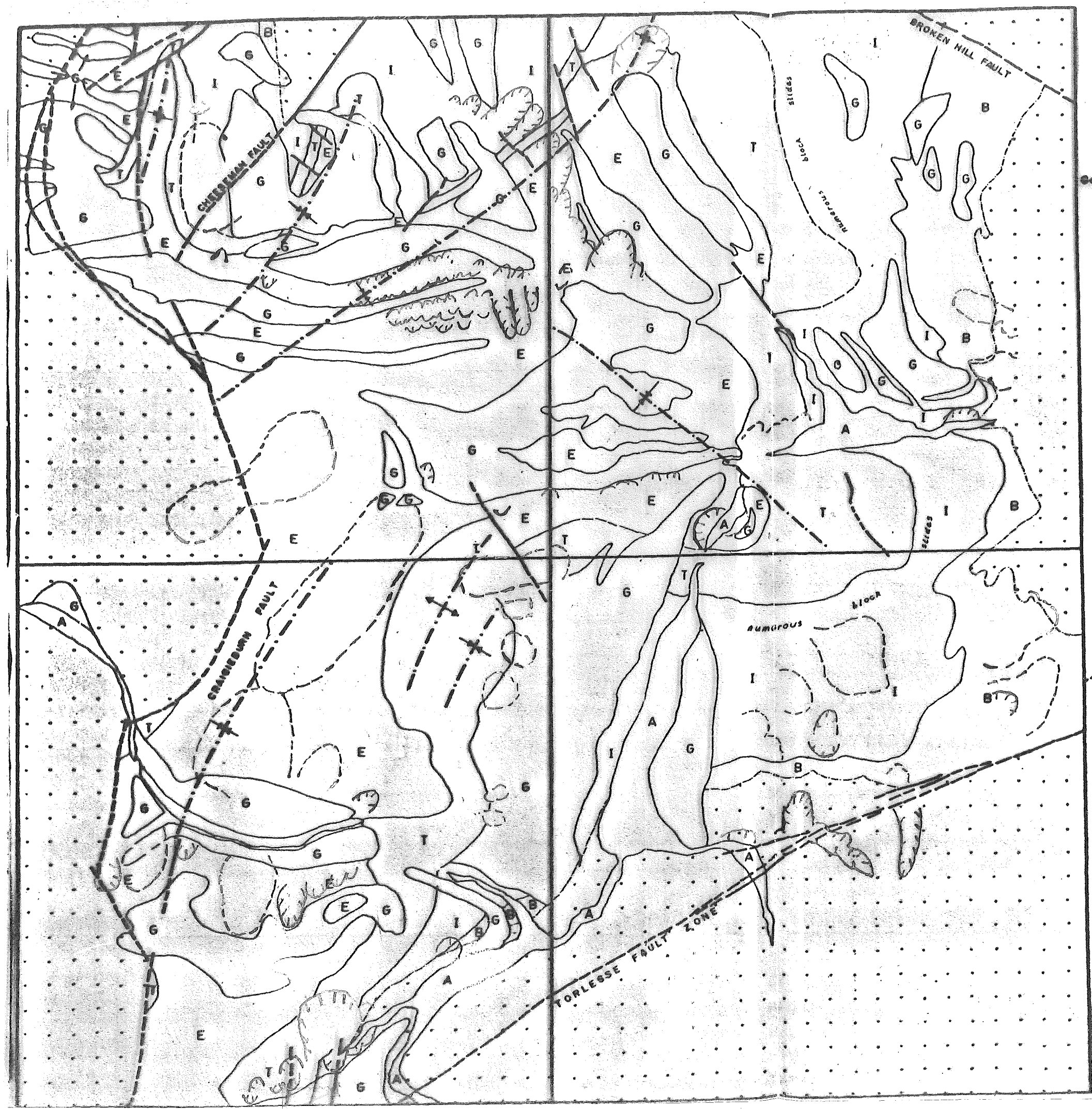
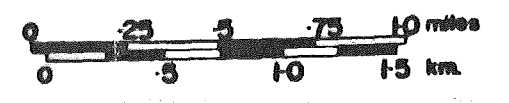


FIGURE 24

SLOPE INTENSITY MAP
OF CASTLE HILL BASIN

Boundary spacing = $\frac{\text{contour spacing}}{\tan \text{ angle scale}}$

SCALE 1:32800



BASE MAP - 366/8

Key

- 0°—10°
- 10°—20°
- 20°—30°
- > 30°

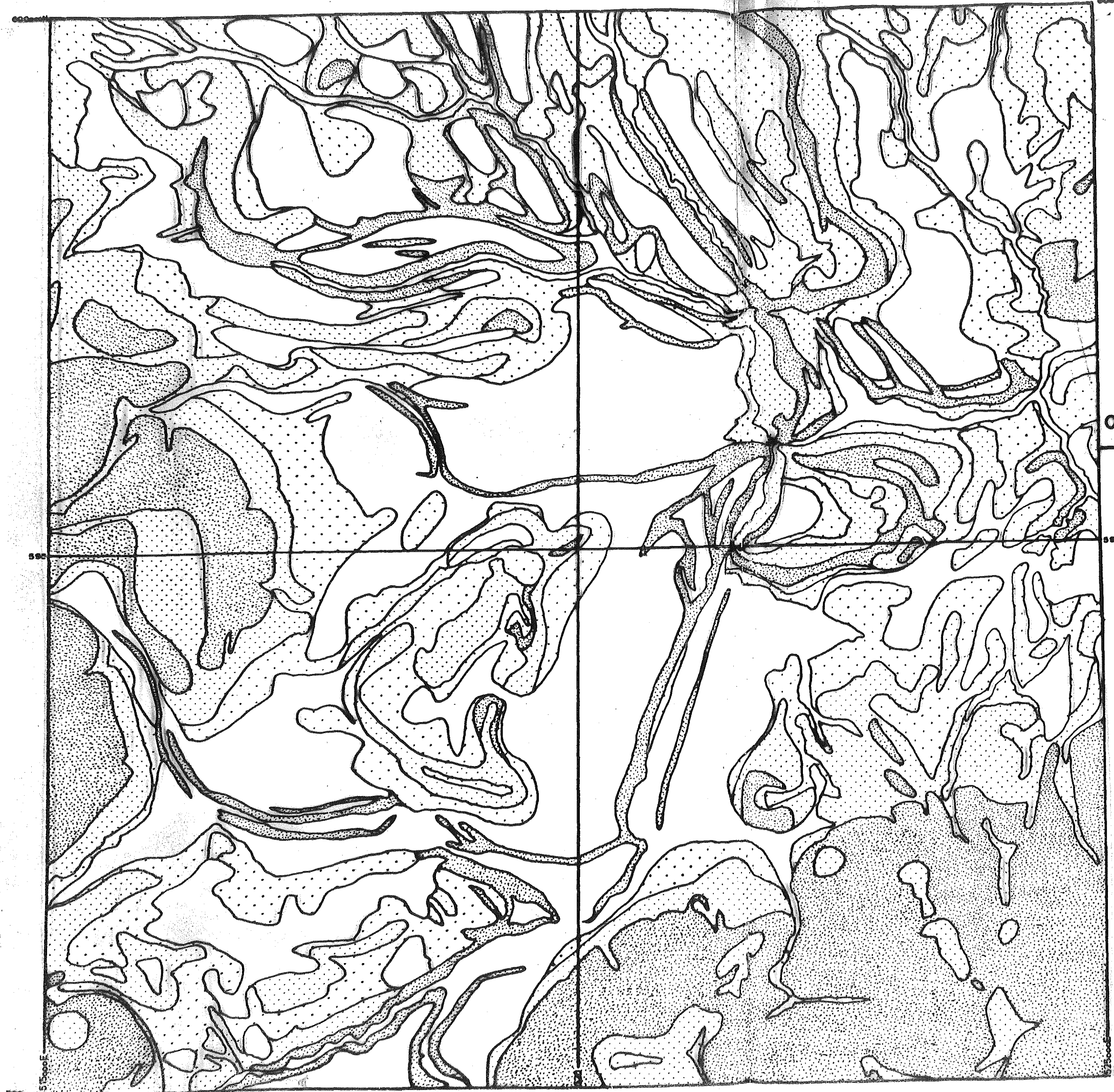


FIGURE 25




LANDSLIDE SUSCEPTIBILITY MAP OF CASTLE HILL BASIN

BASED ON FIGURES 22, 23 AND 24

SCALE 1:32800

0 0.5 1.0 mile
0 0.5 1.0 1.5 Km

KEY

-  **ZONE 1:** Areas of probable slope failure including all recent landslides, reactivated parts of older landslides and oversteepened terrace risers of weak sediments.
-  **ZONE 2:** Areas of possible slope failure including the more stabilised fossil landslides, stable areas bordering active landslides, oversteepened and high terrace risers and areas of accelerated mass wasting.
-  **ZONE 3:** Areas considered to be essentially stable with only a remote possibility of slope failure under present day conditions.

